12-2016

Structural Evaluation of SCDOT Prestressed Channel Bridges

Robert Steven Gunter
Clemson University

STRUCTURAL EVALUATION OF SCDOT PRESTRESSED CHANNEL BRIDGES

A Thesis
Presented to
the Graduate School of
Clemson University

In Partial Fulfillment
of the Requirements for the Degree
Master of Science
Civil Engineering

---

by
Robert Steven Gunter
December 2016

Accepted by:
Thomas E. Cousins, Committee Chair
Bryant G. Nielson
Brandon E. Ross

ABSTRACT

The Five Forks Bridge in Liberty, SC (Figure 7-1) is one of approximately 450 prestressed concrete channel bridges that the SCDOT oversees. Some of these channel bridges, such as the Five Forks Bridge, have unknown structural properties and flexural capacity. The Five Forks Bridge is a prestressed concrete channel bridge consisting of 33 girders that form three simple spans each 30 ft. in length. There are no formal design calculations available for some of these bridges and there are multiple prestressed strand designs that may describe the physical properties of each bridge.

This project seeks to reveal the structural characteristics of the Five Forks Bridge and similar bridges through live load tests, laboratory channel tests, and analysis. A channel girder similar to those in the Five Forks Bridge was tested in a four point bending arrangement to experimentally determine the cracking moment and nominal strength of the girders that make up these bridges. Hand calculations were also carried out to compare the theoretical values for nominal strength, cracking moment, distribution factor for moment, and dynamic load allowance. After completion of the channel test, a forensic investigation was carried out in which the end of the girder was chipped away to discover the actual strand properties and layout.

Comparisons of the live load test, channel test, and hand calculations revealed that the experimental nominal strength of the girders is 3% greater than theoretical calculations predict, the bridge possesses less load transfer than the AASHTO LRFD equations assume, and the bridge is insufficient to support the demand of the HL-93

design load set. The original load rating factors were modified with the experimental results and the Forks Bridge passed the legal load rating level with a rating factor of 1.14.

No posting is needed for the Five Forks Bridge for all legal loads, but it is recommended that the SCDOT carry out future load ratings with assumed conservative bridge properties unless a nondestructive test is conducted.

ACKNOWLEDGEMENTS

First, I would like to thank Dr. Nielson for reaching out to me and inviting me to take part in this project. I would not have even known where to start when it came to finding a project and funding had I not spoken with you. Dr. Cousins and Dr. Ross, thank you so much for mentoring me throughout this process and for being so involved with my work. I am grateful for your willingness to teach me and your patience when things didn't go quite as planned.

Next I would like to thank Danny Metz, Sam Biemann, and Scott Black for all of your help. Orchestrating the live load test of the Five Forks Bridge and conducting the channel test at WISER would have been near impossible without your help. Ashton Pentico and Jesse Grimson, thank you for assisting me with the BDI equipment and helping me out whenever we ran into issues.

Thank you to all of the students who helped me along the way. Mahmood, thank you for helping me acquire the data during the channel test. Learning how to use the National Instruments equipment and figuring out how to wire everything was much easier with you by my side. Carrie Fields up at Virginia Tech, thank you for allowing me to help with your live load test back when I first started my research. Learning from your experiences and heeding your advice gave me a great jump start when I began my testing.

And last but not least I would like to thank my friends and family. It was always nice to have someone to vent to and to have a sympathetic ear. Your support and advice has been immeasurable.

I am very thankful for my 5 ½ years here at Clemson. This last year as a graduate student wouldn't have been nearly as enjoyable or memorable without the help of everyone.

TABLE OF CONTENTS

TABLE OF CONTENTS (CONTINUED)

Page

TABLE OF CONTENTS (CONTINUED)

Page

TABLE OF CONTENTS (CONTINUED)

Page

TABLE OF CONTENTS (CONTINUED)

Page

TABLE OF FIGURES

Page

TABLE OF FIGURES (CONTINUED)

Page

TABLE OF FIGURES (CONTINUED)

Page

TABLE OF FIGURES (CONTINUED)

Page

TABLE OF FIGURES (CONTINUED)

Page

TABLE OF TABLES

Page

TABLE OF TABLES (CONTINUED)

Page

TABLE OF TABLES (CONTINUED)

Page

TABLE OF EQUATIONS

Page

Chapter 1: Introduction

The American Society of Civil Engineers (ASCE) maintains a report card where the quality of the nation's infrastructure is graded. This consists of an overall grade as well as grades for each type of infrastructure such as ports, roads, bridges, etc. for the country and each state. The 2013 report card says the following about the quality of the bridges in the nation: "In total, one in nine of the nation's bridges are rated as structurally deficient, while the average age of the nation's 607,380 bridges is currently 42 years. The Federal Highway Administration (FHWA) estimates that to eliminate the nation's bridge deficient backlog by 2028, $20.5 billion would need to be invested annually, while only $12.8 billion is being spent currently." Those are numbers for the nation as a whole while in South Carolina (SC) approximately 21% of the state's bridges are either structurally deficient or functionally obsolete (FHWA 2013).

Based on this report card, the number of bridges in South Carolina that need repair or replacement is high and needs to be addressed. Of the 9,344 bridges in SC approximately 450 of them use a design utilizing 30 ft. simple spans made of prestressed channel girders (see Appendix A). For a typical two-lane bridge, each span consists of 11 girders with tie rods at the quarter points to facilitate transverse load sharing. A two inch wearing surface is placed on top of the girders and barrier rails made of timber and steel are attached to the external girders. The majority of these bridges were built in the 1950s and 1960s and many have surpassed their original 50 year design life. They were designed for a smaller design truck (H15-44) than the standard design truck used today (HL-93). Figures 1-1 and 1-2 show the truck geometries and loads.

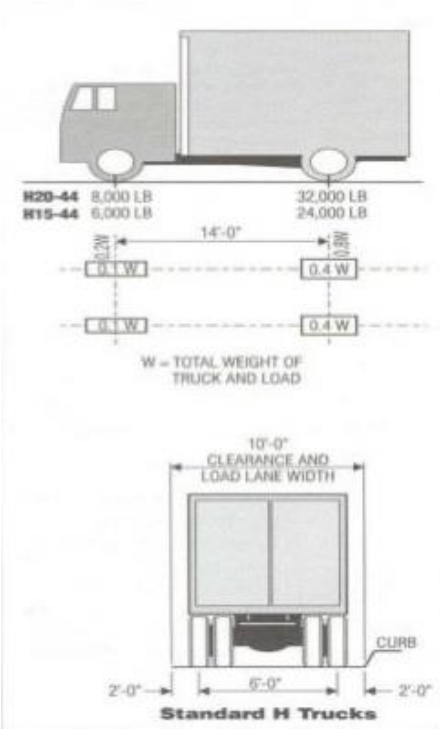

Figure 1-1: H15-44 Truck (AASHTO 1993)

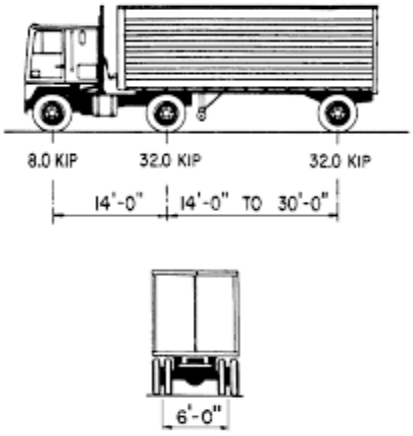

Figure 1-2: HL-93 Truck (AASHTO 2010)

Due to the condition of these bridges and the smaller truck used for design, it is not known whether bridges of this design need to be posted, replaced, or are structurally sufficient.

The Five Forks Bridge over Eighteenmile Creek in Liberty, SC is an example of this prestressed channel design and is the focus of this research. Figure 1-3 shows a view of the bridge from the north. The three simply supported spans can be seen as well as the substructure beneath.

Figure 1-3: Five Forks Bridge

Figure 1-4 is a westward view of the two traffic lanes and the road surface of the bridge. All three spans are visible and cracks can be seen in the wearing surface at each longitudinal girder-to-girder joint. The approach on the eastern span can be seen in Figure 1-4. There is a slight bump in the approach that bounces vehicles as they drive across the bridge.

Figure 1-4: Traffic Lanes

The bottom of the bridge superstructure and the substructure are shown in Figure 1-5. This offers a plain view of the girder geometry; the channel flange and both webs can be seen. The substructure beneath consists of timber piles supporting a concrete bent cap.

Figure 1-5: Bottom of Superstructure and Substructure

The cross section in Figure 1-6 shows a cross section of one half of the symmetric Five Forks Bridge. The barrier rail can be seen attached to the exterior girder, and a tie rod connecting the girders can also be seen. The concrete bent cap and a portion of the timber piles is also visible.

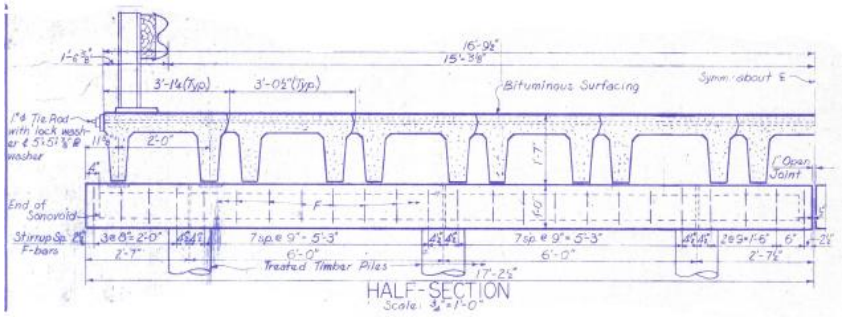

Figure 1-6: Half of Superstructure Cross Section (SCDOT)

Figure 1-7 is a plan view of the girder layout. The girders are numbered 1 through 11. Span designations of East and West are used to clearly indicate which

girders are being referenced. The damaged girder is shown with a dashed line at girder 11 of the West span.

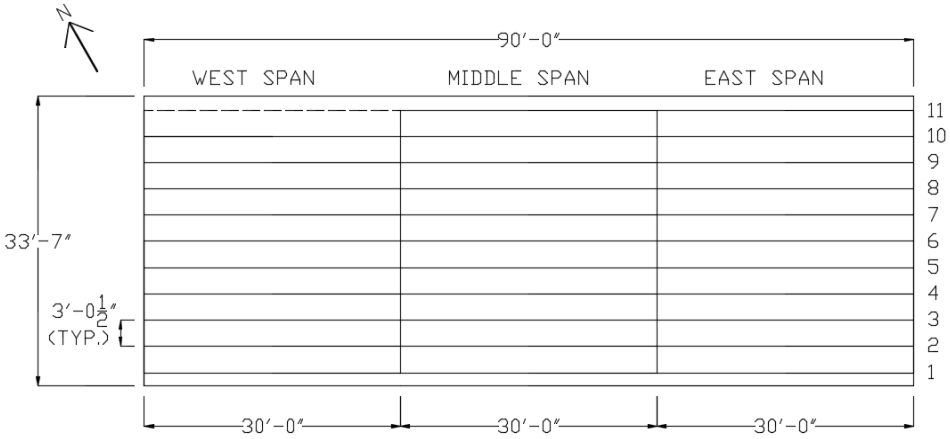

Figure 1-7: Plan View and Girder Designation

1.1 Purpose and Scope

The purpose of this project is twofold: 1) to evaluate the condition of and develop a posting recommendation for the Five Forks Bridge and 2) to use the Five Forks Bridge as a basis for creating a system for SCDOT to assess the health of the other bridges in the state that use the same superstructure. The Five Forks Bridge is a three span, simply supported bridge where the West span has a damaged exterior girder and the East and Middle spans have all visually-determined healthy girders. The damage to the girder is shown in Figure 1-8. The bottom of one of the flanges has concrete that has spalled off resulting in some prestressing strands being exposed and partially corroded.

Figure 1-8: Exterior Girder Damage

These purposes were first achieved by performing a live load test of the Five Forks Bridge using various truck weights. The truck weights were varied from light loads up to the legal limit for this bridge. Strain and deflection were the two parameters recorded during the test. The responses in the healthy and damaged girders were compared to evaluate the condition of the damaged girder. The strains and deflections at varying truck weights were used to determine if the channel girders (specifically the damaged girder) were behaving linear elastically under legal loads.

Next a healthy surplus girder identical to those in the Five Forks Bridge was obtained from SCDOT and tested to failure in Clemson's Structural Engineering Research Lab. The results from the field test were compared to the failure curve of the lab test to get a clearer picture of girder behavior. With the full load versus deflection

behavior known from the lab test, the condition of the Five Forks Bridge could be more definitively determined.

The final portion of the scope was achieved through calculations based on the American Association of State Highway and Transportation Officials (AASHTO) Manual for Bridge Evaluation (MBE 2011). The manual provides guidelines for load rating in-service bridges from experimental results and calculations. The Five Forks Bridge was load rated using these guidelines and a posting recommendation is provided. In addition, the results found for the Five Forks Bridge are used to developed recommendations for rating other channel girder bridges in SC.

1.2 Objectives

There are five objectives set out to be answered from this research as follows:

1. Does the bridge need to be posted? Should a weight limit be set for trucks that are allowed to cross this bridge?
2. What implications does this have for similar bridges? How can the load rating and posting recommendations for the Five Forks Bridge be applied to the other bridges across the state that use a similar superstructure?
3. What is the assessment of the structural health of the damaged girder compared to the healthy girders? How does the damaged girder see and respond to load differently?
4. How do the girders transversely distribute the load and what is the dynamic load allowance of the bridge?
5. What is the flexural capacity and cracking moment of the girders in the Five Forks Bridge?

1.3 Organization

This thesis is organized into five chapters. A literature review of live load testing is presented in Chapter 2. Chapter 3 focuses on the set up and execution of the live load and lab test. Chapter 4 presents the results of the live load test, lab test, and hand calculations. Chapter 5 discusses the recommendations made to SCDOT and presents the conclusions found from this research.

Chapter 2: Literature Review

2.1 Channel Bridges

Both prestressed and nonprestressed concrete bridges make use of girders with channel-shaped cross-sections. These cross-sections resemble those of steel channels; the web forms the horizontal bridge deck and the flanges act as two shallow beams. This is a practical design since the web doubles as the deck and the flanges resist shear and moment (Durham 2003). Steel reinforcement can be found in the bottom of each flange to provide additional flexural reinforcement (Wipf 2006).

2.1.1 Bridge Geometry

A study by Durham found that at least 12 states use these channel bridges. Most channel bridges utilize the same design, having similar geometric properties such as width, span length, and girder cross section. Figures 2-1 and 2-2 show a typical channel girder cross section and a typical channel bridge cross section from a project by Wipf.

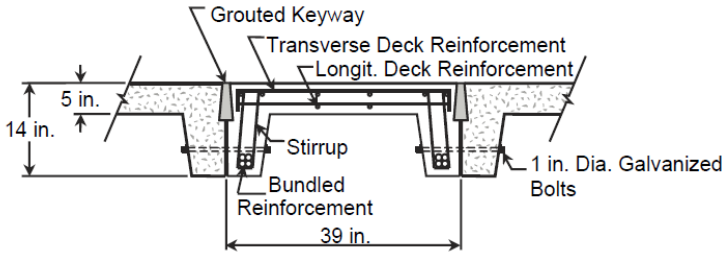

Figure 2-1: Typical Channel Girder Cross Section (Wipf 2006)

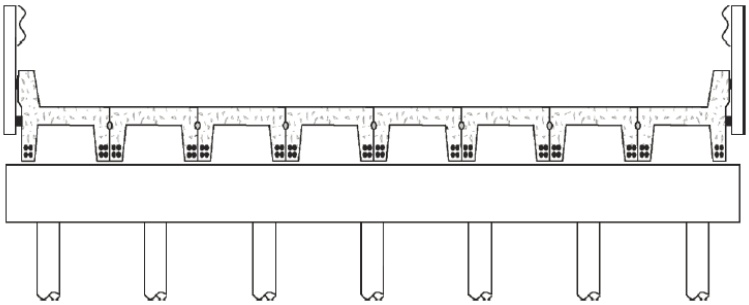

Figure 2-2: Typical Channel Bridge Cross Section (Wipf 2006)

Most of these bridges were similar to the Five Forks Bridge with spans ranging from 19 to 36 ft. with an average length of 32'-0" and a curb-to-curb width of 28'-10½". The girders fit together into the overall bridge structure in a slightly different way compared to the Five Forks Bridge though. In the studies done by Klaiber, Wipf, and Durham (2001) the flanges of each channel form a joint along the entire downward length of each flange. The channels in the Five Forks Bridge have webs that extend beyond the edge of the flanges so the webs of each girder are connected instead of the flanges; this cross section can be seen in Figure 2-3.

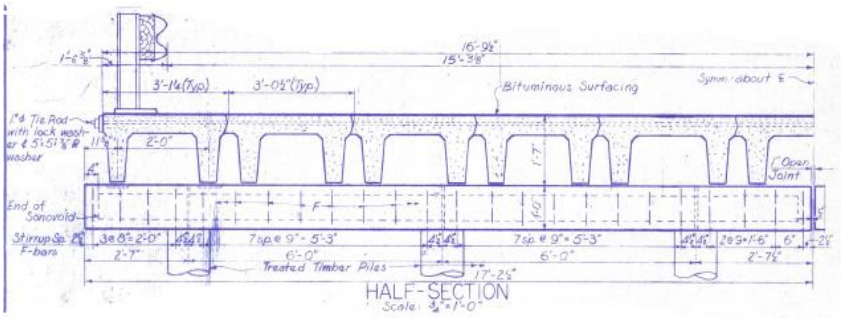

Figure 2-3: Half Cross Section of Five Forks Bridge

2.1.2 Bridge Damage

Almost all of the states with these channel bridges reported damage similar to what is found in the Five Forks Bridge. This damage includes concrete that has spalled

off the flanges and corrosion present on the flexural reinforcement. Figure 2-4 below shows a common example of this type of damage.

Figure 2-4: Example of Corrosion and Spalling (Klaiber, et al 2001)

A common design with channel bridges is for there to be no additional deck structure outside of the channel web. The web is topped with asphalt to form the roadway surface of the bridge. Asphalt is a more permeable surface than concrete so it is common for water to permeate the asphalt and pool on top of the concrete web. Water can then penetrate the channel flanges and eventually reach the flexural reinforcement. In current design the standard practice is to have an impermeable water barrier placed between the asphalt and wearing surface to prevent this water penetration. In older designs this may not be present and the asphalt wearing surface can hide some of the concrete damage.

The chemical reaction that forms rust causes the reinforcing bars to expand and crack the surrounding concrete. Cracked concrete can speed up the corrosion process

until concrete spalls at the flanges. Corroded reinforcing bars have a decreased cross-sectional area and a weaker bond with the surrounding concrete than reinforcing bars that aren't corroded. This corrosion results in a decreased flexural strength (Durham 2003). Conclusions from an Iowa State study identified this widespread and identical damage in concrete channel bridges as a national issue that needs addressing (Klaiber, et al 2001).

2.2 Dynamic Load Allowance

There is no perfectly smooth bridge or roadway, all surfaces have some degree of roughness. This inherent roughness in bridges causes an oscillation in the weight of vehicles as they bounce up and down on their suspension system. During the compression of the vehicle's shock absorbers, the gravitational force from the vehicle's weight is larger than the static gravitational force. This increase in force is called dynamic load allowance (IM) (Barker and Puckett 2007). Figure 2-5 is a time vs. deflection plot that shows the responses from static and dynamic loading. Figure 2-6 accounts for the difference in time and shows the superimposed responses from static and dynamic loading as a function of the truck position on the bridge. The increase in the dynamic loading caused by oscillation is clear in Figure 2-6.

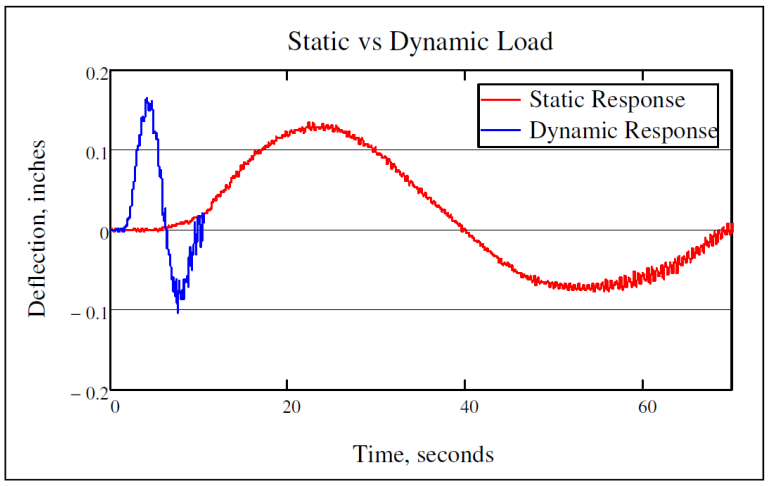

Figure 2-5: Static vs. Dynamic Loading (Collins 2010)

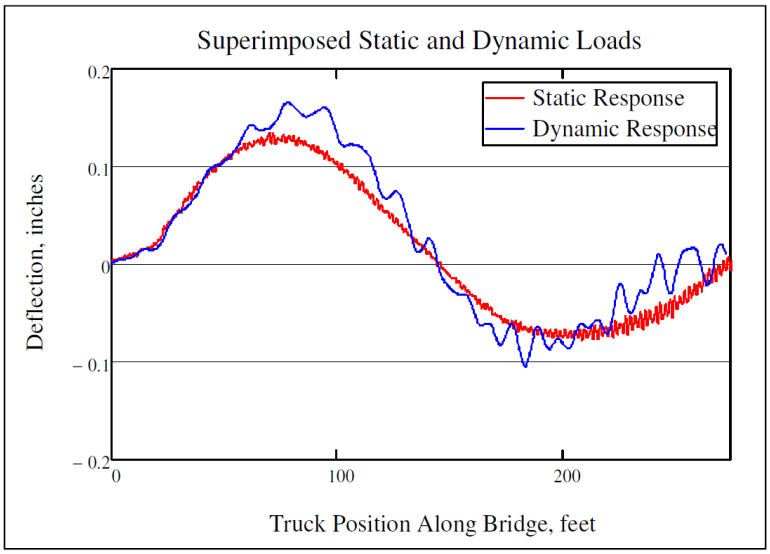

Figure 2-6: Dynamic Load Superimposed over Static Load (Collins 2010)

Extensive studies have been conducted to understand IM and to find the best methods of estimating its value. Paultre, et al. (1992) looked into what factor was needed to increase the static load to account for the dynamic load allowance. No single method is adhered to across the globe; most countries have their own process to estimate the dynamic loading. There are some factors such as bridge frequency, span length, truck weight, and roadway roughness that all international agencies use in their calculations.

The settlement of the roadway at the approach can also create a "ramping effect" that should be considered as well (Restrepo, et al 2005).

2.2.1 AASHTO Dynamic Load Allowance

A simplified approach to estimate IM analytically can be used for design though. Based on an analysis conducted by AASHTO, a single value can be applied to account for the dynamic effects of vehicular load. The table below comes from the *AASHTO LRFD Bridge Design Specifications* (AASHTO LRFD 2010) and is used to conservatively estimate the design IM for different bridges and bridge components.

Table 2-1: AASHTO LRFD IM Factors (AASHTO LRFD 2010)

Component	IM (%)
Deck joints – all limit states	75
All other components Fatigue and fracture limit states All other limit states	 15 33

This test was not concerned with fatigue or fracture limit states so an IM of 33% would typically be used for the Five Forks Bridge.

2.2.2 Experimental Calculation of Dynamic Load Allowance

Dynamic and static tests conducted on prestressed bridges in Florida concluded that AASHTO IM are conservative for short spans. The measured IM for the bridges were less than the theoretical IM from AASHTO LRFD (Issa, et al 1993). The IM for an existing bridge can be found experimentally through the use of nondestructive testing.

However, experimental research conducted by Hwang and Nowak (1991a, 1991b) showed that the IM decreased as the truck weight increased. This is because the deflection caused by dynamic loading was largely independent of an increase in truck

weight while there is a linear relationship between the deflection caused by static loading and an increase in truck weight. Thus, since the dynamic deflection is practically constant but the static deflection increases, then the effective IM is smaller for larger trucks. The standard truck used by AASHTO, an HL-93 weighs 72 kips while the largest truck used in testing the Five Forks Bridge weighed 48 kips. This decrease in truck weight should result in a larger IM for the Five Forks Bridge than the IM that AASHTO LRFD lists in its specification. The following equation uses experimental deflection data from a nondestructive test to calculate the IM:

$$IM = \frac{D_{dyn}}{D_{sta}}$$

Equation 2-1

Where D_{dyn} is the response due to the dynamic loading and D_{sta} is the response due to the static loading. IM is the dynamic load allowance that is used as an amplification factor (Barker and Puckett 2007). Research has shown that either deflection or strain can be used as the response variables in the above equation (Kassner 2004). Once the IM is calculated then the dynamic loading can be found. The equation below is used to amplify the static loading to determine the dynamic loading:

$$P_{dyn} = P_{sta}(1 + IM)$$

Equation 2-2

Where P_{dyn} is the dynamic loading, P_{sta} is the static loading, and IM is the dynamic load allowance in decimal form (Kassner 2004). There can be a large variation in these deflection values based off of the truck location but Bakht and Pinjarkar (1991) insist on using the maximum values since this effect accounts for the extremes.

Research conducted by Issa and Shahawy looked at the IM for different types of AASHTO prestressed girders under different truck speeds. The truck used for these dynamic tests was a 200 kip tractor trailer with five axles supplied by the Florida DOT. The IM calculated from deflection for both girder types and for all speeds were less than the 33% IM that AASHTO LRFD specifies for new design as shown in Table 2-1. However, the IM calculated from strain for the same girders and speeds were slightly higher in comparison. These lower values based off of deflection confirm the belief that AASHTO LRFD provides a conservative approximation for IM. The bottom two rows of Table 2-2 show the deflection-based IM values for the different girder types and truck speeds (Issa, et al 1993).

Table 2-2: Experimental IM Values for AASHTO Girders (Issa, et al 1993)

COMPUTATION OF IMPACT FACTOR FOR A TYPICAL INTERIOR MID-SPAN GIRDER						
Method	AASHTO Bm. Type	Interior Girdor No.	Dynamic Results %			AASHTO EQUATION I=50/(L+125)
			55 MPH	45 MPH	35 MPH	
Strain (ue)	II	3	6.3 %	N/A	N/A	29.3 %
	III	3	36.8	31.6	10.5	26.2
	IV	5	30.4	21.7	7.8	20.3
Deflection (in.)	III	3	30.5	12.0	3.5	26.2
	IV	5	29.6	26.6	13.9	20.2

2.3 Transverse Load Distribution

One of the main focuses of structural analysis is determining how forces and loads are distributed through a structure. In bridges it is necessary to understand how vehicular load is shared transversely between girders. Bridge decks, shear keys between girders, and tie rods can facilitate this transverse load distribution. In bridges this

transverse load distribution is determined by distribution factors, also known as wheel or lateral load distribution factors. These factors are quantitative values that illustrate how much of a wheel line each girder supports. The distribution of load to each girder is generally determined by the stiffness of the concrete deck, cross-frames, diaphragms, bearings, and bridge geometry (Barker and Puckett 2007). The wheel line load is then multiplied by these distribution factors to determine the design load for each girder. A larger distribution factor means that the bridge does not distribute the load well, and the girder directly beneath the wheel line experiences more load.

Figure 2-7 illustrates a point load being distributed through a bridge and the difference between good and poor distribution.

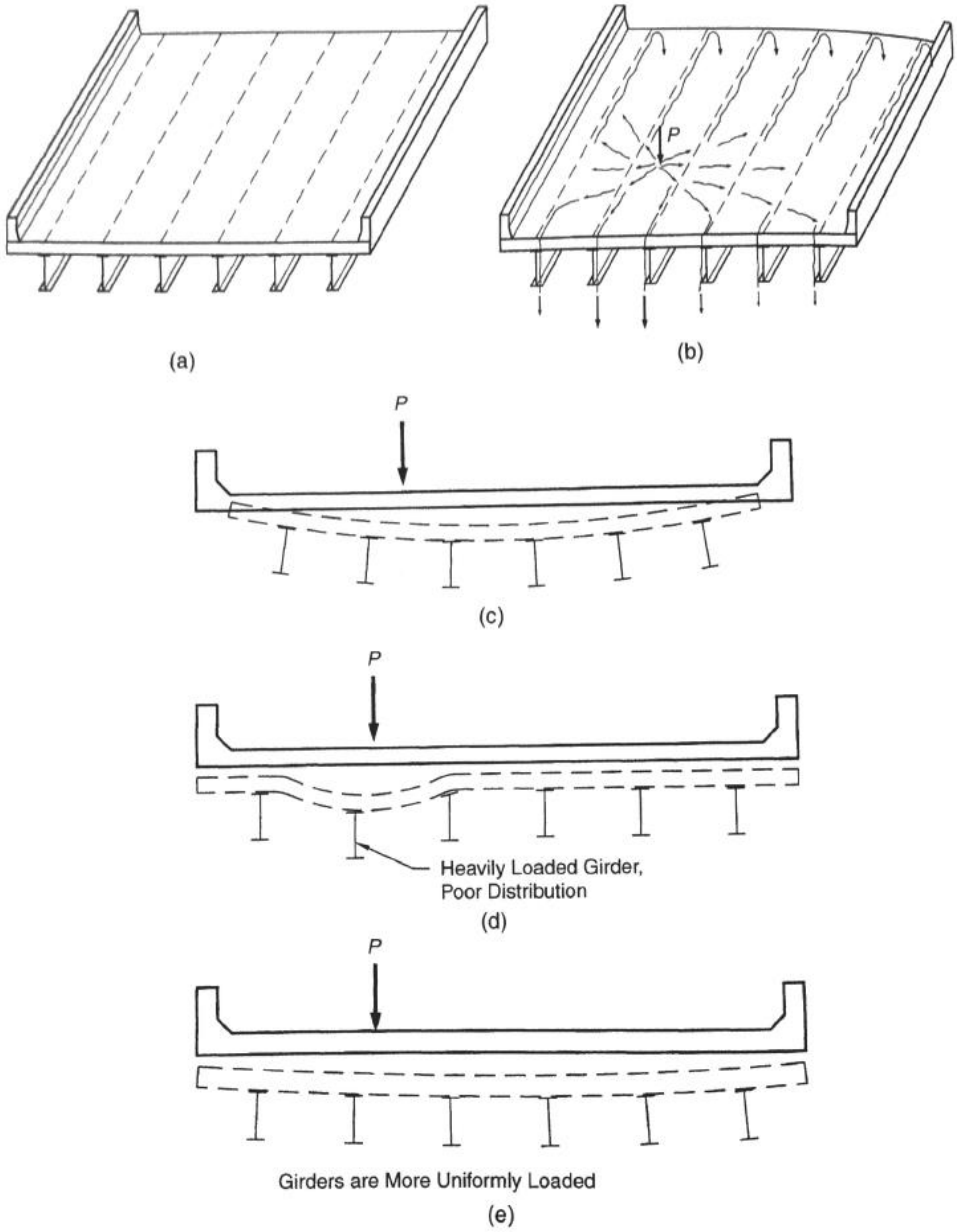

Figure 2-7: Transverse Load Distribution Illustration (Barker and Puckett 2007)

Figure 2-7(a) is an illustration of a slab-girder bridge and Figure 2-7(b) shows how a point load would travel through the slab and into the girders, note that the load going directly into the girders beneath the load is greater than the load going into the surrounding girder. Figure 2-7(c) shows the ideal deflection of the girders assuming

there is linear behavior. Figure 2-(d) shows how the load can be concentrated in a few girders if there is poor distribution. Whereas Figure 2-7(e) shows how a good distribution can allow more equal sharing of the load (Barker and Puckett 2007).There are distribution factors for shear and moment (DFM) (Phelps 2010). The support reactions need to be known to determine the distribution factors for shear. Those responses would be difficult and expensive to record during a load test so distribution factors for shear were not feasible for the Five Forks Bridge.

2.3.1 AASHTO LRFD Distribution Factors for Moment

A number of factors go into calculating distribution factors such as girder spacing, span length, the modular ratio between girder and deck, and girder geometry (Barker and Puckett 2007). AASHTO LRFD presents a table of formulas based off of a parametric study that assists in calculating the distribution factors for single and multi-lane traffic and for interior and exterior girders. From AASHTO LRFD Table 4.6.2.2.1-1 cross section types (h) and (i) most closely resemble the Five Forks Bridge. These cross-sections are then referenced in Table 4.6.2.2.2b-1 to determine the distribution factor for the moment in an interior girder. Cross sections (h) and (i) use the same following equations to determine the distribution factor:

$$DFM = S/D$$

Equation 2-3

Where DFM is the distribution factor for the moment, S is the spacing of the beams or webs, and D is the width of the distribution per lane.

$$C = K(W / L) \leq K$$

Equation 2-4

Where C is the stiffness parameter, K is the constant for different types of construction, W is the edge-to-edge width of the bridge, and L is the span of the beam.

$$K = \sqrt{\frac{(1+\mu)I}{J}}$$

Equation 2-5

Where μ is poisson's ratio, I is the moment of inertia, and J is St. Venant's torsional inertia.

When C ≤ 5 then:

$$D = 11.5 - N_L + 1.4N_L(1 - 0.2C)^2$$

Equation 2-6

Where N_L is the number of design lanes as specified in AASHTO Article 3.6.1.1.1.

And when C ≥ 5:

$$D = 11.5 - N_L$$

Equation 2-7

Article 3.6.1.1.1 states the number of design lanes is found by the following equation:

$$N_L = integer\ of\ ratio\ \frac{w}{12}$$

Equation 2-8

Where *w* is the clear roadway width between the barrier rails.

AASHTO LRFD does not provide a similar equation to calculate the DFM in exterior girders. Instead, the lever rule is applied. Section 4.6.2.2.1 in AASHTO LRFD

explains the lever rule. The lever rule works by placing a hinge at the first interior girder. Moments are summed about the first interior girder and the reaction at the exterior girder is determined. The reaction at the exterior girder is divided by the total load imposed by the truck. This ratio is the DFM for the exterior girder.

2.3.2 Experimental Calculation of Distribution Factors for Moment

The DFM calculated from AASHTO LRFD tend to be conservative and overestimate the load that each girder experiences (Barr, et al. 2001). Experimental values for DFM can also be calculated and may give a more realistic view of how each girder sees the load. During a load test, girders can be instrumented to record the strain that each girder sees. The maximum strain that a girder sees directly under the load can be used to calculate the DFM. It is essential to have the maximum response from the load test so this is best achieved by having the truck drive slowly across the bridge instead of parking it in one spot. The following equation can be used to experimentally calculate DFM (Fu, et al 1996):

$$g_i = \frac{\varepsilon_i}{\Sigma_{j=1}^{n} \varepsilon_j}$$

Equation 2-9

Where g_i is the distribution factor the i^{th} girder, ε_i is the maximum strain in the i^{th} girder, n is the total number of girders in the bridge, and ε_j is the strain response in each of the other girders at the same point in time when the maximum strain was recorded in the ith girder. This assumes that all girders have the same stiffness. Some research has been done to determine an alternate equation that includes the stiffness provided by the barrier rails. This equation is as follows (Barnes, et al 2003):

$$g_i = \frac{w_i R_i}{\Sigma_{j=1}^{n} w_j R_j}$$

Equation 2-10

Where g_i is the distribution factor for the i^{th} girder, R_i is the maximum response in the i^{th} girder, n is the total number of girders in the bridge, R_j is the response of each of the other girders at the time R_i was recorded, and w_i and w_j are the respective section moduli of the ith and jth girders. The alternate equation providing for the additional stiffness is often neglected because it does not necessarily result in a significant difference.

2.3.3 Examples of Experimentally Calculated Distribution Factors for Moment

Figure 2-8 is a graphical representation of the transverse load distribution in a bridge from a project done by Collins (2010). The strain is highest in the girders directly under the wheel loads and decreases in the girders further away from the load. Figure 2-8 includes the results from two sets of data. The service strain is the maximum response seen by each girder and the distribution strain is the response in each girder at the time when the peak response is experienced by the maximally loaded girder.

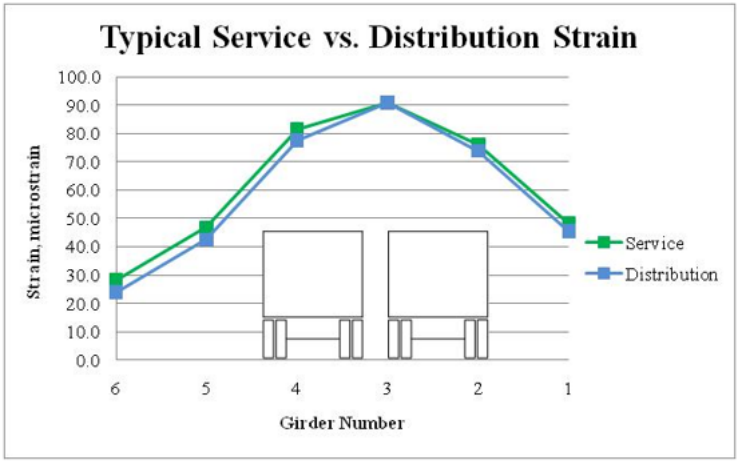

Figure 2-8: Distribution Factors for Moment (Collins 2010)

A study at Iowa State looked at the distribution factors for four different bridges, the reasons for the differences, and the percent difference between the experimentally and analytically calculated DFMs. Table 2-3 through 2-6 lists the distribution factors for reinforced concrete channel bridges one through four, respectively. The values listed are the largest distribution factors for each load position used in the test.

Table 2-3: Maximum DFM for Bridge 1 (Klaiber, et al 2001)

Longitudinal Load Position	Transverse Load Position			
	1-LP24.x	1-LP|56|.x	1-LP79.x	Two Lane
1-LPxx.A	0.45	0.41	0.46	0.53
1-LPxx.B	0.46	0.43	0.49	0.53
1-LPxx.C	0.47	0.43	0.47	0.54

Table 2-4: Maximum DFM for Bridge 2 (Klaiber, et al 2001)

Load Position			
2-LP24.B	2-LP|45|.B	2-LP57.B	Two Lane
0.63	0.51	0.68	0.97

Table 2-5: Maximum DFM for Bridge 3 (Klaiber, et al 2001)

Load Position			
3-LP24.B	3-LP46.B	3-LP68.B	Two Lane
0.39	0.40	0.42	0.56

Table 2-6: Maximum DFM for Bridge 4 (Klaiber, et al 2001)

Load Position			
4-LP24.B	4-LP46.B	4-LP68.B	Two Lane
0.59	0.61	0.59	0.63

Bridges 1 and 3 had built in shear connections between the girders that helped distribute the load more evenly. This can be seen in Tables 2-3 and 2-5, these tables have the lowest DFMs. The experimental DFMs for bridges 1 and 3 were 16% and 28% lower than the theoretical values. Bridges 2 and 4 though had no formal shear connections. Instead Bridge 2 only had bolts intended to hold the panels together and Bridge 4 had dirt and gravel in its shear key instead of grout. These insufficient shear keys resulted in the

girders directly below the trucks seeing a larger share of the load. The experimental DFM for Bridge 2 was 18% larger than the theoretical value and the experimental DFM for Bridge 4 was roughly equivalent to the theoretical value (Klaiber, et al 2001).

2.4 Nondestructive Load Testing

The definition of nondestructive load test is given in a NCHRP Project report as follows (NCHRP, 1998):

"Nondestructive load testing is the observation and measurement of the response of a bridge subjected to controlled and predetermined loadings without causing change in the elastic response of the structure. The principle of load testing is simply the comparison of the field response of the bridge under the test loads with its theoretical performance as predicted by analysis."

AASHTO and other agencies provide guidelines for the design and analysis of bridges but approximating the capacity of an in-service bridge isn't as straight forward. As time passes it is hard to determine material properties, the presence of any composite action, and the influence of damage on bridge behavior. The changing load regulations for new trucks and this difficulty in understanding the actual properties of bridges makes it hard to know the suitable safety level for bridges (Casas and Gomez 2013). Testing through the years though has showed that bridges resist load in ways not considered in design, and they often have a larger strength capacity than expected (ARCHES-D16 2009). A clearer picture of bridge properties can be seen with the help of nondestructive load testing. The best available model for predicting a bridge's behavior is the bridge itself (Chajes, et al 2000).

2.4.1 Types of Nondestructive Loading

The MBE recognizes two kinds of nondestructive load testing, diagnostic and proof testing. Diagnostic testing is performed to determine certain response characteristics of bridges such as load distribution, verify and adjust predictions from an analytical model, and determine the influence of damage. Unknown reserves of capacity and previously ignored composite action can also be identified with diagnostic testing. Diagnostic tests serve to adjust the results from analytical models by imposing the bridge to loads outside of normal traffic but similar to service levels (ARCHES-D16 2009). Proof testing is used to determine the maximum safe load capacity of a bridge while staying in the linear-elastic range. Diagnostic testing can be further divided into two categories, dynamic and static.

Some of the main benefits of diagnostic load testing according to the MBE are as follows:

1. Analytical load rating can be verified. Many AASHTO equations are conservative in nature so the capacity of a bridge may be over or underestimated.
2. Load distribution for specific bridges can be found, these values are used in the load rating equations.
3. The influence of damaged and deteriorated members can be understood.

The design IM is often conservative so load testing can be a more cost effective and reliable method for finding the dynamic load allowance for a certain bridge.

2.4.2 Candidates for Diagnostic Testing

Diagnostic load testing can be costly from both a monetary and time perspective. Due to the cost, not every bridge can be load tested to verify and adjust its approximated strength. Therefore, bridges that are hard to idealize for an analytical model are best verified with a load test. Bridges that don't have reliable documentation or that possibly fail assessment by hand calculations are ideal candidates for load testing (ARCHES-D16 2009).

2.4.3 Implementation of Diagnostic Test

To perform a diagnostic test it is first necessary to have a basic understanding of the bridge being tested. During a diagnostic test specific bridge responses need to be monitored, and an analytical model for comparison needs to be created. Typical bridge responses monitored during a diagnostic test are midspan deflection, deck and girder strain, temperature records, and bearing rotation. Deflection and strain are most often measured at the expected area of maximum response since characteristics such as dynamic load allowance and distribution factors are derived from maximum responses (Collins 2010).

Strain responses are typically measured through the use of electrical strain gages. Strain gages can be embedded within concrete or in the case of the Five Forks Bridge were attached to the surface of the girders. A bond between the gages and the surface of the girders can be attached with epoxy or c-clamps (Nowak, et al 1999).

There are many methods present to measure girder deflection. Displacement transducers can record both absolute and relative girder displacement. Other instruments,

such as string pots, can measure girder deflection from a specified location set at absolute zero. Linear variable differential transformers (LVDTs) are commonly used for relative displacement between adjoining girders in the horizontal and vertical directions.

The loading of a bridge for a live load test usually takes the form of a vehicle being driven across or parked on the bridge. Static loading scenarios can allow a vehicle to travel between 3 to 5 mph across a bridge while dynamic loading sees the vehicle drive close to highway speeds. The position of the vehicle on the bridge may depend on the responses being measured, but typically a number of different truck configurations are used to understand a clear picture of the bridge behavior. Multiple researchers have discovered that trucks weighing between 50 and 75 kips are often sufficient for live load testing even though they are typically lower in weight that the 72 kips of the AASHTO HL-93 design truck (Yang and Meyers 2003).

2.4.4 Iowa State Nondestructive Test

Iowa State conducted nondestructive load tests on four channel girder bridges and the instrumentation included electrical resistance strain gauges to measure concrete and steel strain, and potentiometers to measure deflection (Klaiber, et al 2001). The strain gauges and potentiometers were attached at the midspan of the girders to measure the maximum bottom flange strain and vertical girder deflection. The vertical deflection of each stem on each channel was measured. A central data acquisition system (DAS) recorded all of the data at a frequency of 20 Hz.

Iowa DOT provided tandem axle dump trucks for the loading of three bridges and included a tractor trailer for the fourth bridge. The trucks were loaded up to the Iowa

legal load, 49.32 kips for the dump trucks and 80.18 kips for the tractor trailer. Multiple truck configurations were used during the testing to provide a clear picture of the bridges' behaviors. These configurations included one scenario where the truck wheel line was directly over the center of a girder and another scenario where the wheel line was over the joint between adjacent girders. All tests were conducted at low speeds (1-3 mph) for quasi-static loading. Tape switches attached to the bridge roadway at constant intervals tracked the position of the truck as a function of time. The results from the tests were taken as functions of time, but the tape switches allowed the data to be converted to a function of vehicle position.

The transverse load distribution was found for each bridge. The deflection of each girder's stems was averaged to give a single deflection value for each girder. The equations presented in Section 2.3.3 of this report were also used by Iowa State to determine the DFM for each bridge. Iowa State also plotted the deflection, steel strain, and concrete strain of each girder for all of the loading scenarios. Iowa State used the results from these nondestructive load tests to calculate the DFM and load ratings presented in Sections 2.3.3 and 2.5.5 respectively.

2.5 Bridge Load Rating

The goal of load rating is to confirm the maximum load that a bridge can support. (Casas and Gomez 2013). In traditional load rating a bridge is assigned a rating factor (RF) that represents the ratio of the bridge's total reserve capacity to the maximum live load effect. If a bridge has a rating factor greater than one then the bridge can handle the live load, but if the rating factor is less than one then the bridge lacks the capacity

required (Phelps 2010). This rating applies to all components of a bridge, the lowest rated component is the weak link in the system and controls the capacity (Rogers et al, 2005). Load rating for the Five Forks Bridge is only concerned with the rating factor of the superstructure.

2.5.1 Types of Load Rating

There are two types of load rating, inventory and operational. Inventory rating is the capacity rating for the vehicle type used in the rating that will result in a load level which can safely utilize an existing structure for an indefinite period of time. Inventory load level approximates the design load level under normal traffic conditions. Operational rating will result in the absolute maximum permissible load level to which the structure may be subjected for the vehicle type used in the rating. This rating determines the capacity of the bridge for occasional permitting purposes.

The posting rating is the capacity rating for the vehicle type used in the rating that will result in a load level which may safely utilize an existing structure on a routine basis for a limited period of time. The posting rating for a bridge is based on inventory level plus a fraction of the difference between inventory and operating (Gunasekaran 2010).

2.5.2 AASHTO Load Rating

The AASHTO *Manual for Bridge Evaluation* (MBE) provides guidelines for conducting a load rating. Load rating is based on existing structural conditions, material properties, loads, traffic conditions. The MBE is consistent in philosophy with the AASHTO LRFD. There is an inherent difference in the philosophy between design and rating though. Rating has a larger scope than design; the cost of being conservative in

design is much less than the cost of being conservative in rating. A conservative design decision may call for a larger cross-section but a conservative decision for load rating may result in a posting or bridge replacement. The MBE lays out the following three procedures that make up the whole load rating process.

1. Design load rating – Measure of bridge performance compared to current LRFD standards. Rating Factor (RF) > 1 then satisfactory for all legal loads.
2. Legal load rating – Provides a single safe load capacity for the given truck configuration that applies to AASHTO and state legal loads.
3. Permit load rating – Checks the safety and serviceability of bridges in review of permit applications for overweight trucks (single trip, multi trip, or annual basis). Only applies if legal load rating passed.

Section 6A.4 in the MBE describes how to find the rating factor using the following equations:

$$RF = \frac{C - (\gamma_{DC})(DC) - (\gamma_{DW})(DW) \pm (\gamma_P)(P)}{(\gamma_{LL})(LL + IM)}$$

Equation 2-11

RF is the rating factor and there are two separate equations for C, one for strength limit states and one for service limit states. For the strength limit states:

$$C = \varphi_c \varphi_s \varphi R_n$$

Equation 2-12

Where:

$$\varphi_c \varphi_s \geq 0.85$$

Equation 2-13

For the service limit state:

$$C = f_R$$

Equation 2-14

The C in the equations above is the capacity, f_R is the allowable stress specified in the LRFD code, φ_c is the condition factor, φ_s is the system factor, φ is the LRFD resistance factor, R_n is the nominal member resistance, DC is the dead load effect from structural components and attachments, DW is the dead load from wearing surfaces and utilities, P is the permanent loads other than dead loads, LL is the live load effect, IM is the dynamic load allowance, γ_{DC} is the LRFD factor for structural components and attachments, γ_{DW} is the LRFD factor for wearing surfaces and utilities, γ_P is the LRFD factor for permanents loads other than dead loads, γ_{LL} is the evaluation live load factor.

2.5.3 Load Rating through the MBE

The MBE allows load rating to be adjusted by the use of nondestructive load testing. Load rating is based on conservative assumptions regarding bridge behavior (Gunasekaran 2010). This is why load rating in conjunction with nondestructive load testing is useful. The experimentally determined three dimensional properties of a bridge can be used to adjust the analytical load rating so that the behavior of a specific bridge is more accurately predicted (Iplikcioglu 2012).

2.5.4 Experimental Adjustments for Load Rating

Since AASHTO LRFD provides conservative approximations for the DFM then the MBE also provides conservative approximations for the load rating since DFM determines the load used in the load rating equations. When a nondestructive load test

has been conducted, the experimentally determined DFMs can be used to adjust the analytical load rating factors from the MBE. The modified load rating factor follows the same system as analytically calculated load rating. A value greater than one means the bridge has excess capacity and a value less than one means the bridge lacks the required capacity. Four factors that influence load rating and can be determined from load testing are lateral load distribution, support fixity, composite action, and the effect of secondary members (Phelps 2010.) Section 8.8 from the MBE provides the following equations to modify calculated load rating using the results from a diagnostic load test:

$$RF_T = RF_C K$$

Equation 2-15

Where RF_T is the load-rating factor for the live-load capacity based on the load test result; RF_C is the rating factor based on calculations prior to implementation of diagnostic tests; and K is the adjustment factor resulting from the comparison between the analytical model and test results

$$K = 1 + K_a K_b$$

Equation 2-16

Where: K_a accounts for the benefit derived from the load test and any consideration from the section factor resisting the load test and K_b accounts for the understating of the load test results compared to the theoretical results. If K is greater than one then the response of the bridge is more favorable than predicted by theory and the bridge capacity may be enhanced. But if K is less than one then actual response from the bridge is more severe than predicted and load capacity may have to be reduced.

$$K_a = \frac{\varepsilon_c}{\varepsilon_T} - 1$$

Equation 2-17

Where ε_T is the maximum member strain measured during load test and ε_c is the corresponding calculated strain due to the test vehicle at the same truck position that caused ε_T.

$$\varepsilon_c = \frac{L_T}{(SF)E}$$

Equation 2-18

Where L_T is the calculated theoretical load effect in the member corresponding to the ε_T strain; SF is the member appropriate section factor; and E is the member modulus of elasticity. The factor of K_b should be between 0 and 1 to show the level of benefit at the rating level. The factor is obtained from the level of relationship between T and W. T is the unfactored test vehicle and W is the unfactored gross rating load effect. If equal to 0, the test result cannot be validated. After calculation of T and W the values can be found using the table 8.8.2.3.1-1 in the MBE.

2.5.5 Examples of Load Rating Calculations

The study done at Iowa State referenced in section 2.3.3 also conducted load ratings for each of the bridges. Tables 2-7 to 2-10 show the theoretical and revised load ratings for the inventory and operating levels.

Table 2-7: Bridge 1 Load Ratings (Klaiber, et al 2001)

Level	Theoretical Rating Factor		Revised Rating Factor	
	HS20	Type 3	HS20	Type 3
One Lane				
Inventory	1.06	1.33	1.52	1.90
Operating	1.78	2.22	2.54	3.17
Two Lane				
Inventory	1.02	1.28	1.38	1.72
Operating	1.71	2.14	2.30	2.88

Table 2-8: Bridge 2 Load Ratings (Klaiber, et al 2001)

Level	Theoretical Rating Factor		Revised Rating Factor	
	HS20	Type 3	HS20	Type 3
One Lane				
Inventory	1.15	1.43	0.95	1.19
Operating	1.92	2.39	1.59	1.98
Two Lane				
Inventory	1.13	1.40	0.67	0.83
Operating	1.88	2.34	1.12	1.39

Table 2-9: Bridge 3 Load Ratings (Klaiber, et al 2001)

Level	Theoretical Rating Factor		Revised Rating Factor	
	HS20	Type 3	HS20	Type 3
One Lane				
Inventory	0.83	1.04	1.14	1.43
Operating	1.38	1.73	1.91	2.39
Two Lane				
Inventory	0.81	1.01	0.86	1.07
Operating	1.35	1.68	1.43	1.79

Table 2-10: Bridge 4 Load Ratings (Klaiber, et al 2001)

Level	Theoretical Rating Factor		Revised Rating Factor	
	HS20	Type 3	HS20	Type 3
One Lane				
Inventory	0.90	1.02	0.87	0.98
Operating	1.50	1.71	1.45	1.64
Two Lane				
Inventory	0.86	0.98	0.84	0.95
Operating	1.44	1.64	1.40	1.59

As discussed in section 2.3.3, Bridges 1 and 3 have lower experimental than theoretical DFMs, Bridge 2 has a higher experimental than theoretical DFM, and Bridge 4 has roughly equivalent experimental and theoretical DFMs. The load ratings follow identical trends for each bridge. Bridges 1 and 3 have lower experimental DFMs so each girder

sees a smaller portion of the load than expected. They see less of the load therefore they have a greater overall capacity so the revised rating factor is greater than the theoretical rating factor. Bridge 2 had a higher experimental DFM so it sees more of the load than expected. Since it sees more load than it was designed for, the revised load rating factor is less than the theoretical load rating factor. Finally Bridge 4 has equivalent DFMs and also has equivalent load rating factors. This Iowa State study demonstrated the impact that DFMs can have on the adjusted load rating factor. Figure 2-9 is a graphical representation of the relationship between the DFMs and adjusted load rating factor. The larger the DFM the smaller the load rating factor.

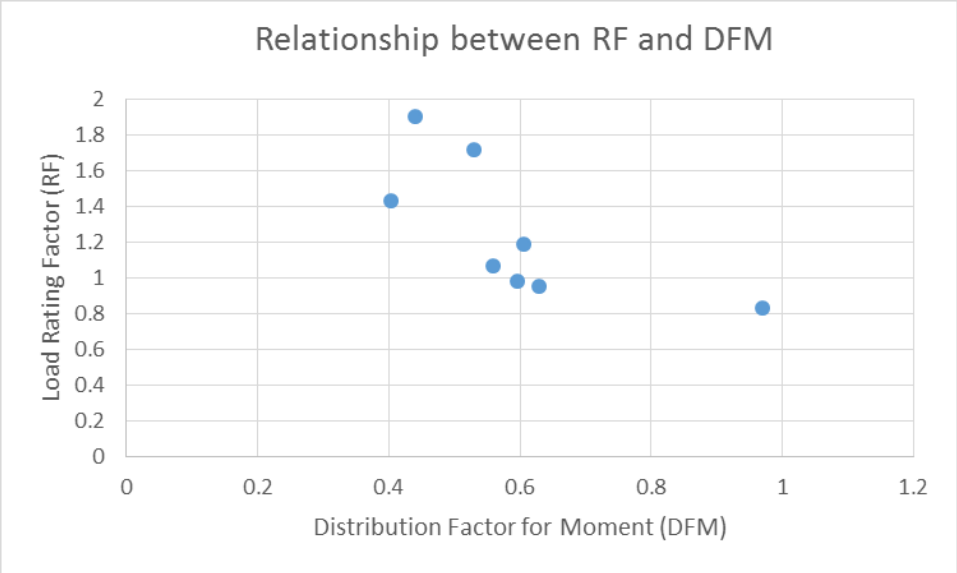

Figure 2-9: Relationship between RF and DFM

2.6 Channel Girder Testing

Iowa State and a few other institutions conducted similar lab testing on concrete channel girders. The girders were tested to failure so the results could be compared to the findings from nondestructive load testing.

A standard test consisted of a 4 point bending arrangement with hydraulic actuators and a reaction frame. The actuators were centered about the middle of the girder and connected in parallel to ensure they applied the same force. The actuators created a section of constant moment at the middle of the girder (Klaiber, et al 2001). Instrumentation was similar to the field tests mentioned in Section 2.4.4 (Wipf 2006).

At Iowa State Klaiber and others tested their girders to failure. Failure was classified as the collapse of the beam or the exceedance of maximum deflection. While the girder was in the elastic region strain, deflection, and load were recorded at specific load intervals. Once the reinforcement yielded the data was then recorded at every 0.1 inch of center deflection until the girder failed. Throughout the test the propagation of flexure and shear cracks was recorded.

2.6.1 Iowa State Channel Test Results

Klaiber used four different girders in the lab test and compared the moment-deflection curve and the ultimate strength of all 4 girders. Cedars 1-3 (the girder designations) were identical interior girders and Cedar 8 (girder designation) was an exterior girder with a concrete curb. Cedars 1-3 each had varying degrees of damage. Figure 2-10 shows a typical cross section and instrumentation setup for the Cedar girders tested. Figure 2-11 shows the moment-deflection curve for each of the 4 girders used.

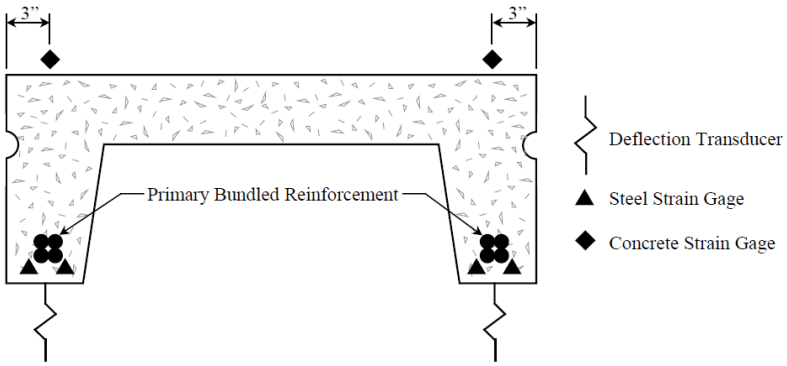

Figure 2-10: Cedar Girder Cross Section and Instrumentation (Klaiber, et al 2001)

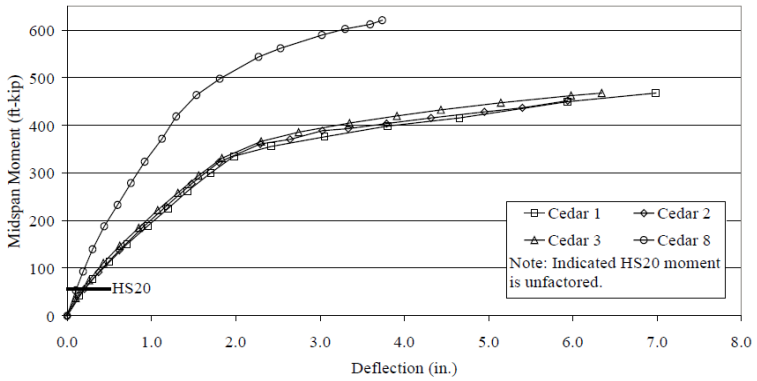

Figure 2-11: Moment-Deflection Curve of 4 Girders (Klaiber, et al 2001)

The ultimate strength of each girder was taken as the maximum midspan moment from Figure 2-11. These ultimate moments were substituted in a theoretical load/deflection equation and back calculated to determine the flexural rigidity (EI) and stiffness (4EI/L where L=span length) for each of the 4 girders. These experimental ultimate strengths were compared to the theoretical and design ultimate strengths. The rigidity and stiffness for each girder was also compared. Table 2-11 presents the ultimate strengths and the rigidity and stiffness for each girder.

Table 2-11: Ultimate Strengths and Stiffnesses (Klaiber, et al 2001)

Panel	Ultimate Strength (ft-kip)			Flexural Rigidity (kip-ft)	Stiffness (kip-ft)
	Experimental	Design	Theoretical		
Cedar 1	466	210	452	122,200	20,100
Cedar 2	488	210	467	128,800	21,200
Cedar 3	469	210	466	129,600	21,300
Cedar 8	621	351	541	233,300	38,400

The results show that all four panels vastly outperformed the design ultimate strength. Cedars 1-3 had similar experimental and theoretical ultimate strengths while Cedar 8 had a larger experimental than theoretical ultimate strength. Even though Cedars 1-3 had varying degrees of damage, they all nearly had the same deflection behavior and ultimate strength. This may indicate that the damage had little effect on the strength of the panels. Cedar 8 was a different girder with a curb laying on it so the increased stiffness and strength as well as the decrease in deflection may be attributed to the concrete curb.

2.7 Summary

Information from the review of each of the above topics was combined for the purposes of this project. The knowledge about channel bridges and the similar issues other state DOT's experience helped the author to understand the scope of the problem and how research here may be applied elsewhere. Dynamic load allowance and the distribution factors for moment are essential bridge properties that are conservatively estimated by AASHTO. Determining these values from the nondestructive load test allowed a more accurate assessment of the Five Forks Bridge's current capacity. The results provided serve as a guide for research conducted on the Five Forks Bridge. The result of load rating will determine the future of the Five Forks Bridge and if it needs

posting. The application of the theoretical equations paired with the results from the nondestructive load test resulted in an accurate picture of the bridge's capacity. Careful review of the process other groups used for nondestructive field testing and lab testing aided in the set up and execution of tests for this project. The lab test of a surplus girder identical to those used in the Five Forks Bridge provided a clear view of the girder's maximum capacity, and where the loads seen by the bridge fall in comparison. The goal of the research on the Five Forks Bridge is to take the information gained from author's better understanding of the nondestructive loading test, the load rating process, and the channel girder test, and combine them to have one overall clear picture of girder and bridge behavior at the Five Forks Bridge

Chapter 3: Nondestructive Test

The field test of the Five Forks Bridge took place over the course of two days in March of 2016. The first day of the test, on March 28, consisted of instrumenting the bridge and preparing equipment for the next day. On the second day of the test, March 29, the acquisition system was set up, the tests were conducted, and the instrumentation was removed.

The bridge responses of interest during this test were the bottom flange concrete surface strain, the absolute vertical deflection of the first interior and exterior girders, and the relative horizontal and vertical deflections of the first interior and exterior girders. These bridge responses provided insight into how the damaged and healthy girders reacted to load and how the bridge distributed load transversely. The damaged girder was less stiff than the healthy girder so the strain transducers and LVDTs captured any overall difference this may have had in the behavior of each girder. The transverse load distribution across the bridge is a function of the condition of the transverse post-tension, the longitudinal girder-to-girder joints, and the girders themselves. The transverse post-tensioning served to tie the girders together and create a solid contact surface between the girders at these joints. The LVDTs captured this relative motion between girders and revealed the quality of the joint condition and post-tensioning.

Strain transducers were used to record the surface strain, string pots were used to record absolute vertical girder deflection, and LVDTs were used to record the relative displacements All of the instruments were located at mid-span of the East and West

Spans. Figures 3-1 and 3-2 show the two instrumentation layouts that were used for the test.

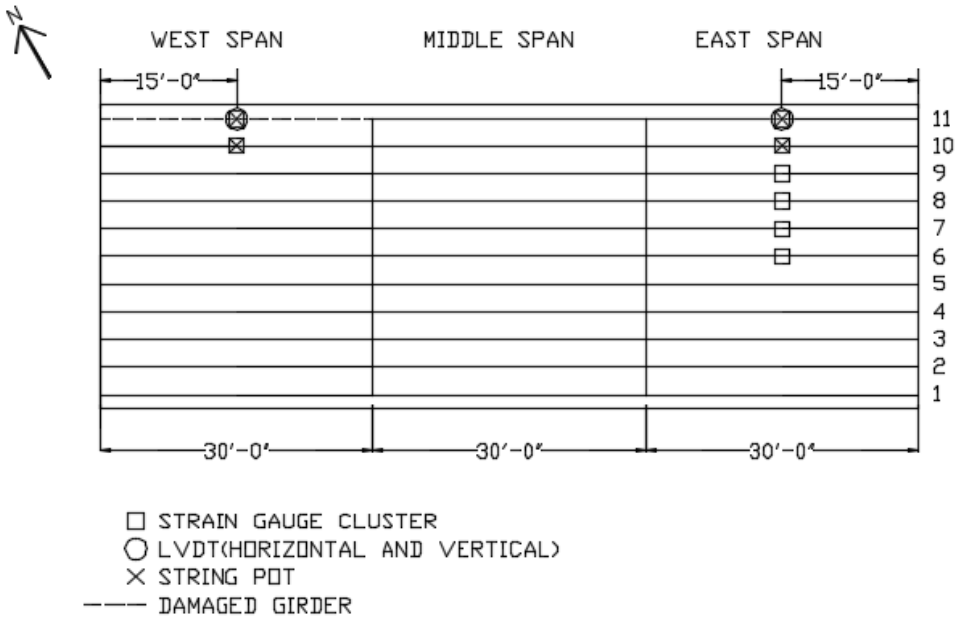

Figure 3-1: Plan View of Instrumentation Layout One

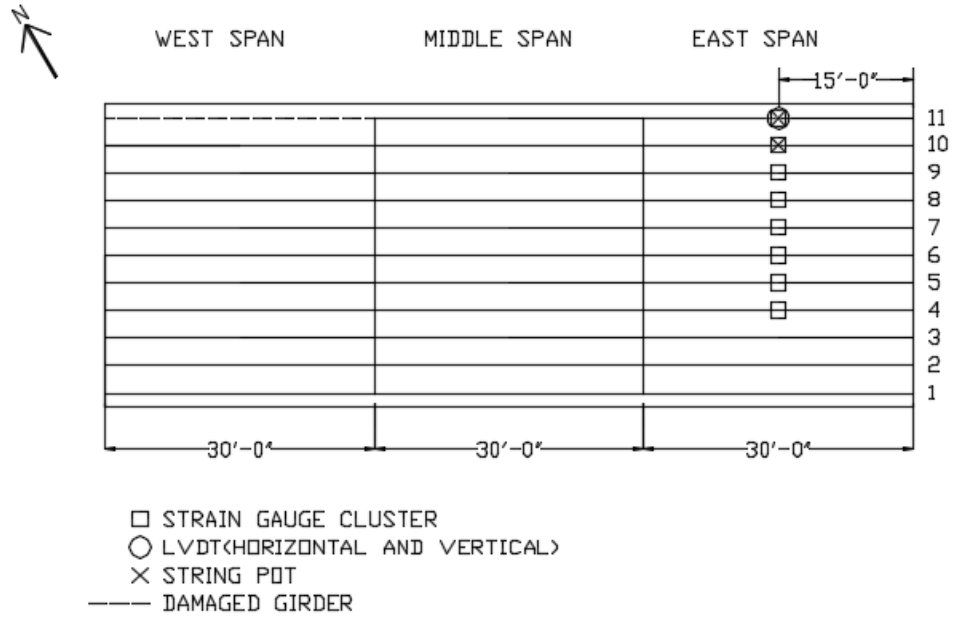

Figure 3-2: Plan View of Instrumentation Layout Two

3.1 Data Needed

Before the field test was conducted the parameters for the test were established. Many different bridge responses can be recorded and collected during live load tests but only certain parameters were needed for the Five Forks Bridge. Some of the goals of this project included assessing the damaged girder, determining the transverse load distribution of the bridge, and establishing a rating factor for the Five Forks Bridge. The essential bridge responses needed to accomplish these goals were girder surface strain and vertical girder deflection measured at mid-span. Instrument selection and instrumentation of the bridge were constrained to these two parameters.

3.2 Bridge Instrumentation

Knowing that deflection and strain had to be recorded led to the selection of instruments. Strain transducers were used to measure concrete surface strain, linear variable differential transformer (LVDTs) were chosen to measure relative girder displacement, and string pots were used to measure absolute vertical girder deflection.

3.2.1 Strain Transducers

Concrete surface strain was measured using sixteen strain transducers manufactured by Bridge Diagnostics Incorporated (BDI). BDI provided calibration for each strain transducer. Figure 3-3 below shows a strain transducer attached to the bottom of a Five Forks Bridge girder.

Figure 3-3: BDI Strain Transducer

The circuit of the strain transducer consists of a full wheatstone bridge with four active foil transducers. The circuit is complete within the transducer so the length of the cable has no effect on the transducer's signal. Strain transducers of this type can be attached to both steel and concrete for recording purposes but they were only used for concrete in this project.

The process of attaching the strain transducers to the concrete surface of the girders was a simple task. BDI provides a set of small metal tabs with each transducer which act as feet to secure the transducers. The nuts seen on each end of the transducers in Figure 3-3 attach these tabs to the transducer. A two-part epoxy was used to glue these feet onto the girders. Figures 3-4 and 3-5 below show the adhesive and accelerant that make up this epoxy.

Figure 3-4: Loctite Adhesive

Figure 3-5: Loctite Accelerant

To ensure a good connection, the surface of the girder was prepared by smoothing any noticeable roughness. The future location of the transducer was coated in a thin layer of adhesive and then sprayed with accelerant. The feet of the transducer were also coated in adhesive and then sprayed with accelerant. The epoxied feet were pressed against the epoxied surface for a few seconds until a secure bond was formed. These strain transducers were attached the night before the test so the intelliducers used to connect them to the channels were wrapped in plastic bags and duct taped closed so no moisture could affect them. These cables were held up with cable ties attached to the underside of the girders.

Longitudinal bending strain of the bottom flanges at the mid-span of the bridge were measured using the strain transducers. These strains were measured at mid-span,

the location of maximum moment and maximum bending strain of the bottom flange. Figure 3-6 is a representative sketch of transducer location at the mid-span of interior and exterior girders. The shear key shown in Figure 3-6 is the assumed geometry based off of drawings provided by SCDOT in Figure 1-6.

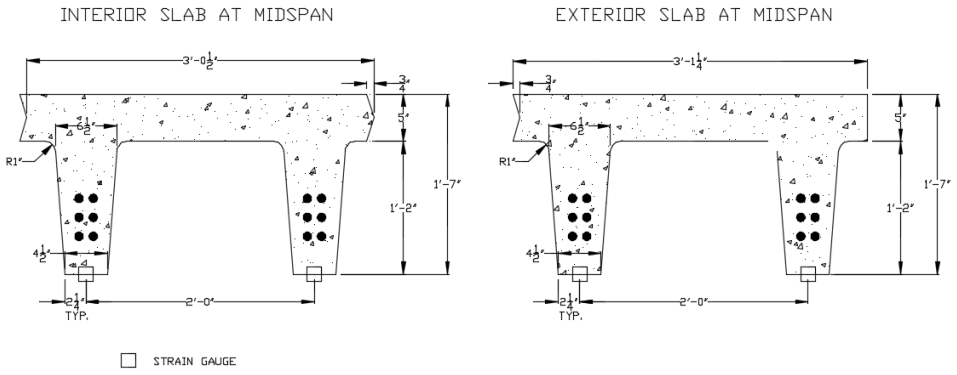

Figure 3-6: Strain Transducer Location at Mid-span

3.2.2 Linear Variable Differential Transformers

LVDTs measure displacement by recording the differential movement of the armature (plunger) relative to the exterior body of the transformer. BDI provided the four LVDTs used for this project and also included the calibrations for each LVDT.

A custom made case was created to hold the LVDTs and attach them to the girders. A one inch PVC pipe was cut to match the length of the transducer's exterior case, approximately seven inches long. Four equal, two inch deep, cuts were made at the quarter points of the PVC cross section to allow the pipe's opening to be closed by tightening a pipe clamp. A strip of Velcro was wrapped around the end of the exterior casing approximately one inch from the end. The Velcro provided a rough surface for the PVC to grip when tightened. This prevented the LVDT from moving within the PVC. A 1½" x 1½" piece of steel angle was cut to match the length of the PVC. Gorilla glue was

applied to the interior of each angle leg and also to the exterior of the PVC. The PVC was then clamped to the reentrant corner of the angle to ensure a good bond. The exterior of the steel angle was coated with the same adhesive and accelerant from Figures 3-2 and 3-3 to attach it to the girder stems.

The relative horizontal and vertical displacements between the exterior and first interior girders were of interest in this project because of the comparison between the healthy and damaged girders and the assessment of the transverse load distribution. A comparison of the relative deflections for each of these scenarios provided insight into how the damaged and healthy girders, longitudinal joints, and transverse post-tensioning responded to load. The longitudinal cracking in the asphalt wearing surface over the girder joints is an example of reflective cracking. The movement between girders at their joints reflected up into the wearing surface causing cracks to form. The LVDTs captured that motion at the joint. The relative horizontal displacement revealed if there was any opening at the longitudinal girder joint, and the relative vertical displacement revealed if there was any slippage at the joint. Both relative displacements also determined to what extent the transverse post-tensioning was facilitating transverse load distribution. One horizontal and one vertical LVDT were used between the first interior and exterior girders on the East and West Spans. The measurement of the horizontal displacement required the LVDT and its case to be glued to the bottom of the exterior girder's innermost stem in a direction orthogonal to the flow of traffic. At the opposite end of the joint between the girders on the first interior girder's outermost stem a piece of 2" x 4" wood was glued with the same adhesive and accelerant. This wood piece extended out

into the gap between the exterior and interior girders and provided a point of contact for the LVDT armature. Measuring the relative vertical displacement used a similar set up as the horizontal configuration. The stems of the girders were tapered so first wooden blocks were cut to negate the angle of the stems. These wooden blocks provided a vertical surface for the LVDTs case to be glued. The LVDT was glued to a wooden block on the same stem as the horizontal LVDT using the same adhesive and accelerant. Higher up on the opposite stem a 2" x 2" x 1/8" steel angle was cut to two inches and attached to the wooden block. This angle served the same purpose as the 2" x 4" and provided a point of contact for the armature. Figures 3-7 and 3-8 show the horizontal and vertical setups of the LVDTs.

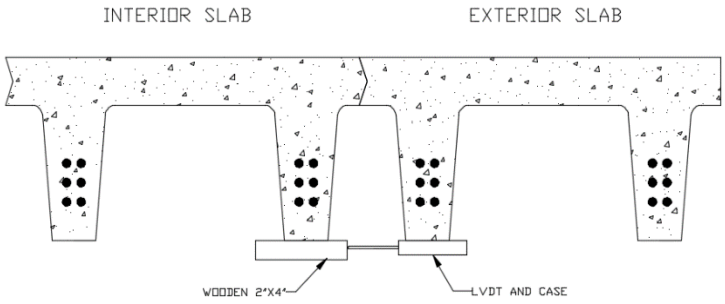

Figure 3-7: Horizontal LVDT Setup

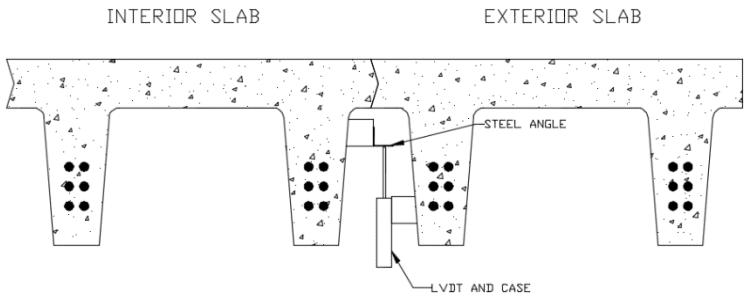

Figure 3-8: Vertical LVDT Setup

Figure 3-9 shows how this setup was implemented at the Five Forks Bridge. A horizontal and vertical LVDT can be seen spanning the distance between the two girders. A strain transducer at the bottom of each girder stem can also be seen.

Figure 3-9: Horizontal and Vertical LVDT Setup

3.2.3 String Pots

While the LVDTs were used to measure relative girder displacement, the string pots were used to measure the absolute vertical deflection of the exterior and first interior girders of the East and West Spans. SM2-25 string pots manufactured by Celesco were used in this project. These string pots have a linear stroke or range up to 25 inches. The

string pots had to be calibrated before the test could begin. This was done by using a set up created by a former student that had fixed distances increasing in one inch increments marked on a board. The string pot was anchored to the board, and then the string was pulled out to each known location marker and the reported deflection was written down. These values were repeated a couple times for each location. The ratio of the actual distance over the reported distance was determined and this calibration factor was input. This was done for each string pot.

The string pots used the ground beneath the bridge as the reference for the absolute deflection. The string pot's exterior consisted of a metal bracket that was attached to a piece of wood. This wood was glued to a concrete block with the same two part epoxy used to attach the instruments to the girders. This concrete block served as an anchor that kept the string pot casing locked in one location while the string itself could move with the bridge. The string could not reach from the ground to the bridge so extension wire was used to bridge the distance. The extension wire was connected to a metal hook glued to the bottom of the girder web at mid-span. The string was pulled out about halfway of its total stroke before being tautly tied to the wire. It was checked that no slack was in the wire or string. The string was pulled out so it could register positive and negative vertical deflection of the girders. Figures 3-10 and 3-11 show the entire setup of the string pots.

Figure 3-10: String Pot Anchor

Figure 3-11: Hook Attaching String Pot to Girder

3.2.4 Instrumentation Plans

Two separate instrumentation plans were used for the field test. The girders' maximum responses were of interest for the test so all instrumentation was attached at the mid-span of the East and West Spans. The Central Span was over the Eighteen Mile Creek and therefore difficult to access. The spans are also identical outside of girder damage so instrumenting the Central Span was not necessary for understanding bridge behavior.

The first instrumentation plan can be seen in Figure 3-1 at the beginning of the chapter. This layout used 16 strain transducers, 4 string pots, and 4 LVDTs. This layout was setup to assess the difference in response between the healthy and damaged exterior girders. The damaged girder is represented by the dashed line on the West Span in

Figure 3-10. To record the appropriate responses, the exterior and first interior girders (girders 11 and 10, respectively) of the East and West Span were instrumented with strain transducers, LVDTs, and string pots. The rest of the available strain transducers were attached to girders numbered nine through six. These additional strain transducers were attached to understand how the truck loads were shared between the girders so the transverse load distribution could be determined. This instrumentation would allow the responses of the healthy and damaged girders to be directly compared.

The second instrumentation layout can be seen in Figure 3-2 at the start of the chapter. This layout used 16 strain transducers, two string pots, and two LVDTs. This instrumentation plan focused on recording all of the data needed to fully determine the transverse load distribution of the healthy East Span. All available strain transducers were used in this layout to determine if there was symmetry between the girders. Ideally, all eleven girders would have been instrumented but only 16 strain transducers were available so only eight girders could be instrumented. The string pots and LVDTs on the West Span were disconnected.

3.3 Data Acquisition

A BDI data acquisition system was used to collect and record the data from the field test. STS4-4 nodes are 4-channel data acquisition devices that were connected directly to all instruments. The strain transducers and LVDTs from BDI connected to the nodes through an intelliducer provided by BDI, however, the string pots were connected manually. Figure 3-12 shows a STS4-4 receiver with manually wired string pots.

Figure 3-12: STS4-4 Receiver with Wired String Pots

Each of the six receivers was placed on top of a cement block directly beneath the four instruments it was attached to. The concrete block was used to keep dirt off of the receiver. These receivers were wirelessly connected to the central base station. The STS4 Base Station created a wireless signal that was used to collect the data from all of the STS4 receivers. Figure 3-13 shows the STS4 Base Station. This wireless connection also connected the base station to the laptop that ran the STS-Live software. The STS-Live application allowed the bridge response to be viewed in real time to ensure all data was usable. Figure 3-14 below shows a schematic of the data acquisition setup and how everything was connected.

Figure 3-13: STS4 Base Station

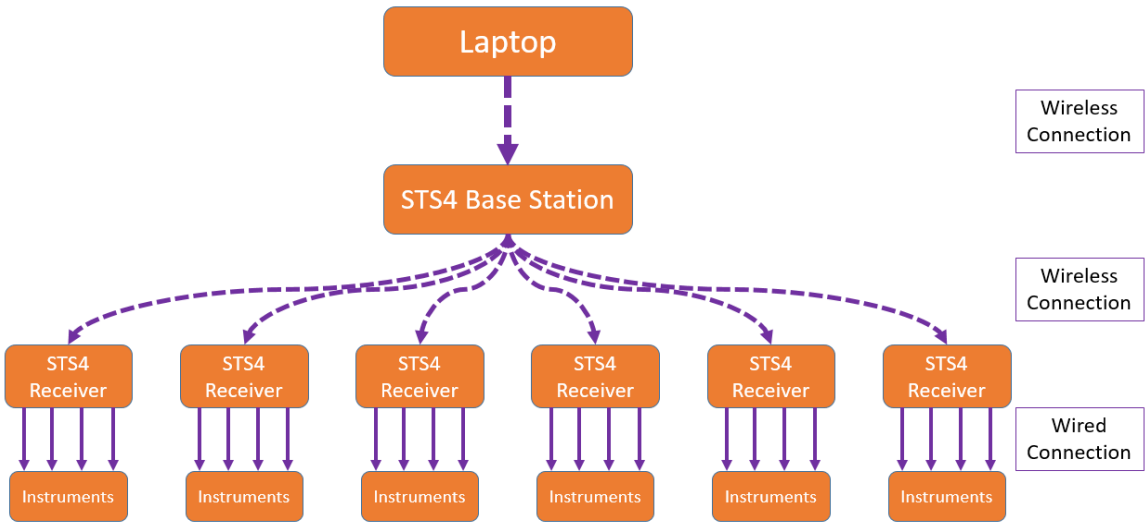

Figure 3-14: Data Acquisition Schematic

3.4 Loading Procedures

3.4.1 Truck Descriptions

SCDOT provided three three-axle dump trucks that were used for the field test. One truck was left empty. A nearby quarry was used to fill the other two trucks with gravel, one was partially filled and the other was filled completely. The trucks had the front axle and back two axles weighed separately at the quarry. The empty truck, half full truck, and full truck had total weights of 18.8 kips, 36.6 kips, and 48.7 kips respectively. Three different truck weights were used to determine if the bridge response was linear. If the deflection and strain responses each exhibited a linear relationship then the bridge was in the linear-elastic range which means the concrete had not cracked yet. This linearity ensures there is some factor of safety between the current bridge loads and the loads required to crack the girders and damage the bridge further. Figure 3-15 shows an example of this linearity in the field test. The points taken from the field test make up the linear portion of the plot while the nonlinear portion of the plot begins upon concrete cracking. The legal load limit for all South Carolina bridges is 80 kips and the maximum load this bridge saw from the field test was 48.7 kips. Based off the great difference in these values it was expected that there would be a large factor of safety between the loads from the test and the loads to force the bridge to behave nonlinearly.

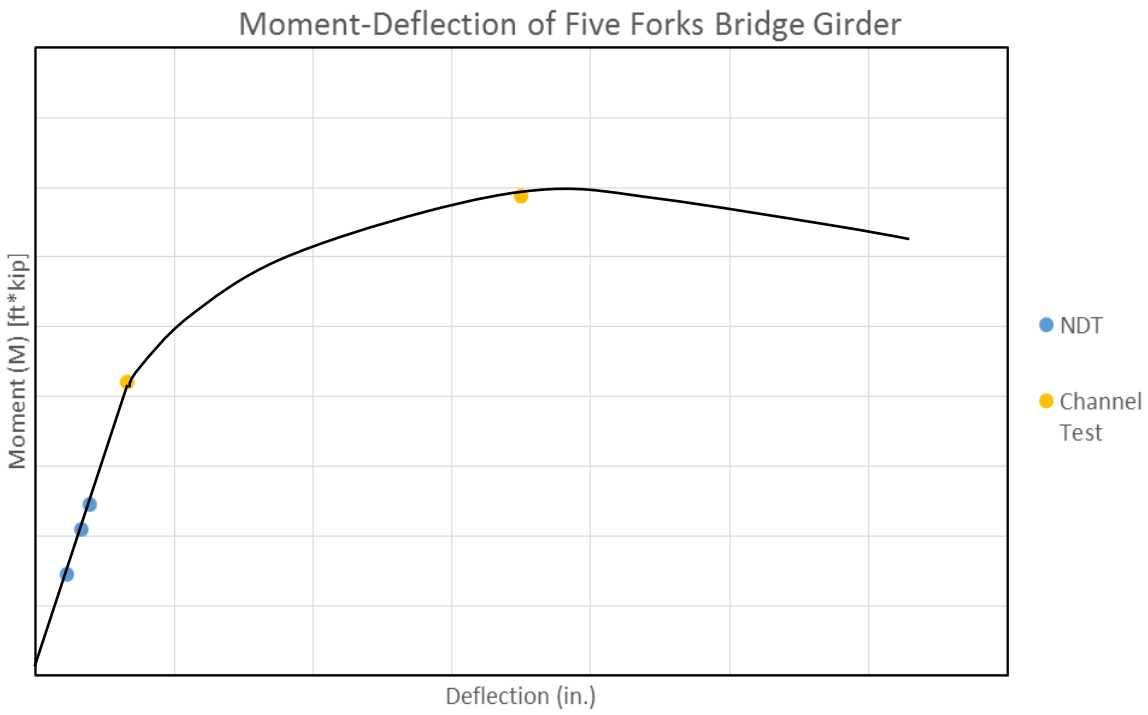

Figure 3-15: Plot Showing Linear Relationship between Field Loads

The trucks' dimensions were taken when they arrived at the bridge. Figures 3-16 through 3-21 show the truck weights and axle dimensions for each of the trucks.

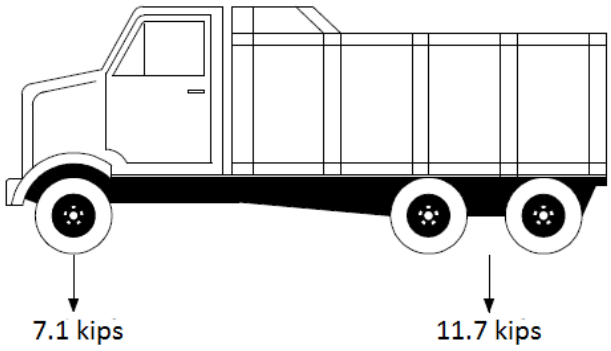

Figure 3-16: Empty Truck Weight

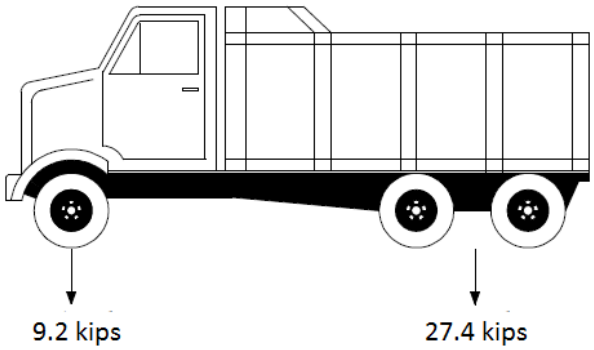

Figure 3-17: Half Full Truck Weight

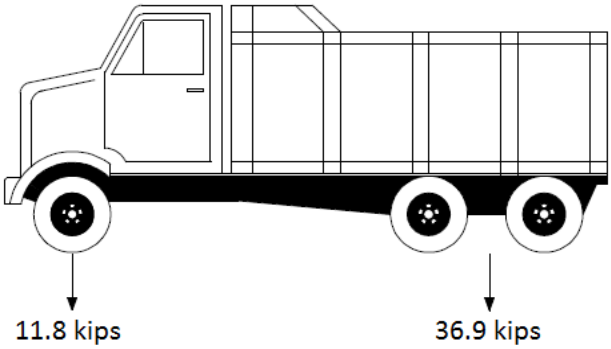

Figure 3-18: Full Truck Weight

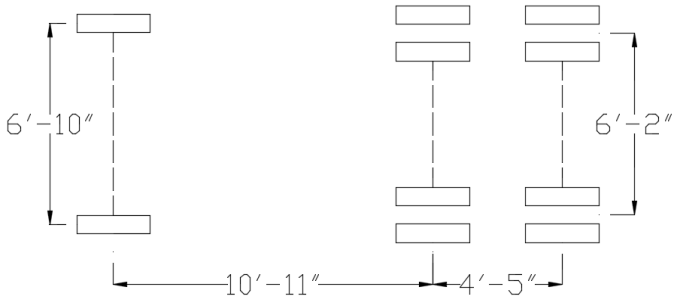

Figure 3-19: Empty Truck Dimensions

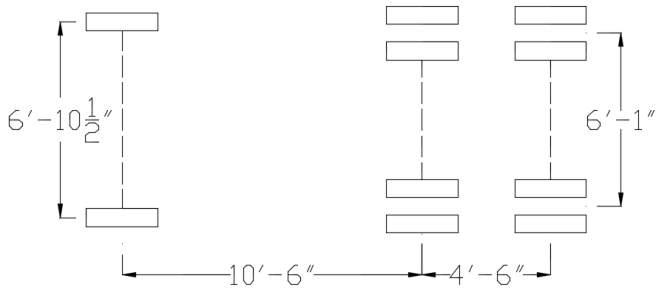

Figure 3-20: Half Full Truck Dimensions

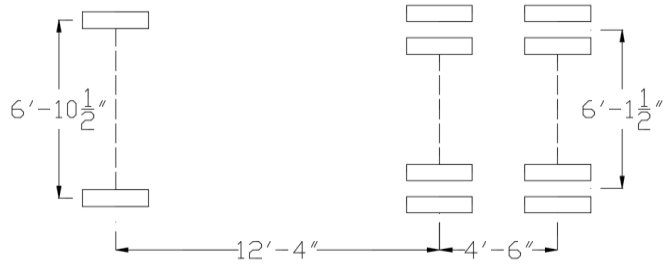

Figure 3-21: Full Truck Dimensions

3.4.2 Loading Configurations

Six different loading scenarios were used during the field test. Each scenario only used one truck at a time. In Figures 3-22 and 3-23 the dashed girder eleven represents the damaged exterior girder. Scenarios one through five were pseudo-static tests (less than 5 mph) and scenario six was a dynamic test (45 mph). During a pseudo-static test the truck crosses the bridge in a pre-determined transverse location at a speed less than 5 mph. This slow speed ensures that the truck is not "bouncing" as it crosses the bridge and that there are no dynamic effects. Scenarios one through three used instrumentation layout one with all three trucks. Figure 3-22 shows the first three loading scenarios.

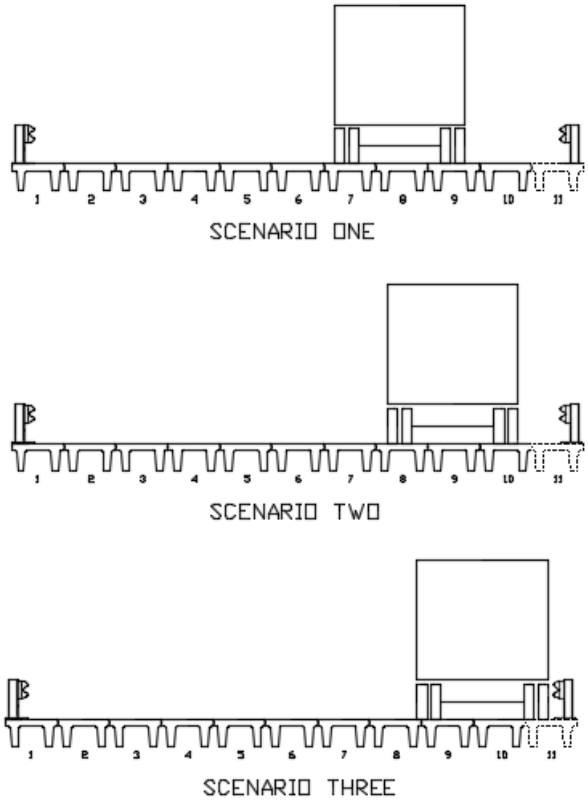

Figure 3-22: Truck Scenarios One through Three

The scenarios in Figure 3-22 were chosen out of caution for the exterior girder's capacity. It would have been undesirable to load the damaged girder immediately with the heaviest load since so many details of the bridge were unknown. Starting the load over the middle girders and then moving the truck closer to the exterior girder allowed the exterior girder to see a slow increase in load. Real-time monitoring of the girder responses ensured that the girder behavior didn't deviate from what was expected as the load moved closer to the exterior girder.

Scenario one had the truck line up its right wheel line over the center of girder nine. The loading location in scenario one is the same location of a vehicle driving in the design lane. Scenario two had the truck line up its right wheel line over the center of

girder ten. Scenario three had the truck get its right side as close to the guard rail as possible so to maximally load the damaged girder eleven. These locations were chosen with the right wheel line over top of the girder centerlines so an individual girder would see as much of the load as possible. These girders needed to be loaded as much as possible to accurately determine the transverse load distribution. First, the empty truck did a total of three runs per each of these scenarios. Then the half full truck did three runs per each of these scenarios. Finally, the full truck did three runs per each of these scenarios. This created a total of nine runs per loading scenario. Three runs were conducted per scenario to reduce the variability in the results. An average of the three runs helps eliminate outliers and provides the most accurate data.

Loading scenarios four through six were done with the second instrumentation plan. These loading scenarios were also only conducted with the full truck. These loading scenarios can be seen in Figure 3-23.

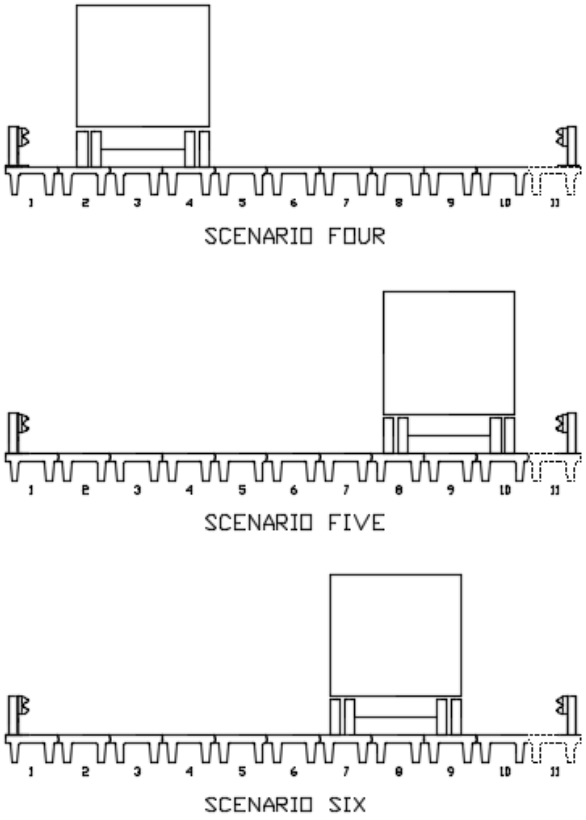

Figure 3-23: Truck Scenarios Four through Six

Loading scenario four had the truck line up its left wheel line over the center of girder two. This scenario was meant to be a direct mirror of scenario two. Scenario five had the truck line up its right wheel line over the center of girder ten. This is also the same location as scenario two. This repeat was done because instrumentation plan two had more strain gauges on the East Span so the data from scenarios four and five should have been symmetrical. Scenario six lined up in the same location as scenario one but instead of moving at pseudo-static speeds this scenario used a dynamic loading. Scenarios four through six were completed with three runs each. Scenario six used four runs but one was discarded due to error as an outlier. Table 3-1 provides a summary for the loading scenarios.

Table 3-1: Loading Scenario Summary

Loading Scenario	Trucks Used	Truck Speed (mph)	Repetitions	Instrumentation Plan	Primary Purpose
1	All	< 5	3	1	Damaged Girder Comparison
2	All	< 5	3	1	
3	All	< 5	3	1	
4	Full Only	< 5	3	2	Transverse Load Distribution
5	Full Only	< 5	3	2	
6	Full Only	45	3	2	Dynamic Load Allowance

3.5 Test Data

3.5.1 Data Organization

After each run was completed the data was saved on a laptop and backup copies were made. The manageable size of the data meant that all manipulation of the data could be done in Excel, no other program was needed for organizing or displaying data. The STS 4 system could be zeroed before each test so each individual set of data did not need to be manually zeroes. The STS 4 base station and channels were all battery powered and wireless so external noise interfering with data recording was not a concern. Data points for analysis were taken directly from the Excel sheets at the maximum and minimum values.

3.5.2 Data Reporting

Resolution and Accuracy of the instruments used determined the precision with which results are presented.

In this report the results are reported to the following resolution:

- Strains reported to the tenth of a microstrain

- Deflection reported to the thousandth of an inch

Chapter 4: Test of Channel Girder

The nondestructive test of the Five Forks Bridge revealed the bridge system behavior and response, and to some extent the behavior of the individual channels. However, the load versus deflection of a channel girder through failure is needed to further evaluate the Five Forks Bridge capacity. A channel similar in cross-sectional geometry and span length to those found in the Five Forks Bridge was provided by the SCDOT for flexural testing. A cross section of the channel can be seen in Figure 4-1 along with the strand profile. The strands in the channel were 3/8" in diameter with an ultimate stress of 270 ksi. The strands were assumed to be harped at the mid-span based off of other drawings provided by the SCDOT shown in Section 5.1.

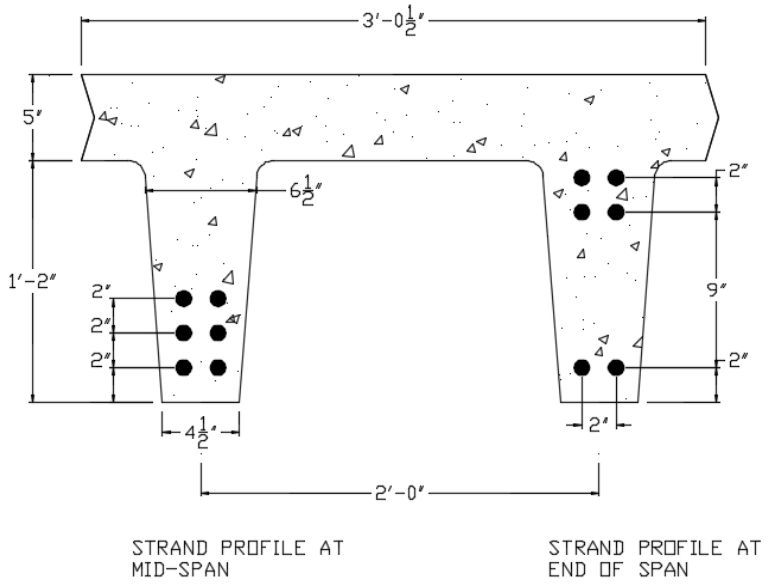

Figure 4-1: Girder Dimensions and Strand Profile

The purpose of the laboratory test was to determine the load versus deflection response of a channel representative of those found in the Five Forks Bridge. The channel was loaded to failure in a four-point bending configuration that created a

constant moment region at mid-span. Failure was determined to be the point where cracks formed in the flange and concrete flaked and crumbled on the top of the channel. Failure occurred at the largest moment resisted by the channel. The load-deflection plot from the laboratory test is used in conjunction with the data from the nondestructive test to evaluate the factor of safety between highway legal loads and the cracking moment and moment capacity of the individual channels.

4.1 Instrumentation

The instrumentation used to record the channel response was similar to the instrumentation used for the nondestructive test of the Five Forks Bridge. Strain gages were used to measure the surface strain, string pots were used to measure vertical deflection, and a dial gage was used to measure support movement. Figures 4-2 and 4-3 below show the layout for the instrumentation.

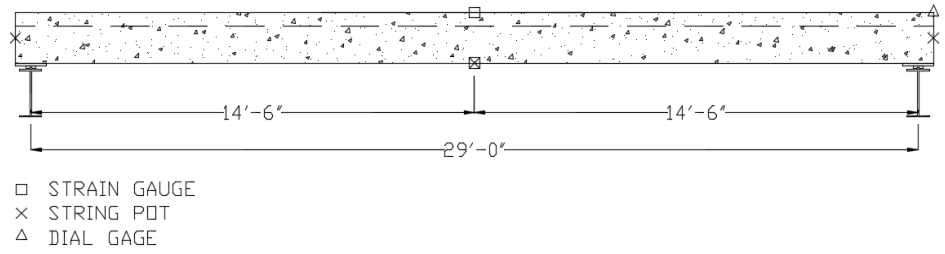

Figure 4-2: Elevation of Instrumentation

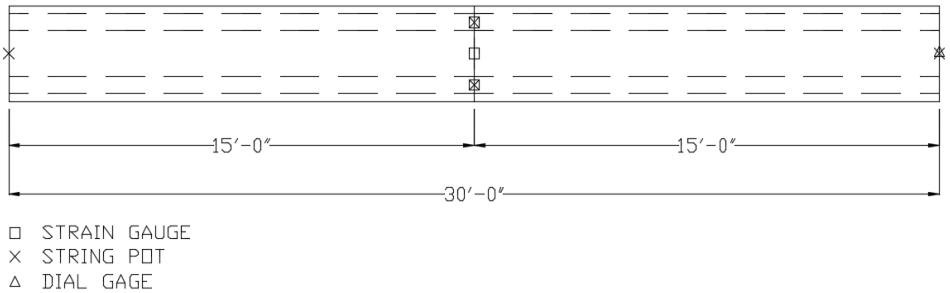

Figure 4-3: Plan View of Instrumentation

4.1.1 Strain Gages

The strain gages used were made by the Tokyo Sokki Kenkyujo Co. These were 60 mm (2.36 in.) long polyester strain gages designed for concrete use. The strain gages did not need to be calibrated, but the strain recorded was compared to the strain recorded by the BDI strain transducers used in the nondestructive test of the Five Forks Bridge. A BDI transducer was placed beside a strain gage and the strains were compared. It was found that the strain transducers and gages recorded very similar values. Strain gages were attached to the top of the channel at mid-span with a Cyanoacrylate-based adhesive. Of these three strain gages, one was placed over top of each stem and one placed in the middle between the stems. Two strain gages were placed on the bottom of each stem at mid-span; these gages were centered on the stems. Figure 4-4 shows the gages attached to the channel.

Figure 4-4: Attached Strain Gages

4.1.2 String Pots

Four of the same Celesco SM-25 string pots used for the nondestructive test of the Five Forks Bridge were used for the laboratory test. The accuracy of these string pots is 0.0625 in. The string pots were calibrated using a dial gage stand. The string pots were pulled to a known deflection. The deflection and corresponding resistance were plotted

for multiple distances. A linear equation was fit to the plot, this equation was used to convert the recorded resistances to distances. A separate equation was used for each of the four string pots. Deflection at mid-span was of interest so two string pots were attached to each web of the channel at mid-span. The string pot strings were attached to plastic hooks glued to the side of the channel at the neutral axis. To attach the string pots stiff wire was wrapped around the hooks and looped through the string pot ends. Concrete blocks were used as anchors for the casings of the string pots. Figure 4-5 shows a string pot attached to the channel. The other two string pots were attached 12 in. from the ends of the beam to measure the deflection near the supports. These string pots were attached to hooks glued to the side of the channel at the neutral axis. Some pieces of cross-laminated timber were used to anchor the casings of the string pots.

Figure 4-5: String Pots on Channel

4.1.3 Dial Gage

A dial gage from Mitutoya with an accuracy of 0.0001 in. was used at the end of the channel to record compression of the bearing pads. This overall channel settlement was subtracted from the deflection that the string pots recorded at mid-span to ensure more accurate recordings. Figure 4-6 shows the dial gage at the bearing of the channel.

Figure 4-6: Dial Gage at Bearing of Channel

4.2 Loading Setup

The channel was loaded in a four-point bending arrangement that can be seen in Figures 4-7, 4-8, and 4-9. Figures 4-7 and 4-8 show the elevation and plan views of the load test setup. Figure 4-9 is a picture taken before the test.

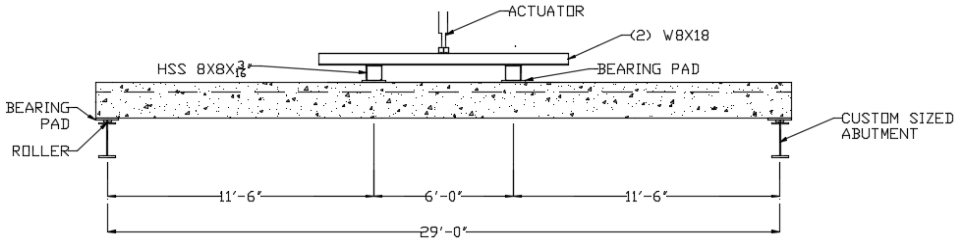

Figure 4-7: Elevation of Channel Test

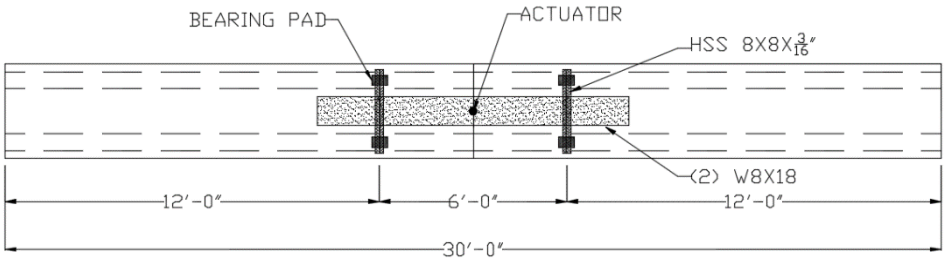

Figure 4-8: Plan of Channel Test

The setup consisted of a reaction frame, hydraulic actuator, and a spreader beam to distribute the load. The actuator and jack hung from the cross head of the reaction frame. The pressure was applied to the center of a spreader beam consisting of two W8x18 beams welded together. The spreader was centered on the channel transversely and longitudinally. It was supported by two transverse tubes (HSS 8x8x$\frac{3}{16}$ in.). The tubes were centered transversely but offset 3 ft. on each side of the channel center line. The tubes were 6ft. apart and created a constant moment region at the middle 6 ft. of the channel. The tubes rested on 1 in. thick bearing pads located directly above the channel stems. The channel was supported by custom-made W-shaped members 18 in. deep and with flange widths of 8.66 in. These custom beams were bolted to the reaction floor. The custom beams were located 14'-6" from the center of the frame creating a total span length of 29'-0" between the custom abutments. Between the channel and abutment were 1 in. thick bearing pads and rollers that allowed lateral movement of the channel. Figure 4-9 shows the loading setup.

Figure 4-9: Channel Setup

4.3 Test Procedure

Prior to loading, the strain gages and string pots were zeroed by the DAS. The dial gage was zeroed manually. Load was slowly applied in 5 kip increments. The Enerpac pressure gauge used has an accuracy of ± 1.0%. The load applied by the Enerpac pump was compared to the load recorded by a load cell placed between the actuator and channel in order to determine the relationship between hydraulic pressure and applied load. The pump was not calibrated by the load cell, but the load cell was used to ensure the load being recorded from the pump was accurate. The loads recorded by the pump and load cell were similar. At each 5 kip mark the current from the pressure gage was recorded as well as the pressure in psi. After initial cracking, cracks were marked at 5 kip increments. Due to safety concerns, cracks were no longer marked near

the expected failure load. The crack pattern on one side of the web at a load of 40 kips can be seen in Figure 4-10. The beam was loaded until failure.

Figure 4-10: Crack Pattern at 40 kips

4.4 Data Acquisition

LabVIEW from National Instruments was used to record and save data from the laboratory test. The system recorded the load as a function of current, the deflection as a function of resistance, and the strain as strain. Calibration files from previous experiments were used to convert the current into load. Calibration with a ruler was completed to convert the resistance into deflection. Deflection from the dial gage was recorded and used to set the baseline for the string pots. Figure 4-11 shows the data acquisition system.

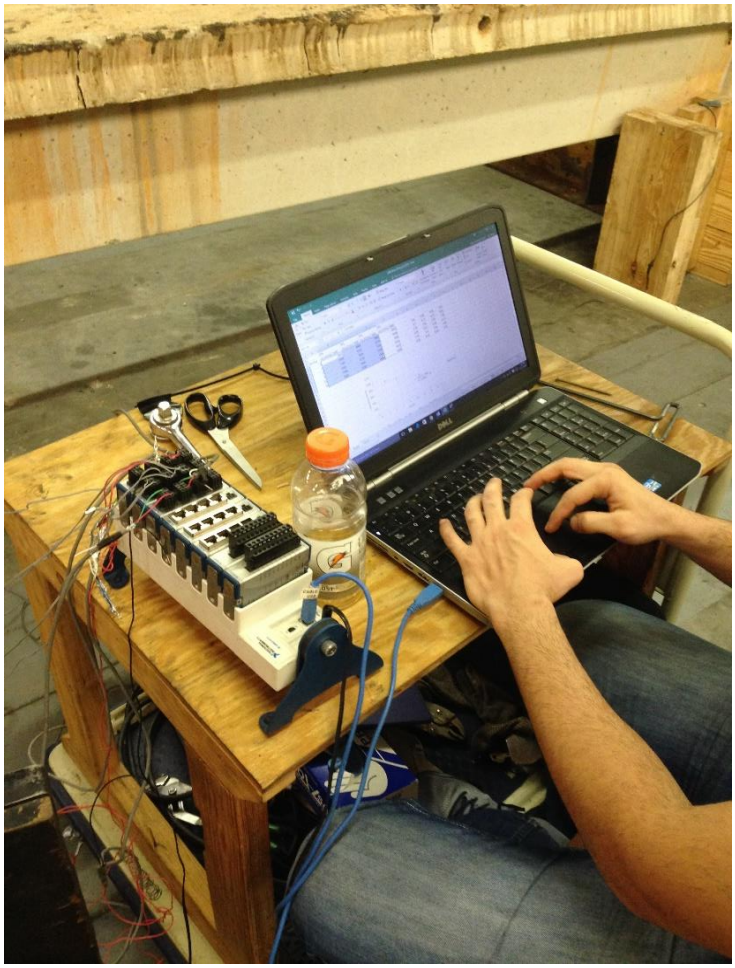

Figure 4-11: Data acquisition system

Chapter 5: Nondestructive and Channel Test Results

This chapter focuses on the results from the nondestructive test of the Five Forks Bridge and the laboratory test conducted on the channel provided by the SCDOT. A comparison of experimental and theoretical values for bridge and girder characteristics are also discussed.

Data was recorded for the duration of the truck's travel across all three spans of the Five Forks Bridge. All instrumentation was at the mid-span of the east and west spans so only data recorded when the trucks were at mid-span was of interest to this study. It was determined that the trucks were at the middle of the spans when the maximum values were recorded by the instrumentation. All strains presented in this chapter are an average of the readings from strain transducers on both girder stems. In addition, the results from the three repetitions of each truck orientation are averaged unless otherwise stated.

All deflection values are reported as positive for downward displacement and negative for upward lift. Tensile strain is presented as a positive value and compressive strain is shown as a negative value. The nondestructive test and the laboratory test both present strain and deflection as a result of applied live load. The effect from dead loads are not considered in the strain and deflection data presented. When applicable, the moment caused by the self-weight of the girder is added to the applied moment to determine the total load on the girder.

5.1 Investigation of Girder Properties

To the best knowledge of the SCDOT there were no formal designs or plans unique to the Five Forks Bridge on record. The SCDOT provided two separate sets of drawings used for channel bridges built in SC. Girder cross sections from each design are presented in Figures 5-1 and 5-2 as Design 1 and Design 2, respectively.

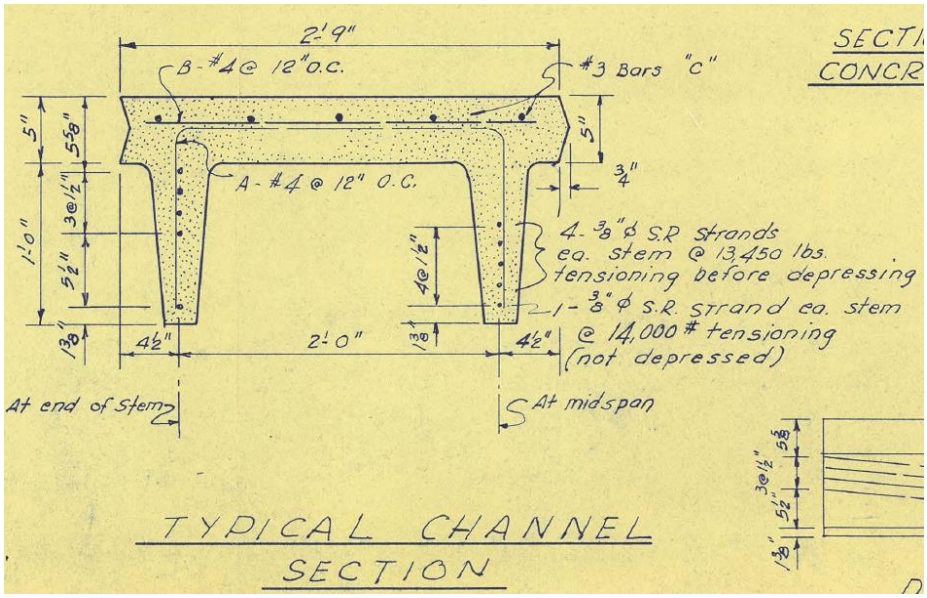

Figure 5-1: Design 1 Girder Cross Section

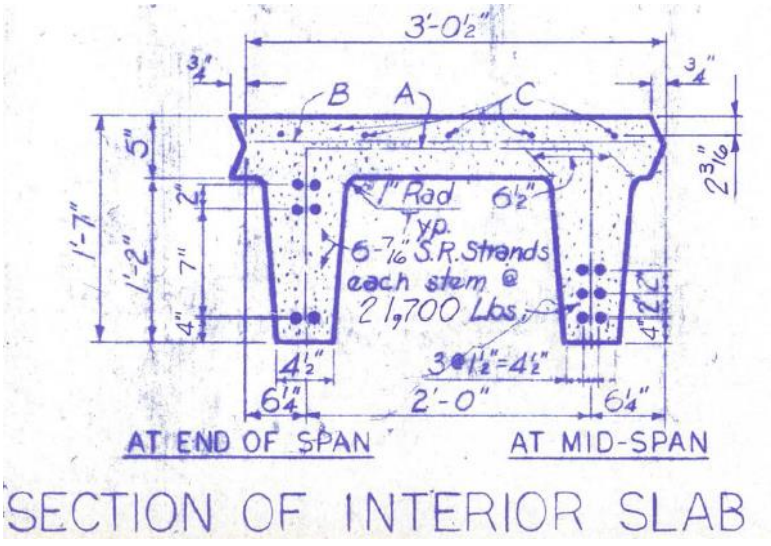

Figure 5-2: Design 2 Girder Cross Section

There are multiple differences between the two designs. The strand layout is different in each plan; Design 1 has 5 strands arrayed in a single column in each channel stem while Design 2 has 2 columns of 6 strands in each stem. The spacing of the strands and the center of gravity of the strands relative to the channel's neutral axis are different in each design. The strand eccentricity along the length of the span can be seen for Design 1 and Design 1 in Figures 5-3 and 5-4.

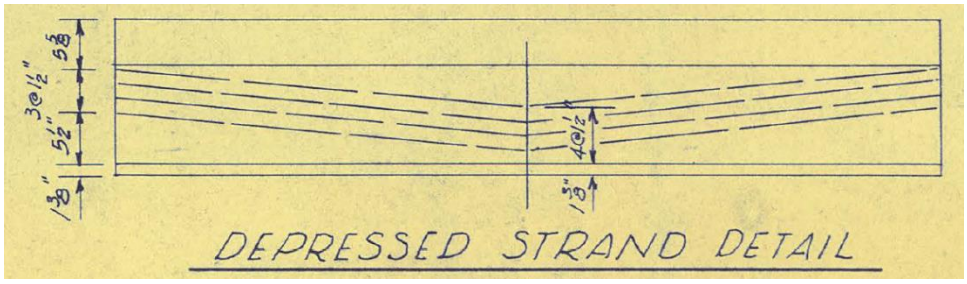

Figure 5-3: Design 1 Strand Profile

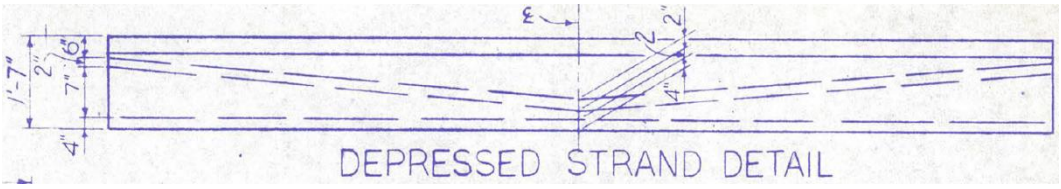

Figure 5-4: Design 2 Strand Profile

The strand material properties are different in each design as well. Design 1 contains 3/8 in. strands with a nominal capacity of 250 ksi. Design 2 contains 7/16 in. strands with a nominal capacity of 270 ksi. Due to these differences the flexural capacities of each design are significantly different.

After the flexural test was conducted it was determined that the difference in Designs 1 and 2 were too large to blindly choose either. A jack hammer was used to chip the concrete away at the end of the girder so the end of the strands could be exposed. All of the concrete was removed from the face of one of the stems. It was assumed that the

layout of one stem was identical to the layout of the other. A picture of the exposed strands from the channel can be seen in Figure 5-5.

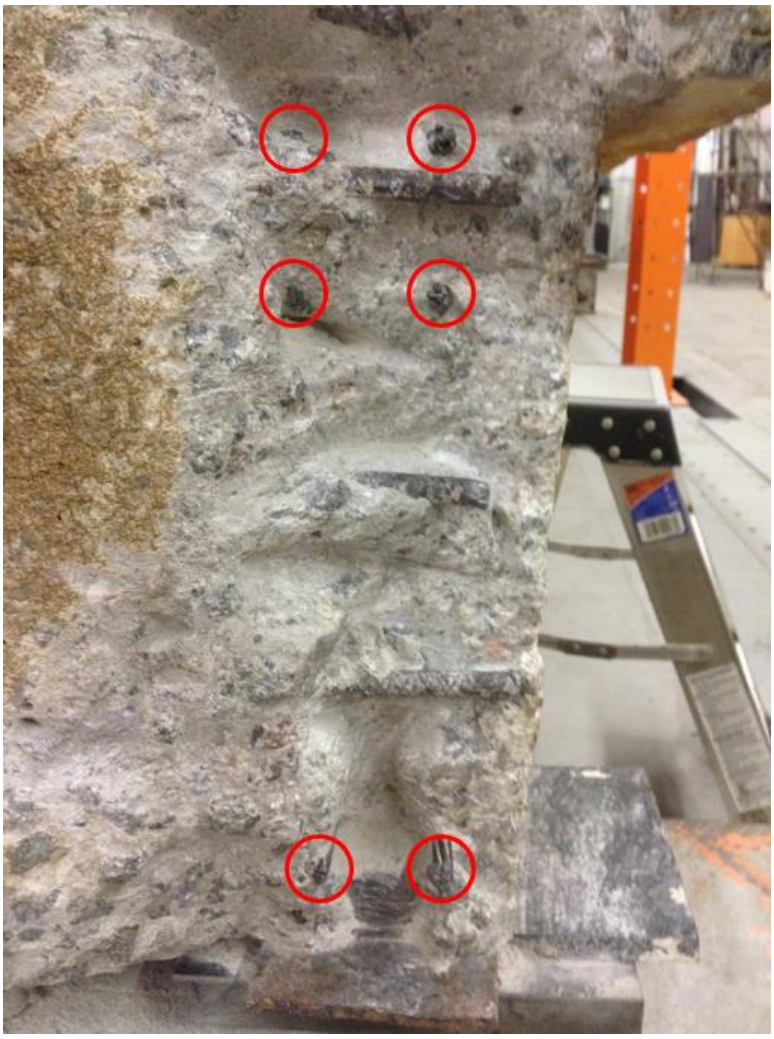

Figure 5-5: Exposed Strands of Channel

The end of each exposed strand is outlined by a red circle. Once the strands were exposed the position of each strand was measured and the diameter of each strand was recorded. The bottom layer of strands were measured at 2 in. from the bottom of the channel. The second and third layers of strands were measured at 11 and 13 in. from the

bottom, respectively. This layout of strands is different from both Design 1 and 2. Figure 5-6 below shows the assumed strand eccentricity along the length of the span.

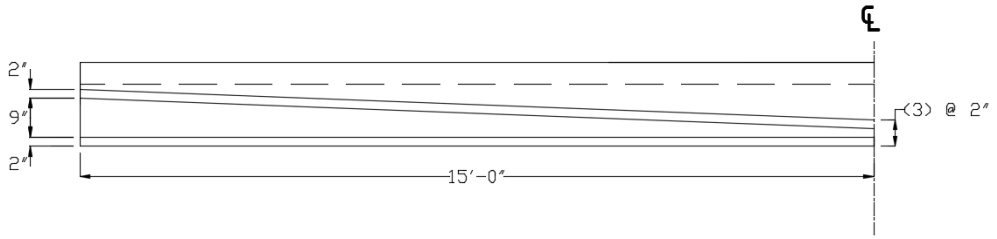

Figure 5-6: Channel Strand Profile

Table 5-1 shows the differences in strand area as a function of nominal diameter and nominal capacity.

Table 5-1: Area of Prestressing Strands

	270 ksi	**250 ksi**
3/8 in.	0.085 in^2	0.08 in^2
7/16 in.	0.115 in^2	0.108 in^2

Using these values the area of the strands in the channel were measured and compared against the table to determine what size strands were in the channel. To do this, the nominal diameter of the four accessible strands were measured with a digital caliper. The average nominal diameter of the strands came out to be 0.369 in. This is very close to the nominal diameter of the 3/8 in. strands. To determine the area of the strands, the diameter of the individual wires were measured. The area of these wires were calculated and then multiplied by seven to determine the area of the whole strand. The average strand area of the six strands that could be measured was 0.0870 $in.^2$. Using the average nominal diameter and average strand area it was concluded that the strands in the channel had an ultimate stress of 270 ksi with a diameter of 3/8 in. These properties were different than those in both the Design 1 and 2 drawings. The girder geometry from

the Five Forks Bridge matched the girder geometry from the channel test and the girder in Design 2. The strand properties found in the forensic investigation resulted in a smaller nominal strength than the nominal strength calculated from the strand properties in Design 2. Because the strand properties from the forensic investigation resulted in a more conservative nominal strength, these properties were used for all subsequent calculations.

5.2 Discarded Data

Each truck scenario was tested with at least three runs to ensure consistency and to attempt to reduce the chance of outliers. Scenario four is the only test that required more than three runs. The first run of scenario four resulted in a very high strain being recorded by BDI strain transducer B5337. The strain in B5337 for each of the runs from scenario four can be seen in Table 5-2.

Table 5-2: B5337 Strain Comparison from Scenario Four

Run	Strain (με)
1	445
2	163
3	154
4	152

This transducer was located on girder 4 which was directly beneath one wheel line of the truck. The other transducers in run one recorded similar values to the other runs but transducer B5337 recorded almost three times the amount of strain found in the other runs. Using the instrumentation available it appeared that run one recorded about 300 με more than any other run. It is unlikely that this run actually recorded more overall

load than the other runs so the data from run one was discarded and three other runs were conducted.

Recording the surface strain in the girders was the main focus of the nondestructive test of the Five Forks Bridge but the deflections of the exterior girder (11) and first interior girder (10) in the east and west spans were also recorded. The deflection data was intended to be compared against the deflection data from the channel test conducted at Clemson University. There was an unexplained phenomena in the deflection data from the nondestructive test though. Figure 5-7 below compares the plots of the recorded deflection and strain experienced by girder 10 in scenario two. The strain and deflection data in Figure 5-7 are the average of the two stems of girder 10. The wheel line was directly above the girder in this scenario.

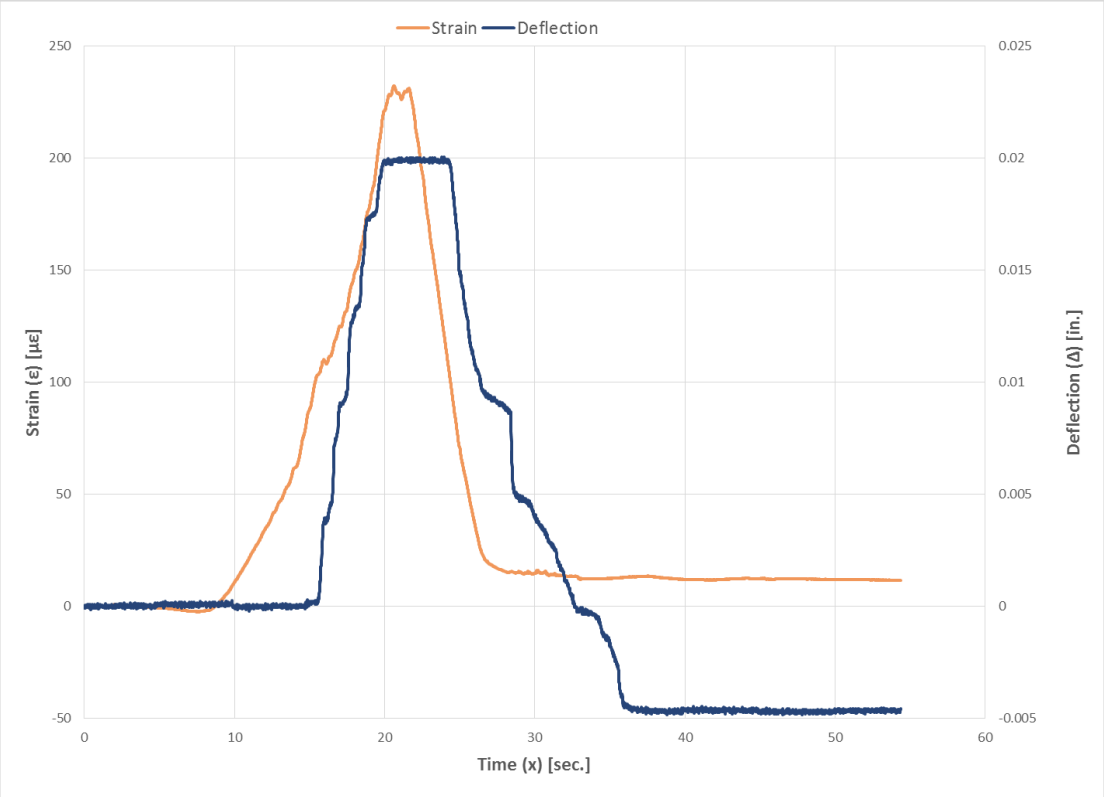

Figure 5-7: Strain and Deflection Values for Girder 10, Scenario Two

The data from the strain transducer on the left axis plots as expected, with one exception. There is one large peak that corresponds to the truck nearing the center of the span and there are two small peaks as a result of each truck axle. However, there is residual tensile strain equal to approximately 10 με in the girder after the truck passes. Ideally, there would be no residual strain but this is a small amount compared to the maximum strain under loading. Due to the complex nature of the overall bridge system the reason for this strain is unknown.

The deflection data on the right axis does not follow the same trend. It would be expected for the deflection of the girder to closely mirror the plot of the strain. Instead the deflection data plateaus near the peak and maintains the plateau for a few seconds.

The deflection plots for each of the four string pots used in the nondestructive test look similar to the plot in Figure 5-7. The peak of the plateau for each plot is different and the peak recorded by each individual string pot is different for the multiple scenarios. As seen in Chapter 3, the string pots were pulled a certain distance before being set in place to allow upward and downward movement. The setup allowed for multiple inches of movement in either direction so it is not a case of the string pot reaching its limit. After the nondestructive test the string pots were recalibrated, and then the string pots underwent a series of exercises to attempt to recreate this plateau behavior. No movement was able to mimic the plots from the nondestructive test.

It is unknown whether the string pots accurately recorded the peak deflection experienced during the test. One hypothesis is that the string pots were not able to coil and uncoil quick enough to accurately record the movement of the trucks as they crossed over the bridge. There is nothing known for certain. Since the deflection data may not be accurate and there is an unexplained plateau in the plots it was decided to discard the deflection data from the nondestructive test. Only strain data from the nondestructive test was used in the analysis and comparison of the Five Forks Bridge.

5.3 Service Strain Results

This section focuses on reporting the surface strains from the nondestructive load test of the Five Forks Bridge. A majority of the discussed results are from the pseudo-static or creep tests, but the strains from the dynamic loading are reported as well. An in-depth comparison of the static and dynamic strains are presented in Section 5.5. Table 5-3 provides a summary of the loading scenarios used in the nondestructive test.

Table 5-3: Loading Scenario Summary

Loading Scenario	Trucks Used	Truck Speed (mph)	Repetitions	Primary Purpose
1	All Weights	< 5	3	Damaged Girder Comparison
2	All Weights	< 5	3	
3	All Weights	< 5	3	
4	Full Only	< 5	3	Transverse Load Distribution
5	Full Only	< 5	3	
6	Full Only	45	3	Dynamic Load Allowance

5.3.1 Service Strain Results of all Truck Scenarios for the East Span

This section reports the average and maximum strain for every instrumented girder in the east span as well as the coefficient of variation. The coefficient for variation is a tool to determine how much the sample values deviate in relation to the average value. Only one other nondestructive test could be found where the coefficients of variation for the strain were able to be determined, and the paper reported coefficients of variation as high as 10% for girders further away from the load. Most coefficients of variation for girders under the load were in the 1% to 3% range (Collins 2010). The coefficients of variation are tabled for each loading scenario and truck size. The service strains for the east span from scenario one are reported in Tables 5-4, 5-5, and 5-6. The loadings for scenario one consisted of an empty truck, half-full truck, and full truck driving at pseudo-static speeds over top of girders 7 and 9.

Table 5-4: Strain from Scenario One with Empty Truck

Girder Number	6	7	8	9	10	11
	Tension Strains (με)					
Average	8.58	***55.7***	38.0	***65.2***	12.4	0.949
Maximum	9.15	56.9	38.4	66.4	12.6	1.16
Coeff. of Variation	6.82%	1.62%	0.862%	1.54%	1.33%	28.3%

Table 5-4 above shows the results from scenario one with the empty truck. As expected the largest strains were recorded in girders 7 and 9 with averages of 55.7 με and 65.2 με, respectively. The coefficient of variation was largest at the girders furthest from the load. This could be attributed to noise interfering with the sensitive measurements of the strain.

Table 5-5: Strain from Scenario One with Half-Full Truck

	East Span					
Girder Number	6	7	8	9	10	11
	Tension Strains (με)					
Average	21.0	***135***	85.6	***142***	22.7	2.3
Maximum	21.3	136	86.5	144	24.3	2.5
Coeff. of Variation	1.05%	0.94%	0.84%	0.85%	8.05%	12.9%

Table 5-5 above shows the results from scenario one with the half-full truck. As expected the largest strains were recorded in girders 7 and 9 with averages of 135 με and 142 με, respectively. The coefficient of variation was largest at the girders furthest from the load. This could be attributed to noise interfering with the sensitive measurements of the strain.

Table 5-6: Strain from Scenario One with Full Truck

	East Span					
Girder Number	**6**	**7**	**8**	**9**	**10**	**11**
	Tension Strains (με)					
Average	29.4	***193***	107	***196***	30.9	3.1
Maximum	30.4	196	108	198	32.4	3.7
Coeff. of Variation	2.51%	1.39%	0.67%	1.07%	4.15%	15.4%

Table 5-6 above shows the results from scenario one with the full truck. As expected the largest strains were recorded in girders 7 and 9 with averages of 193 με and 196 με, respectively. The coefficient of variation was largest at the girders furthest from the load. This could be attributed to noise interfering with the sensitive measurements of the strain.

The service strains from scenario two are reported in Tables 5-7, 5-8, and 5-9. The loadings for scenario two consisted of an empty truck, half-full truck, and full truck driving at pseudo-static speeds over top of girders 8 and 10.

Table 5-7: Strain from Scenario Two with Empty Truck

Girder Number	**6**	**7**	**8**	**9**	**10**	**11**
	Tension Strains (με)					
Average	4.10	30.0	***50.9***	29.3	***68.4***	6.64
Maximum	4.12	30.1	51.5	29.8	69.9	6.92
Coeff. of Variation	0.296%	0.383%	1.26%	1.13%	2.58%	4.20%

Table 5-7 above shows the results from scenario two with the empty truck. As expected the largest strains were recorded in girders 8 and 10 with respective averages of 50.9 με and 68.4 με. The coefficient of variation was only slightly larger in girder 11 compared to the other girders.

Table 5-8: Strain from Scenario Two with Half-Full Truck

Girder Number	6	7	8	9	10	11
	Tension Strains (με)					
Average	7.75	60.9	***114***	67.3	***161***	13.0
Maximum	8.05	61.8	116	68.2	165	13.5
Coeff. of Variation	4.56%	1.28%	1.29%	1.58%	1.73%	3.51%

Table 5-8 above shows the results from scenario two with the half-full truck. As expected the largest strains were recorded in girders 8 and 10 with respective averages of 114 με and 161 με. The coefficient of variation was largest at the girders furthest from the load. This could be attributed to noise interfering with the sensitive measurements of the strain.

Table 5-9: Strain from Scenario Two with Full Truck

Girder Number	6	7	8	9	10	11
	Tension Strains (με)					
Average	9.59	78.2	***148***	87.9	***227***	16.1
Maximum	9.98	78.9	150	88.5	232	16.6
Coeff. of Variation	4.42%	1.06%	0.771%	0.719%	1.40%	3.98%

Table 5-9 above shows the results from scenario two with the full truck. As expected the largest strains were recorded in girders 8 and 10 with respective averages of 148 με and 227 με. The coefficient of variation was largest at the girders furthest from the load. This could be attributed to noise interfering with the sensitive measurements of the strain.

The service strains from scenario three are reported in Tables 5-10, 5-11, and 5-12. The loadings for scenario three consisted of an empty truck, half-full truck, and full

truck driving at pseudo-static speeds as close to the guard rail as possible to maximize the load in girder 11.

Table 5-10: Strain from Scenario Three with Empty Truck

Girder Number	6	7	8	9	10	11
	Tension Strains (με)					
Average	1.48	10.8	21.1	***56.5***	***69.4***	49.2
Maximum	2.03	11.0	21.5	58.1	70.5	50.3
Coeff. of Variation	26.9%	1.88%	1.54%	2.41%	1.46%	2.08%

Table 5-10 above shows the results from scenario three with the empty truck. Even though it was attempted to load girder 11 as much as possible, the physical constraint of the guard rail resulted in the largest strains being recorded in girders 9 and 10 with respective averages of 56.5 με and 69.4 με. The coefficient of variation was largest at the girders furthest from the load. This could be attributed to noise interfering with the sensitive measurements of the strain.

Table 5-11: Strain from Scenario Three with Half-Full Truck

Girder Number	6	7	8	9	10	11
	Tension Strains (με)					
Average	2.40	20.4	42.2	***134***	93.3	***131***
Maximum	2.79	21.0	43.3	139	109	145
Coeff. of Variation	12.3%	3.07%	2.84%	3.06%	12.6%	11.1%

Table 5-11 above shows the results from scenario three with the half-full truck. This test was able to produce the largest strains in girder 9 and 11 as desired. The truck wheels over girders 9 and 11 resulted in the largest strains being recorded in girders 9 and 11 with respective averages of 134 με and 131 με. The coefficient of variation was larger further away from the load and in girders 10 and 11.

Table 5-12: Strain from Scenario Three with Full Truck

Girder Number	6	7	8	9	10	11
	Tension Strains (με)					
Average	2.72	28.2	66.5	***159***	***166***	130
Maximum	2.98	30.1	71.7	160	178	139
Coeff. of Variation	7.97%	4.71%	5.64%	0.56%	5.05%	6.18%

Table 5-12 above shows the results from scenario three with the full truck. Even though it was attempted to load girder 11 as much as possible, the physical constraint of the guard rail resulted in the largest strains being recorded in girders 9 and 10 with respective averages of 159 με and 166 με in the east span. The coefficient of variation was larger further away from the load and in girders 10 and 11.

The service strains from scenario four are reported in Table 5-13. The loading for scenario four consisted of a full truck driving at pseudo-static speeds over girders 2 and 4. In this presentation of data there are only the undamaged girders from the east span. There were no strain transducers on girders 1, 2, or 3.

Table 5-13: Strain from Scenario Four with Full Truck

Girder Number	4	5	6	7	8	9	10	11
	Tension Strains (με)							
Average	***152***	42.3	10.3	2.66	1.21	0.440	0.431	0.341
Maximum	155	45.4	11.1	2.94	1.44	0.785	0.753	0.514
Coeff. of Variation	1.70%	5.11%	5.58%	8.64%	20.6%	69.8%	69.2%	60.2%

As expected, the table above shows girder 4 as being the most heavily loaded. The load over girders 1, 2, and 3 can't be seen, but Section 5.3.2 will demonstrate the girder symmetry. The average strain recorded in girder 4 was 152 με. The coefficient of variation was larger further away from the load.

The service strains from scenario five are reported in Table 5-14. The loading for scenario five consisted of a full truck driving at pseudo-static speeds over girders 8 and 10. In this way, scenario five is identical to the full truck scenario two loading. In this presentation of data there are only the undamaged girders from the east span. There were no strain transducers on girders 1, 2, or 3.

Table 5-14: Strain from Scenario Five with Full Truck

Girder Number	4	5	6	7	8	9	10	11
	Tension Strains (με)							
Average	1.11	2.37	7.93	75.4	***153***	84.3	***239***	13.4
Maximum	1.37	2.66	8.33	76.9	155	85.2	241	13.8
Coeff. of Variation	23.4%	13.0%	4.53%	1.39%	1.36%	0.880%	0.606%	2.38%

As expected, the table above shows girders 8 and 10 as being the most heavily loaded. The average strain recorded in girders 8 and 10 were 153 με and 239 με, respectively. The coefficient of variation was larger further away from the load.

The service strains from scenario six are reported in Table 5-15. The loading for scenario six consisted of a full truck driving at highway speeds over girders 7 and 9. This loading is similar to scenario one except for the speed of the truck. In this presentation of data there are only the undamaged girders from the east span. There were no strain transducers on girders 1, 2, or 3.

Table 5-15: Strain from Scenario Six with Full Truck

Girder Number	4	5	6	7	8	9	10	11
	Tension Strains (με)							
Average	11.5	21.5	52.9	***184***	142	***170***	50.7	20.4
Maximum	12.2	23.7	68.1	225	158	202	61.1	24.2
Coeff. of Variation	5.96%	7.47%	22.4%	15.8%	8.17%	14.7%	16.1%	17.4%

As expected, the table above shows girders 7 and 9 as being the most heavily loaded. The average strain recorded in girders 7 and 9 were 184 με and 170 με, respectively. There was fairly high coefficient of variations for all of the girders. The truck in this test was driving approximately 45 mph so there was a much greater chance of the truck course changing between runs.

The measured strain data presented in this section was expected for each of the loading scenarios because the largest strains were typically directly under the load, with the exception of scenario three, and the strain in the girders far from the load was negligible. The recorded strain became negligible only a couple of girders away from the load. The coefficients of variation were consistent with those reported by Collins for the girders under the load and for those far away from the loaded girders. Figure 5-8 below is a plot of the coefficient of variation of the average girder strains for each girder over all scenarios. The plot shows that the largest coefficients of variation almost always occur at the smallest strain values where they are most susceptible to ambient noise. The smallest strain values are also those furthest from the load. Four data points are circled that show the abnormally large coefficients of variation that were found at exterior girders where the location of the load was not tightly controlled (scenario three).

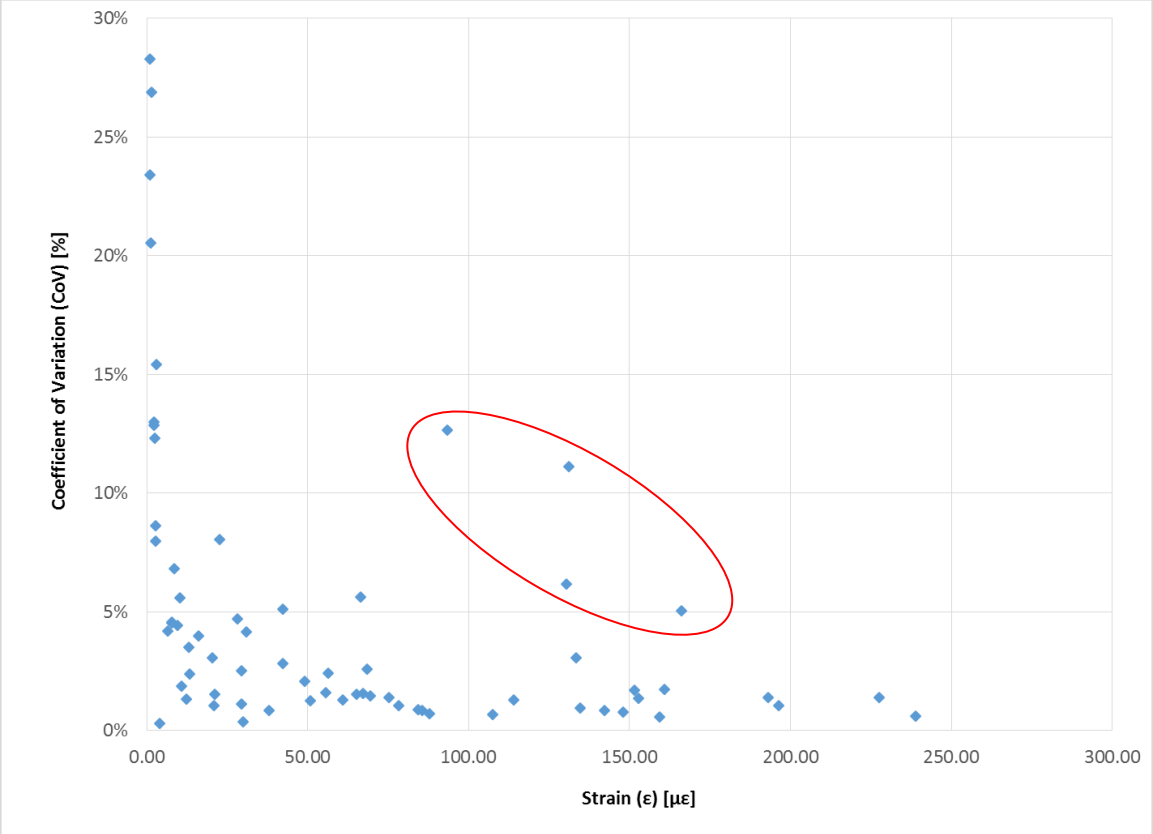

Figure 5-8: Coefficient of Variation Plot

5.3.2 Service Strain Comparison for the East and West Spans

This section focuses on the comparison of the exterior girder (11) and first interior girder (10) responses for the east and west spans. The west span has damage present on the exterior girder whereas the east span is undamaged. A table for each loading scenario and truck size is presented below to determine if the damage influences the response each girder sees.

Tables 5-16, 5-17, and 5-18 below compare the east and west spans for all truck sizes of scenario one.

Table 5-16: Span Comparison for Scenario One with Empty Truck

	Empty Truck			
	East Span		West Span	
Girder Number	10	11	10	11
	Tension Strains (με)			
Average	12.4	0.949	20.4	6.49
Maximum	12.6	1.16	20.7	6.64
Coeff. of Variation	1.33%	28.3%	0.98%	2.61%

Table 5-17: Span Comparison for Scenario One with Half-Full Truck

	East Span		West Span	
Girder Number	10	11	10	11
	Tension Strains (με)			
Average	22.7	2.26	40.6	13.7
Maximum	24.3	2.52	41.1	14.0
Coeff. of Variation	8.05%	12.9%	1.24%	1.52%

Table 5-18: Span Comparison for Scenario One with Full Truck

	East Span		West Span	
Girder Number	10	11	10	11
	Tension Strains (με)			
Average	30.9	3.08	51.5	18.0
Maximum	32.4	3.71	52.1	18.9
Coeff. of Variation	4.15%	15.4%	1.41%	3.88%

All three tables above present a larger strain in girder 10 compared to girder 11. Each table also shows a larger overall load in the girders of the west span compared to the east. The coefficient of variation is larger in the east span but this is likely due to noise as the girder is further away from the load.

Tables 5-19, 5-20, and 5-21 below compare the east and west spans for all truck sizes of scenario two.

Table 5-19: Span Comparison for Scenario Two with Empty Truck

	East Span		West Span	
Girder Number	**10**	**11**	**10**	**11**
	Tension Strains (με)			
Average	68.4	6.64	55.1	16.7
Maximum	69.9	6.92	59.1	18.0
Coeff. of Variation	2.58%	4.20%	5.16%	5.61%

Table 5-20: Span Comparison for Scenario Two with Half-Full Truck

	East Span		West Span	
Girder Number	**10**	**11**	**10**	**11**
	Tension Strains (με)			
Average	161	13.0	125	38.0
Maximum	165	13.5	128	38.4
Coeff. of Variation	1.73%	3.51%	1.55%	0.863%

Table 5-21: Span Comparison for Scenario Two with Full Truck

	East Span		West Span	
Girder Number	**10**	**11**	**10**	**11**
	Tension Strains (με)			
Average	227	16.1	168	40.3
Maximum	232	16.6	176	41.2
Coeff. of Variation	1.40%	3.98%	3.28%	2.23%

All three tables above present a larger strain in girder 10 of the east span and a larger strain in girder 11 of the west span. Each table also shows a slightly larger overall load in the girders of the east span compared to the west. There is no significant difference in the coefficient of variation between the four girders presented in the tables.

Tables 5-22, 5-23, and 5-24 below compare the east and west spans for all truck sizes of scenario three.

Table 5-22: Span Comparison for Scenario Three with Empty Truck

	East Span		West Span	
Girder Number	**10**	**11**	**10**	**11**
	Tension Strains (με)			
Average	69.4	49.2	70.4	52.6
Maximum	70.5	50.3	72.4	54.0
Coeff. of Variation	1.46%	2.08%	2.13%	2.64%

Table 5-23: Span Comparison for Scenario Three with Half-Full Truck

	East Span		West Span	
Girder Number	**10**	**11**	**10**	**11**
	Tension Strains (με)			
Average	93.3	131	65.5	182
Maximum	109	145	70.4	191
Coeff. of Variation	12.6%	11.1%	6.71%	3.62%

Table 5-24: Span Comparison for Scenario Three with Full Truck

	East Span		West Span	
Girder Number	**10**	**11**	**10**	**11**
	Tension Strains (με)			
Average	166	130	146	165
Maximum	178	139	155	175
Coeff. of Variation	5.05%	6.18%	4.49%	8.43%

All three tables above present a larger strain in girder 11 of the west span compared to girder 11 of the east span. The strain in girder 10 is larger in the east span for two of the tables and larger in the west span for the other table. Each table also shows a larger overall load in the girders of the west span compared to the east. Nothing conclusive can be determined from the coefficient of variation due to the absence of a trend between the girders and the spans.

Tables 5-16 through 5-24 show that the damaged girder 11 takes more load than the healthy girder 11 as the truck moves closer to the exterior of the bridge. In Table 5-

23 the damaged girder 11 takes 39% more load than the healthy girder. Scenario three shows the largest strain in girders 11 and 11D compared to 10 and 10D. The largest strain experienced in scenario three is smaller than the largest strain in scenario two. Therefore, while it is possible to maximally load girders 11 and 11D in scenario three, they still won't see the same magnitude of strain as the maximally loaded girders in scenario two.

The coefficients of variation for the girders in scenario one are larger due to being further removed from the loaded girders, and the coefficients for variation are larger in scenario three due to variation in the position of the truck. The coefficients of variation are within the expected range outside of the exceptions just listed. The strain in the damaged girder 11 never exceeded the maximum strain seen by the east span girders in Section 5.3.1. The following section will further explore the condition of girders 10 and 11 in the west span by investigating the linearity of the bridge response under increasing load.

5.3.3 Strain Linearity

An important assumption in concrete is that the material response behaves in a linear elastic fashion until it cracks. This plays a role in the analysis of existing bridges because nonlinear behavior can indicate if a structure is nearing its nominal capacity. One way to determine linearity of a data set is through the calculation of the linear correlation coefficient (R) and the coefficient of determination (R^2). The linear correlation coefficient measures the strength and direction of a linear relationship between two variables. A linear correlation coefficient of 1 indicates perfect, positive

linearity and a correlation greater than 0.8 can be described as strong and positive. The linear correlation coefficient doesn't tell the whole story though so the coefficient of determination is also used. The coefficient of determination predicts the amount of fluctuation in one variable based off of the other variable. It represents the percent of data that is closest to the line of best fit (PennState 2016). The equation used to find correlation can be found below.

$$R = \frac{n(\sum xy) - (\sum x)(\sum y)}{\sqrt{[n\sum x^2 - (\sum x)^2][n\sum y^2 - (\sum y)^2]}}$$

Where R is the linear correlation coefficient, x are the individual data points for the x-axis, y are the individual data points for the y-axis, and n is the number of data sets. This equation can be applied to the data from the Five Forks Bridge by setting the moment caused by each truck size as the "y" variable and the strain recorded for each girder as the "x" variable. In this presentation of data each strain transducer is looked at individually. The nomenclature used names the stems from left to right when looking west. The correlation coefficients were determined using all 9 data points, 3 data points per each truck size. Tables 5-25, 5-26, and 5-27 show the R and R^2 values for scenarios one through three. Girders with a "D" after the number indicate girders on the west span were damage is present.

Table 5-25: Linearity of Scenario One Strain

Girder	R	R^2
6	0.998	0.995
6.5	0.993	0.985
7	0.990	0.981
7.5	1.000	1.000
8	0.998	0.997
8.5	0.998	0.997
9	0.997	0.994
9.5	0.998	0.997
10	0.965	0.931
10.5	0.989	0.979
11	0.899	0.808
11.5	0.937	0.878
10D	0.999	0.998
10.5D	0.999	0.998
11D	0.996	0.991
11.5D	0.996	0.992

The strain linearity for scenario one is shown above. Scenario one placed the truck over girders 7 and 9. The lowest correlation coefficient for scenario one is 0.8988 located at girder 11 in the east span. This correlation indicates a strong linear relationship. The lowest coefficient of determination is 0.8079 which means that 80.79% of the data falls along the line of best fit. The correlation is not weaker for the west span compared to the east span so it appears that even the damaged girders behave linearly when load is located in a typical design lane.

Table 5-26: Linearity of Scenario Two Strain

Girder	R	R^2
6	0.991	0.981
6.5	0.989	0.978
7	0.999	0.999
7.5	0.999	0.998
8	0.998	0.996
8.5	0.996	0.991
9	0.999	0.998
9.5	0.999	0.999
10	0.996	0.991
10.5	0.998	0.995
11	0.988	0.977
11.5	0.993	0.987
10D	0.995	0.990
10.5D	0.996	0.993
11D	0.944	0.892
11.5D	0.971	0.943

The strain linearity for scenario two is shown above. Scenario two placed the truck over girders 8 and 10. The lowest correlation coefficient for scenario two is 0.9444 located at the damaged girder 11 in the west span. This correlation indicates a strong linear relationship. The lowest coefficient of determination is 0.8919 which means that 89.19% of the data fall along the line of best fit. The correlation coefficients for the west span girders are approximately equal to the correlation coefficients for the east span. The correlation is not weaker for the west span compared to the east span so it appears that even the damaged girders behave linearly when load is located in a typical design lane.

Table 5-27: Linearity of Scenario Three Strain

Girder	R	R^2
6	0.777	0.603
6.5	0.878	0.770
7	0.991	0.982
7.5	0.985	0.970
8	0.980	0.961
8.5	0.967	0.935
9	0.995	0.989
9.5	0.986	0.972
10	0.911	0.830
10.5	0.863	0.745
11	0.889	0.791
11.5	0.912	0.831
10D	0.784	0.615
10.5D	0.676	0.456
11D	0.850	0.722
11.5D	0.894	0.799

The strain linearity for scenario three is shown above. Scenario three placed the truck as close to the guardrail as possible. The lowest correlation coefficient for scenario three is 0.6755 located at the damaged girder 10 in the west span. This correlation indicates a weaker linear relationship than in scenarios one and two. The lowest coefficient of determination is 0.4563 which means that only 45.63% of the data falls along the line of best fit. The correlation is weaker for the west span compared to the east span so it would appear that the behavior is less linear when the load is placed next to the guardrail. Scenario three was expected to have a weaker linear relationship due to each truck being driven at different distances from the guardrail. Each truck had a different driver so it is expected that each driver would not drive at the exact same distance from the guardrail. Even with this taken into account, it would appear that the

girders behave in a more nonlinear fashion when the load is placed over the exterior girders.

If the moment-strain plot is completely linear then the material is behaving in a linear elastic fashion and has not reached capacity. Once a material's behavior goes nonlinear it shows that the material is behaving in a plastic fashion and it is near failure. The difference in linearity between the healthy and damage girders would indicate any difference in girder behavior due to the damage. Scenario two is when girders 10 and 10D experienced their maximum strain. Scenario three is when girders 11 and 11D experienced their maximum strain. Figure 5-9 shows a direct comparison in the linearity and magnitude of strain for girders 10 and 10D under scenario two loading. Scenarios one and two had all of the girders behave linearly. Figure 5-10 shows a direct comparison in the linearity and magnitude of strain for girders 11 and 11D under scenario three loading.

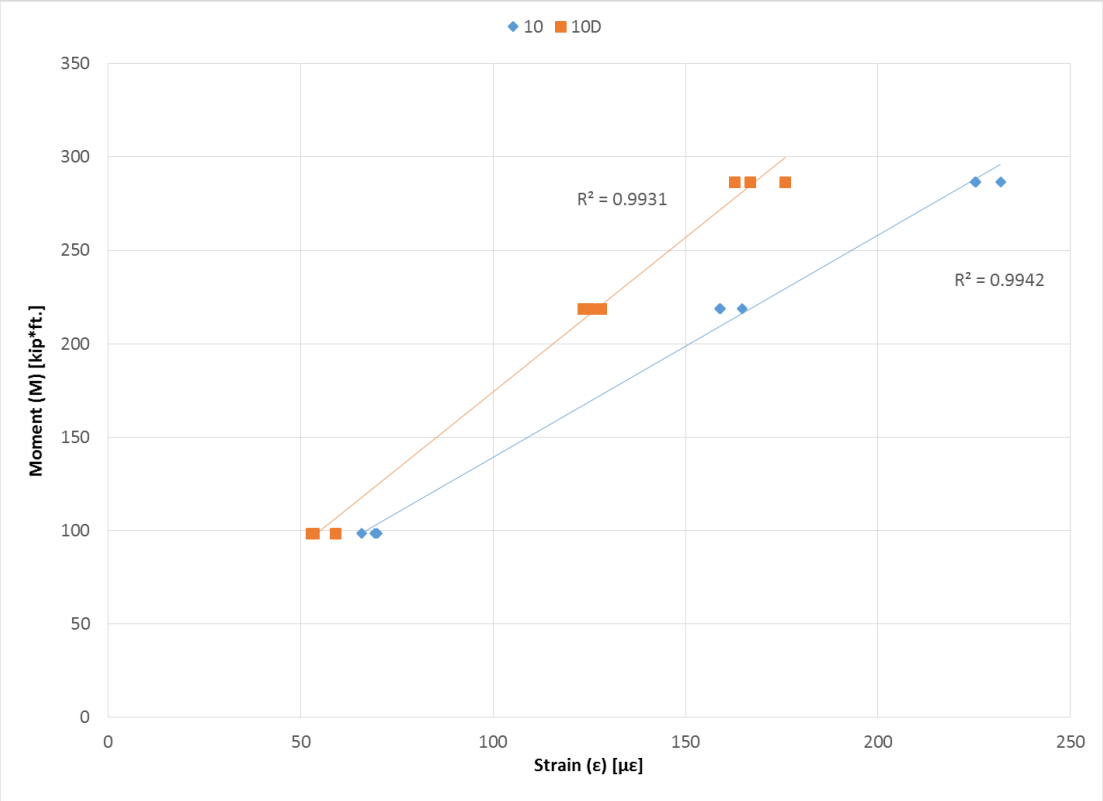

Figure 5-9: Scenario Two Damaged Girder Comparison

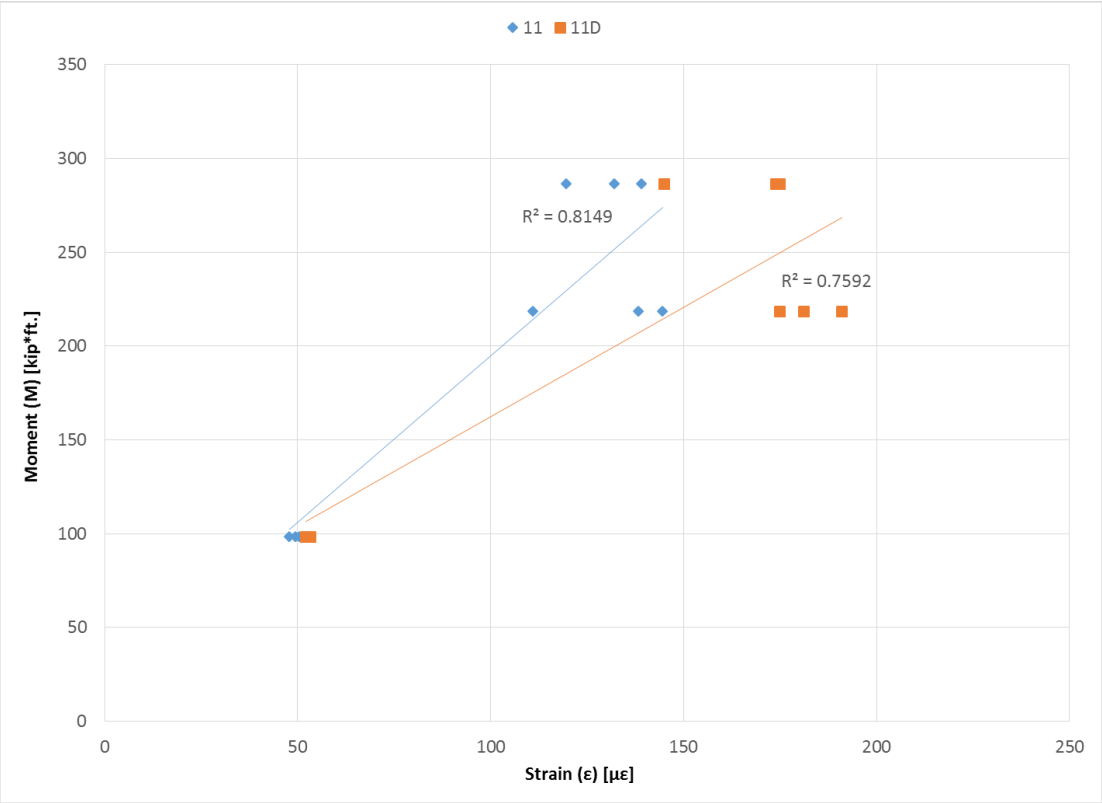

Figure 5-10: Scenario Three Damaged Girder Comparison

Figure 5-9 shows that the relationships of the moment vs. strain behavior for girders 10 and 10D are strongly linear. The healthy girder 10 sees more load than the damaged girder 10D but both have an approximately linear moment versus strain relationship. Figure 5-10 shows that the damaged girder 11D sees more strain than the healthy girder 11 for all three truck sizes. The moment vs. strain relationship for girder 11D exhibits weaker linearity than girder 11. Girder 11 has a weaker linear relationship that both girder 10 and 10D so this may indicate that the location of loading in scenario three was not as consistent as that of scenario two. More variability in the location of loading for girder three could also explain why girder 11D saw less strain for the largest moment in Figure 5-10.

Although the data in Figure 5-10 does not exhibit a strong linear relationship for girder 11D it appears to be a function of the location of loading and not because the girder is nearing its capacity. If the girder was nearing its capacity then it would be expected that the strain for the heaviest truck would be much larger than the strain for the half-full truck, this is not the case though. The exterior girder is also difficult to load due to the bridge geometry and the presence of the barrier rail. Figure 5-11 shows the truck location necessary to load the exterior girders. Due to the difficulty in loading and the magnitude of the strain under the exterior loading, the damage in the west span is not a concern. Under normal traffic circumstances the damaged girder in the west span would not see a significant amount of load. Girders 10 and 11 are outlined in Figure 5-11 below and called out as "G10" and "G11" respectively.

Figure 5-11: Loading the Exterior Girder

5.3.4 Strain Comparison Charts

Data from the east span in Tables in Section 5.3.1 is presented in Figures 5-12 through 5-15. Scenarios one through three are plotted on three separate figures where the average strain for each girder is compared for each truck size. The only known data is plotted as a data point for each girder, the straight lines drawn between each data point provide an easier way to understand the image. The downward pointing arrows represent where the wheel lines of the truck were for that loading scenario.

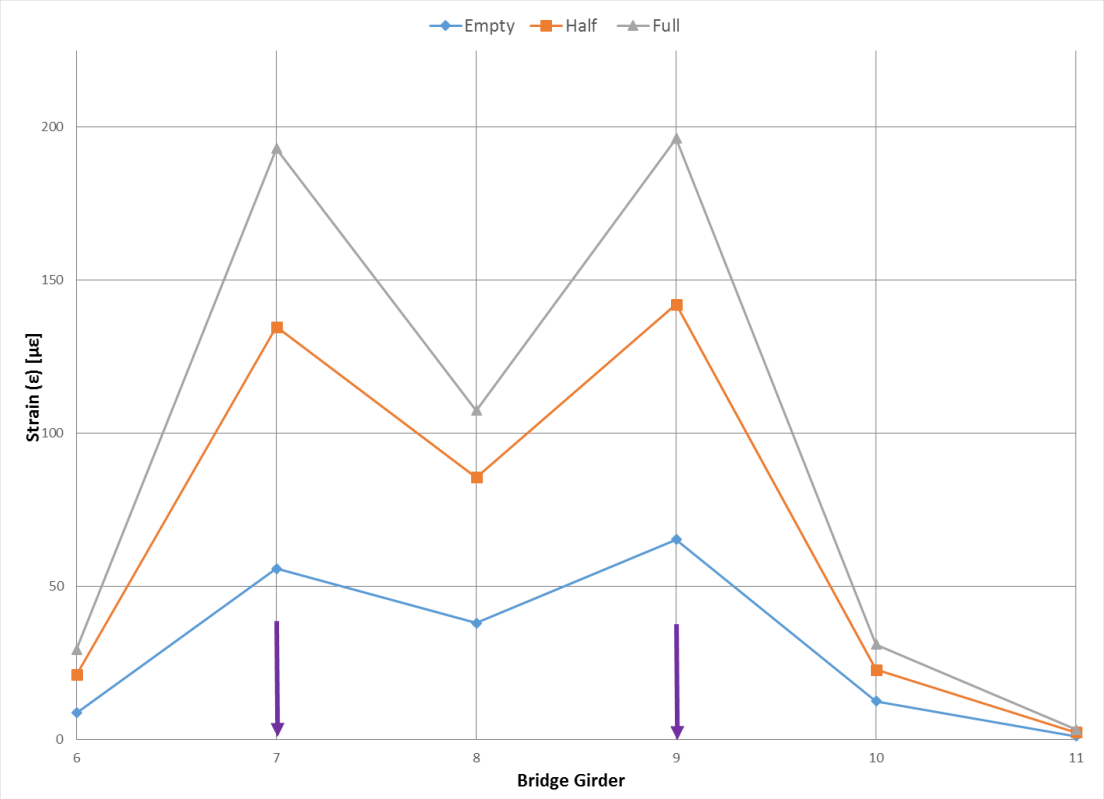

Figure 5-12: Scenario One Strain Comparison

Figure 5-12 above shows the strain associated with scenario one loading. The maximum strains in the span for all three truck sizes was directly under the wheel lines. All three truck sizes follow the same pattern where a negligible strain was experienced in

the exterior girder 11 and the strain experienced by girder 6 and 7 was mirrored in girders 9 and 10.

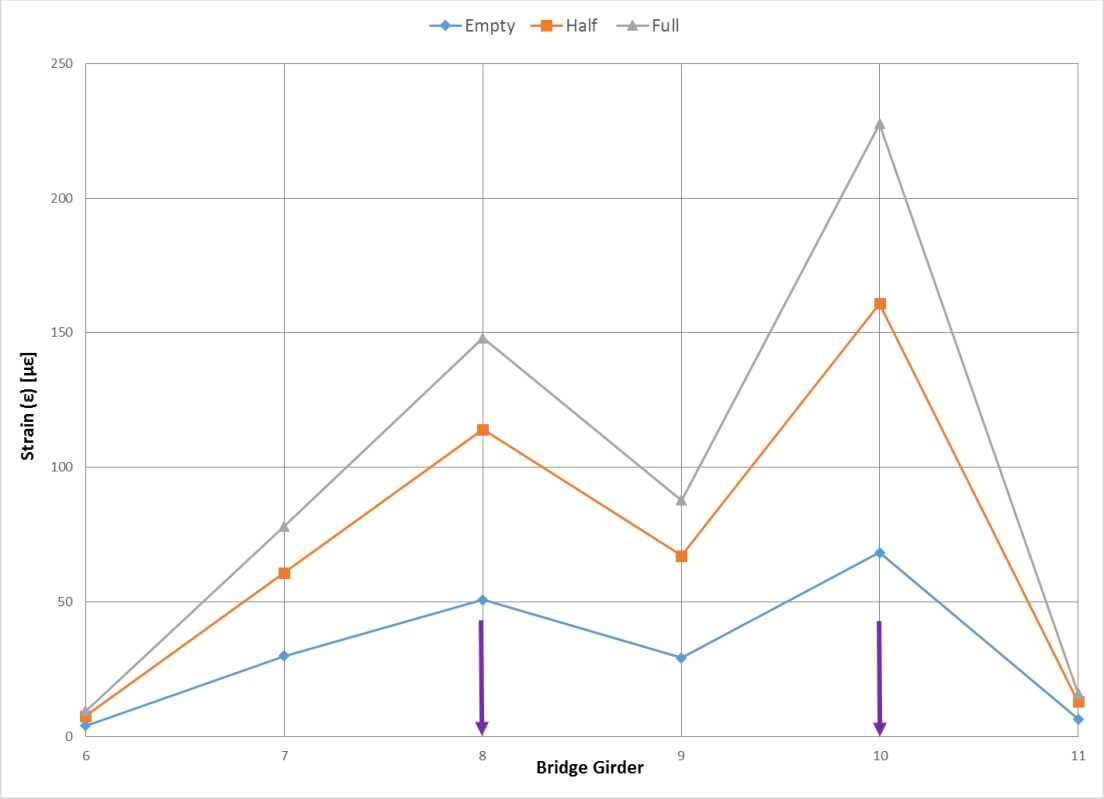

Figure 5-13: Scenario Two Strain Comparison

Figure 5-13 above shows the strain associated with scenario two loading. The maximum strain in the span for all three truck sizes was directly under the wheel lines. All three truck sizes follow the same pattern where a negligible strain was experienced in the exterior girder (girder 11). All three truck sizes saw the largest strain in girder 10 and a smaller strain under the other wheel line in girder 8. The gap between the strain in girders 8 and 10 increased with the increase in truck size. A negligible strain was seen in girder 6 for all truck sizes and the strain experienced in girders 7 and 9 were

approximately equivalent. Scenario two does not exhibit the same symmetry that scenario one showed.

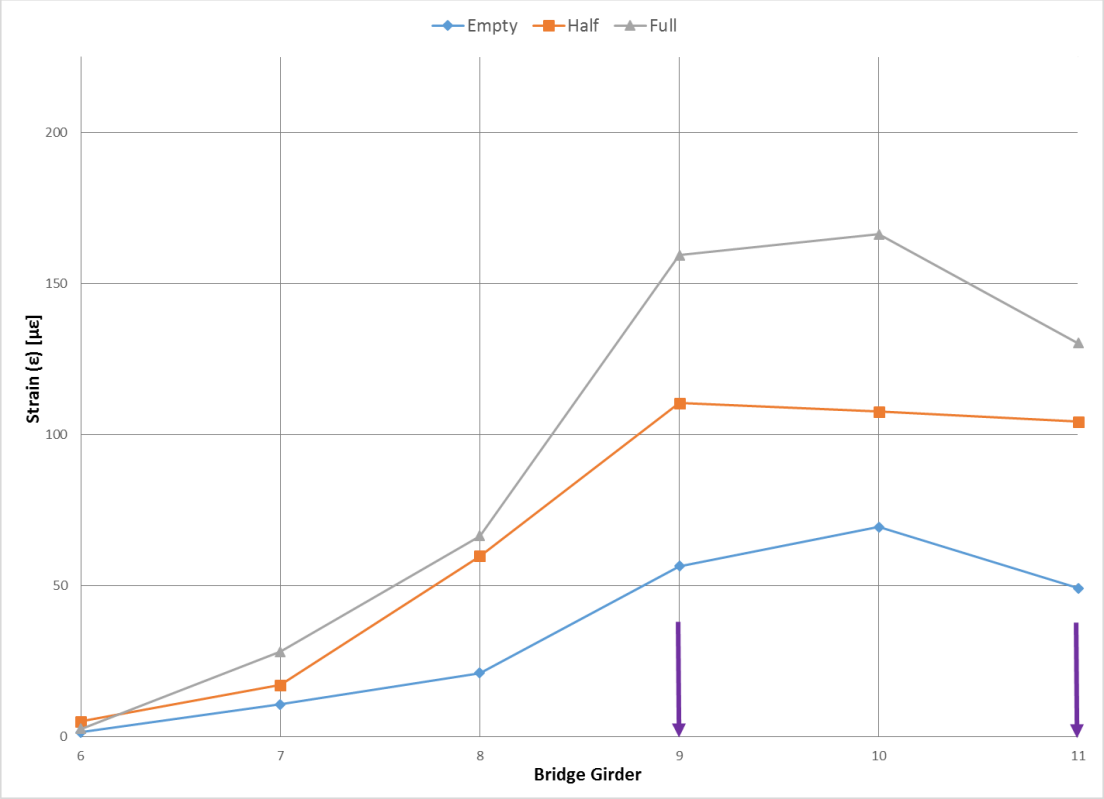

Figure 5-14: Strain Three Strain Comparison

Figure 5-14 above shows the strain associated with scenario three loading. Unlike in the other two scenarios, the maximum strain did not always occur under the wheel lines. The maximum strains for the empty and full truck were under girder 10 and the maximum strain for the half-full truck was under girder 9. It was theorized that the exterior girder 11 may have attracted more load due to the increased stiffness provided by the barrier rail adjacent to girder 11. This was not the case though, girder 11 never saw more load than girders 9 or 10. The strain quickly dropped off past girder 9 though and the strain in girder 6 was negligible for all three truck sizes.

5.3.5 Symmetry of Bridge System

Figure 5-15 shows a comparison of the strain in scenarios two, four, and five from the full truck. The solid downward arrows show the location of the truck for scenarios two and five. The locations of the trucks and instrumentation for scenarios two, four, and five are shown in Figure 5-16.

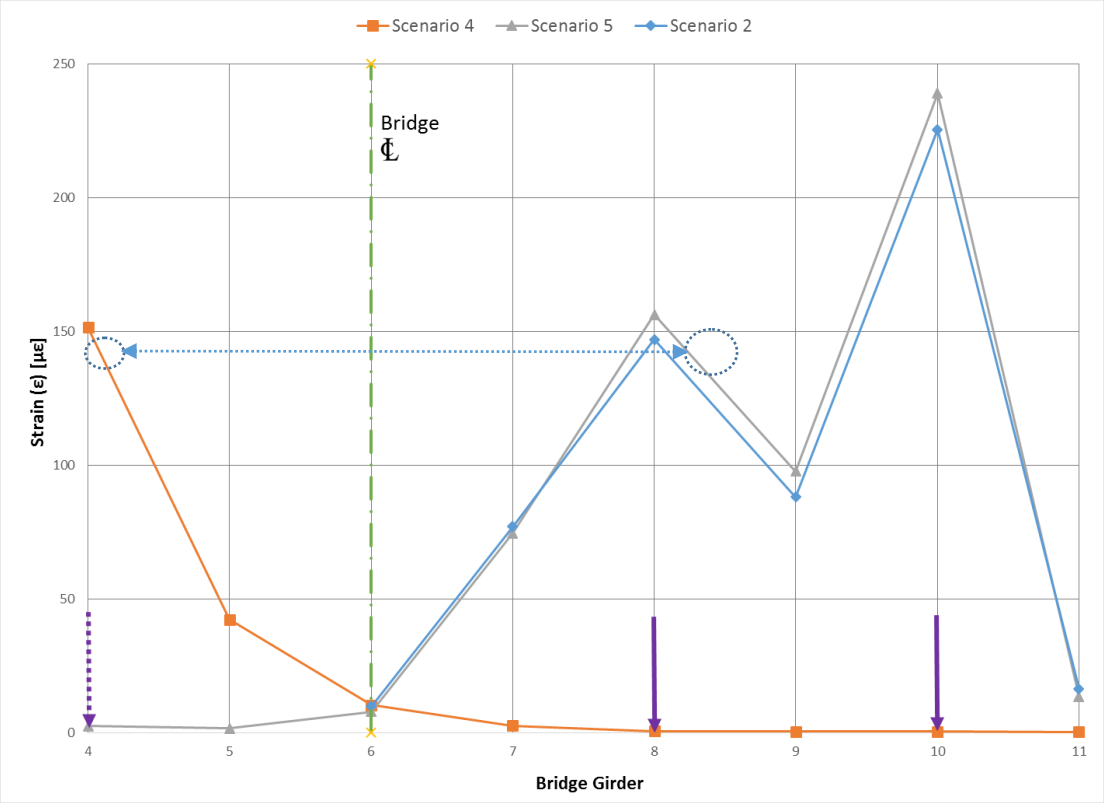

Figure 5-15: Strain Symmetry

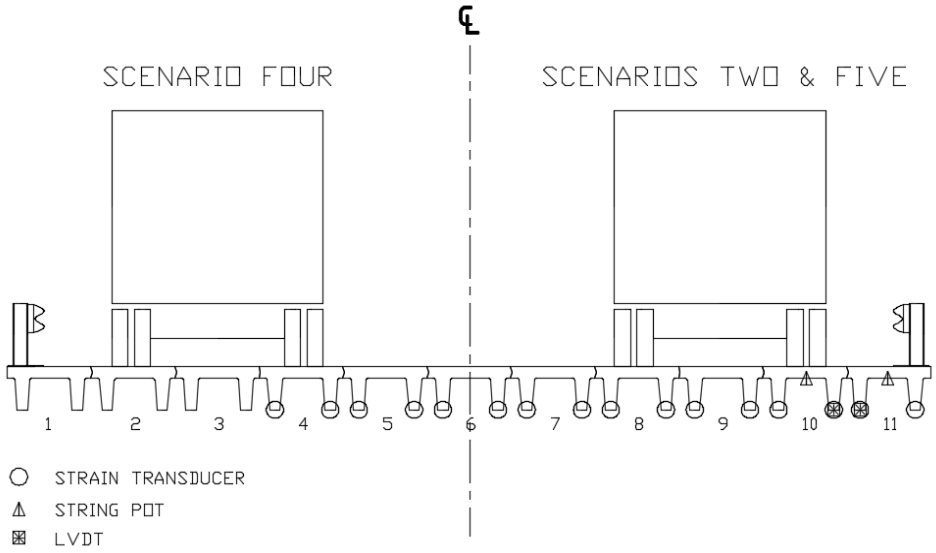

Figure 5-16: Truck Positions for Scenarios Two, Four, and Five

The dashed arrow represents the innermost wheel line of the truck in scenario four. The strains from scenarios two and five are almost identical which is expected given the identical loading conditions. The strains for girder 8 in scenarios two and five are similar to the strain for girder 4 under scenario four. The three data points representing these strains are circled with an arrow drawn between in the figure above. The loading scenarios are identically mirrored about girder 6 so it is expected that the strain seen by the girders would be similarly mirrored. For all three scenarios, the strain is negligible for the girders on the opposite side of the load from girder 6. These negligible strains away from the load show that the strain at the non-instrumented girders is small and not crucial to consider when calculating and comparing DFM's. The symmetry about girder 6 for scenarios two and five compared to scenario four confirm that it was sufficient to concentrate instrumentation on one side of the bridge.

Concentrating instrumentation on one side of the bridge requires a smaller number of strain transducers and can be applied to future instrumentation plans for nondestructive bridge testing.

5.4 Load Distribution Results

5.4.1 AASHTO DFM

In Section 2.3.1 it was discussed that AASHTO presents design equations for determining the distribution factors for moment. These equations were used to determine the design distribution factors for the Five Forks Bridge. The DFMs calculated using AASHTO LRFD Table 4.6.2.2.2b-1 are presented in Table 5-28. An excerpt from the AASHTO LRFD Table can be found in Appendix C.

Table 5-28: AASHTO DFMs

Girder	DFM
Interior	0.293
Exterior	0.293

Typically the exterior girder DFM is determined using the Lever Rule from Section 4.6.2.2.1 AASHTO LRFD. This equation cannot be accurately used for the girders in the Five Forks Bridge. The Lever Rule assumes that a deck/slab carries the load between girders and that a hinge is allowed to form that transfers shear but not moment. There is no slab present at the Five Forks Bridge, and a shear-carrying hinge cannot form between the exterior and interior girder. Because of this, the Lever Rule was not used to find the exterior girder DFM. The AASHTO equation was used for the exterior DFM in addition to the interior DFM. The layout of the Lever Rule's application for the Five Forks Bridge can be seen in Figure 5-17 below. If applicable, the moment

would be taken around the first interior girder (2) which results in a negative contribution from the exterior girder (1).

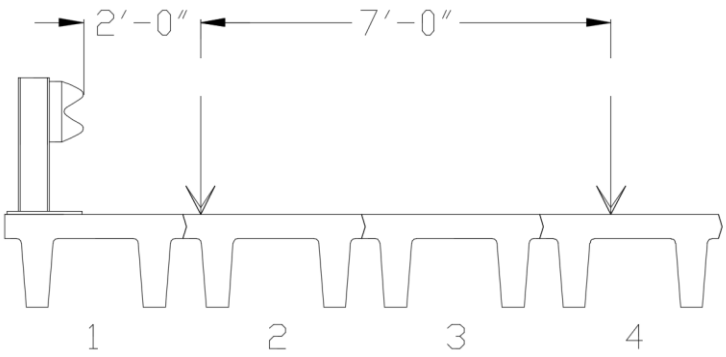

Figure 5-17: Lever Rule Illustration

Although not used, the Lever Rule calculations for the exterior girder DFM as well as the AASHTO followed calculations for the interior girders can be found in Appendix C.

5.4.2 Procedure for Experimental DFM

Section 2.3.2 discussed how to experimentally determine the DFM using the results from a nondestructive live load test. The deflection data was discarded from the test so the strain data was used to determine the experimental DFMs. All Experimental DFMs were calculated using the strain transducers attached to the east span. The maximum DFM for each truck run was calculated, and then the maximum DFM for each loading scenario was considered in Section 5.4.3.

5.4.3 Experimental DFM

Table 5-29 below shows the maximum DFM found for each of the loading scenarios except for scenario six. DFMs are not typically calculated from dynamic testing because it is more difficult to ensure the loading occurs at the same location for all

of the truck crossings. The maximum DFM from each truck run can be found in Appendix D.

Table 5-29: Maximum DFM for Each Loading Scenario

Distribution Factor for Moment			
Scenario	**Experimental**	**Assumed**	**AASHTO**
One	0.374	0.5	0.293
Two	0.418	0.5	0.293
Three	0.394	0.5	0.293
Four	0.438	0.5	0.293
Five	0.414	0.5	0.293

The DFMs in the table above all fall within the range from 0.37 to 0.44. The only data manipulation needed was for scenario four. There was no strain transducer under girder 2 where the other wheel line was located. The average total strain experienced by girders directly under the truck was found for each full truck run. The girder 4 strain recorded in scenario four was subtracted from this average and the remaining strain was assigned to girders 1, 2, and 3. The equation to determine experimental DFMs was then used as normal.

5.4.4 Comparison of AASHTO and Experimental DFM

Figure 5-18 below shows a comparison of the experimentally determined DFMs against the initial assumption for the DFM and the theoretical DFM from AASHTO LRFD.

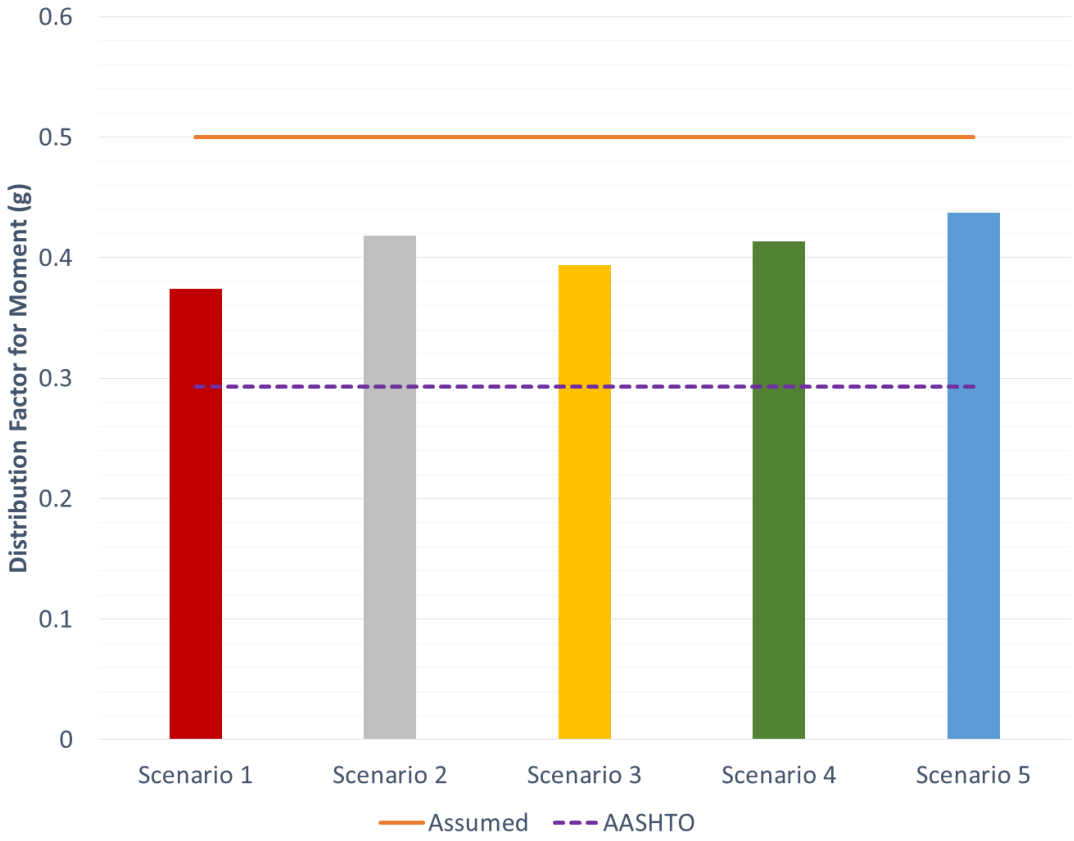

Figure 5-18: DFM for Each Loading Scenario

The AASHTO DFM presented in the figure above is taken from Table 5-28, and represents the DFM for interior and exterior girders. The initial assumption for DFM was taken as the worst case scenario, 0.5. It was assumed that if there was absolutely no load sharing between girders then the maximum load that a single girder could take would be one wheel line, or half of the overall truck weight.

The data falls within the bounds set by the AASHTO-determined DFM (0.293) and the assumed for the DFM. The experimental values are all higher than the DFM determined from AASHTO. AASHTO LRFD Table 4.6.2.2.2b-1, where the equation for

the theoretical DFM was found, assumes a monolithic structure and, therefore, minimal relative vertical movement between adjacent girders.

To evaluate the applicability of the AASHTO DFMs to the Five Forks Bridge, vertical movement of the girder-to-girder joints was measured during loading with LVDTs. No relative movement between girders would indicate very good load transfer between girders which facilitates load sharing. Diagnostic tests conducted by Kedar Halbe that measured relative vertical displacement of adjacent box beam girders recorded no relative vertical displacements greater than 0.03 in. The experimental DFMs calculated from the diagnostic tests were very similar to the theoretical values calculated from AASHTO LRFD. The closeness of the experimental and theoretical DFMs in Kedar's project shows that a relative vertical displacement in the range of 0.03 in. indicates good load transfer. (Kedar 2014). Figure 5-19 below shows the relative vertical displacement measured by the LVDTs in the nondestructive test. The setup of the vertically oriented LVDTs is shown in the corner of Figure 5-18.

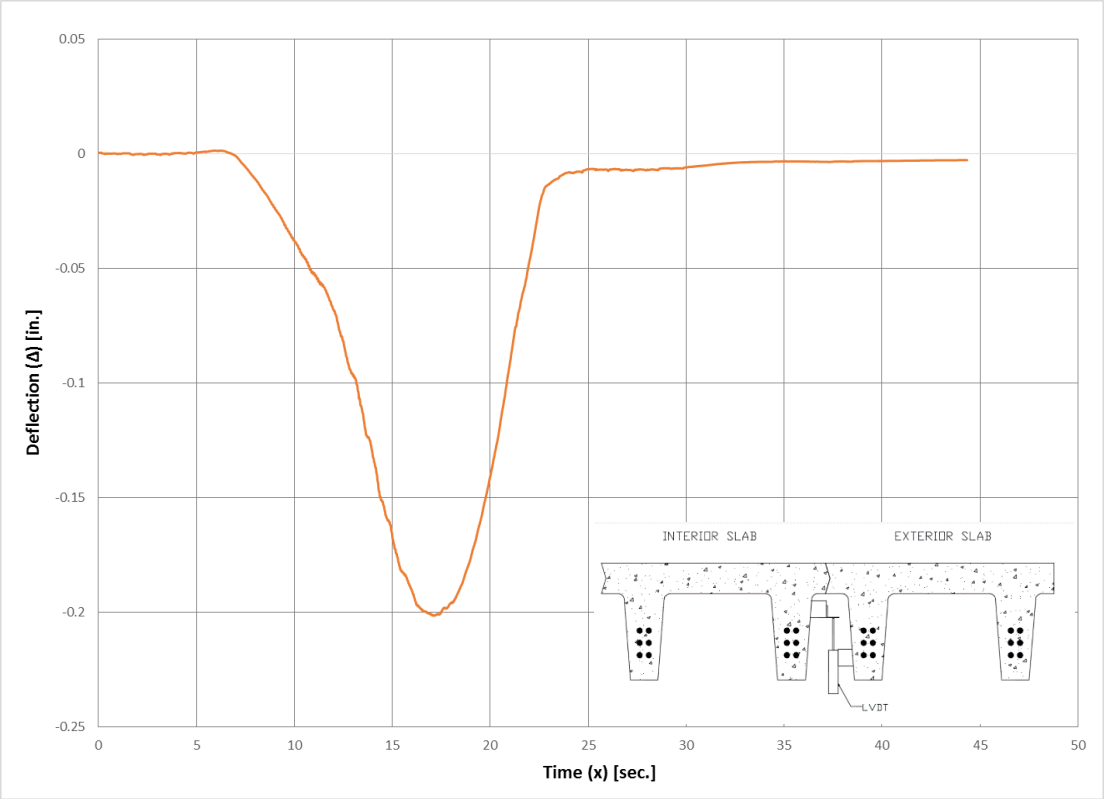

Figure 5-19: LVDT Movement from Scenario Two

The relative displacement of 0.2 in. compared to the displacement of 0.03 in. measured in Kedar's test shows that there was indeed a large vertical displacement between girders. Since there was a lot of relative movement it indicates load transfer was not good and a poor connection exists. The result of this behavior would be that the AASHTO equations would yield lower DFMs than measured. All of the experimentally measured DFMs fell below the initial assumption (DFM = 0.5) which indicates that there is some degree of load sharing.

The significance of these results is that the condition of load transfer in the field is lower than what the AASHTO equations assume since the experimental DFM is greater than the AASHTO DFM. The Five Forks Bridge does have tie rods at quarter points that

are intended to facilitate load sharing, but these tie rods are in derelict condition and do not fulfill their purpose. An analysis of the Five Forks Bridge using the AASHTO LRFD DFMs would be unconservative. This finding proves that for the Five Forks Bridge, and bridges similar to it, the AASHO equations may not be appropriate for the calculation of DFMs. A load test may be conducted to determine the experimental DFM's or an assumption of 0.5 (one wheel line) must be made for the DFM.

5.5 Dynamic Load Allowance Results

5.5.1 AASHTO IM

As discussed in Section 2.2, the dynamic load allowance accounts for the increased bridge response from dynamic loading. AASHTO provides a single factor of 1.33 that can be applied to the static load to conservatively simulate the effect of dynamic loads.

5.5.2 Procedure for Experimental IM

An experimental DLA can be determined from the results of a nondestructive test as well. The comparison of the bridge response from a pseudo-static test and a dynamic test can determine the unique impact factor for that bridge and loading. The following equation uses experimental deflection data from a nondestructive test to calculate the IM:

$$IM = \frac{D_{dyn}}{D_{sta}}$$

Equation 5-1

Where D_{dyn} is the response due to the dynamic loading and D_{sta} is the response due to the static loading. IM is the dynamic load allowance that is used as an

amplification factor. Either deflection or strain can be used as the chosen response, but strain was used in this analysis since the deflection data was discarded.

5.5.3 Experimental IM

The dynamic load allowance is of interest at the location of maximum response since it will be amplified. The dynamic loading scenario placed the wheel lines over girders 7 and 9. Figure 5-20 below shows the static and dynamic strain from girder 9. A dimension on the plot highlights the difference between the dynamic and pseudo-static responses. These strains are averages of both girder 9 stems for all three runs.

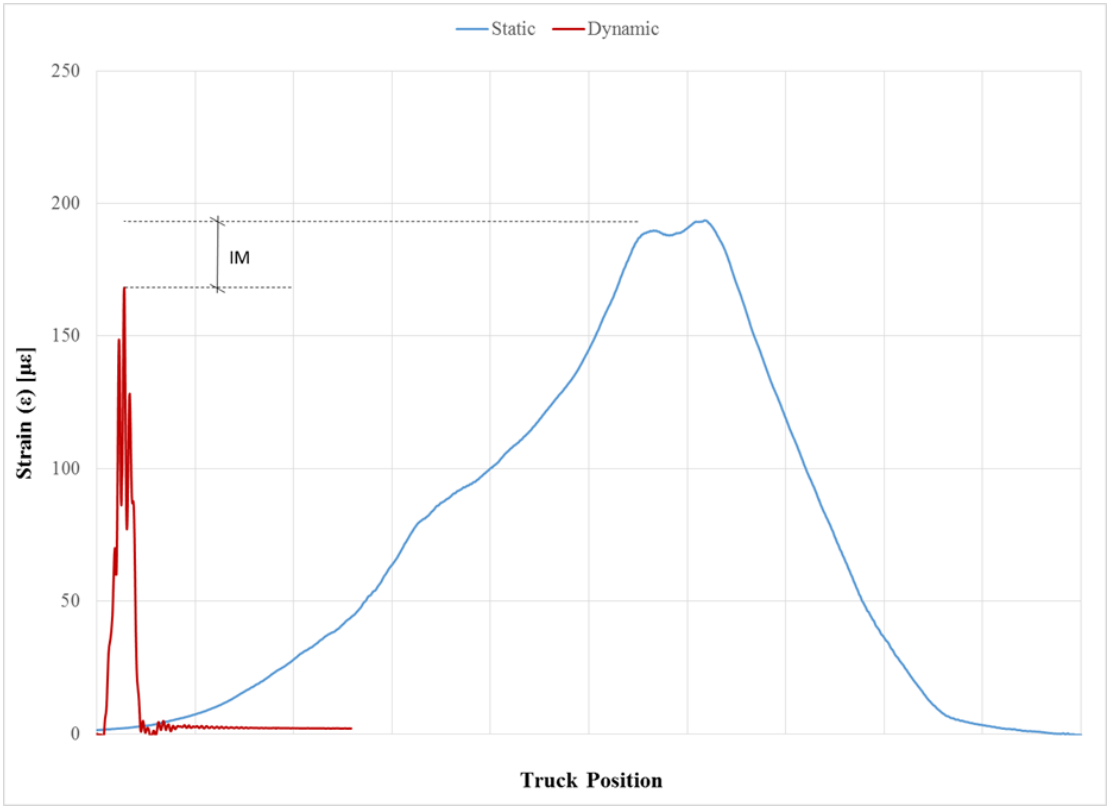

Figure 5-20: Static and Dynamic Strain Results

Figure 5-21 below superimposes the dynamic strain recorded by girder 9 over top of the static response from girder 9. The dynamic strain data was "stretched" so the truck position of the dynamic and static tests aligned.

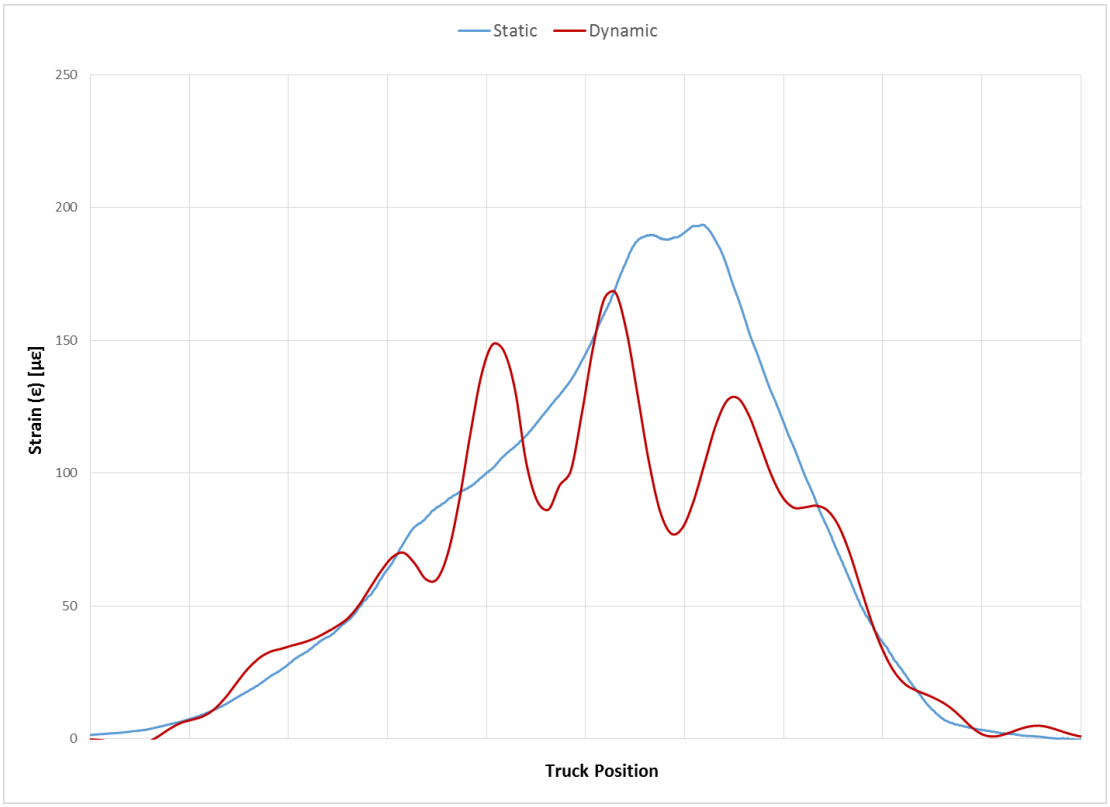

Figure 5-21: Dynamic Strain Superimposed over Static Strain

Figure 5-21 shows that the strain caused by the dynamic test was less than the strain due to the static loading. A similar plot for girder 7 can be found in Appendix D.

5.5.4 Comparison of AASHTO and Experimental DLA

The AASHTO IM is conservative in most cases so it is assumed that the experimental IM will be less than the 1.33 that AASHTO allows. The Five Forks Bridge experimental IM for girder 9 came out to be approximately 0.871. There are a variety of factors that could result in a dynamic response being less than the static response.

Section 2.2 mentioned multiple factors that affects IM such as bridge frequency, span length, truck weight, truck suspension, approach quality, and roadway roughness. All of these variables can't be quantified for the Five Forks Bridge and the dump trucks used in the scope of this project. A similar result occurred in a test conducted by Structural Testing Incorporated where a negative dynamic load effect was attributed to the combination of a short span and the contours of the approach (STI 1998). A picture of the approach for the Five Forks Bridge can be seen below in Figure 5-22.

Figure 5-22: Five Forks Bridge Approach

The approach is highlighted by the yellow circle in the picture above. It can be seen that the there is a depression in the approach of the bridge. This depression with the short span may be the reason for the negative impact factor.

5.6 Load Rating and Permitting Results

The goal of load rating, as discussed in Section 2.5, is to determine the true strength of a bridge and uncover any reserve capacity the structure may possess. The Five Forks Bridge was load rated because the SCDOT had questions about its true capacity and whether or not the bridge needed to be posted. The MBE provides a guide for design load rating and legal load rating. Section 8 of the MBE outlines provisions for modifying the load rating factor using the results of a nondestructive load test. Two types of design load rating are described in the MBE, inventory and operating. Inventory load rating approximates the design load level under normal traffic conditions and the operating load rating gives the maximum possible load that the bridge is rated for. Both the inventory and operating load ratings are carried out for the AASHTO design load, an HL-93 truck. If a bridge has either an operating or inventory rating factor less than one after modification then the bridge must be rated for legal loads. The process is the same as for design load rating but legal load rating only uses one rating factor. In addition to this the bridge is rated for a set of standard AASHTO legal loads and the live load factor is a function of the bridge's average daily traffic. The Five Forks Bridge was rated for both design and legal loads.

5.6.1 Procedure for Load Rating from Nondestructive Test

The MBE equation for bridge load rating is outlined in Section 2.5.2. The general load rating was completed using the load from the tandem axle of the HL-93 truck. The span length of 30 ft. results in the front axle of the HL-93 truck sitting at or near the supports of the bridge when the maximum moment occurs, therefore, only the tandem

axle of the HL-93 truck was considered for the maximum moment. The original load rating was conducted for the initial and assumed conditions of the bridge so a DFM of 0.5 was used. For the modified load rating factor, the experimental DFM was used. A load rating for the inventory and operating levels was calculated for the Five Forks Bridge. The calculations for determining both the original and modified load ratings can be found in Appendix C.

5.6.2 Modified Load Rating Results

Once the nondestructive test of the Five Forks Bridge was completed the experimental strain values were used to modify the original load rating. The full steps to determine the modified load rating can be found in Section 8 of the MBE, where the original load rating is modified by two separate factors, K_a and K_b. K_a is a comparison of the expected theoretical strain and the recorded experimental strain from the test load. In determining the K_a factor for this load rating the strain from the full truck, 25 tons, was used as the test load. The largest experimental DFM (0.44) from Table 5-29 was used in the calculation of K_a to provide a conservative modification using the experimental results. The equation used to solve for K_a is:

$$K_a = \frac{\varepsilon_c}{\varepsilon_T} - 1$$

Equation 5-2

Where ε_T is the maximum member strain measured during load testing and ε_c is the corresponding calculated strain due to the test vehicle at the same truck position that caused ε_T. K_a was found to be equal to 0.884.

K_b estimates the level to which the results of the nondestructive load test can be extrapolated to 133% of the rating vehicle load. In this case the design load is the tandem axle of the HL-93 truck. An excerpt from Section 8.8.2 of the MBE that shows the values for K_b can be found in Table 5-30 below.

Table 5-30: K_b Values

Can member behavior be extrapolated to 1.33*W*?		Magnitude of Test Load			
Yes	No	$\frac{T}{W} < 0.4$	$0.4 < \frac{T}{W} \leq 0.7$	$\frac{T}{W} > 0.7$	K_b
√		√			0
√			√		0.8
√				√	1.0
	√	√			0
	√		√		0
	√			√	0.5

In Table 5-30 "T" is the unfactored effect from the 25 ton truck and "W" is the unfactored effect from rating load of the HL-93 truck. "T" for this project was the 126 kip*ft. moment caused by the 25 ton truck and "W" was the 148 kip*ft. moment caused by the HL-93 load set. The channel's ability to take up to 133% of "W" was determined by comparing the moment caused by the HL-93 truck to the experimental cracking moment determined in the channel test. The theoretical moment caused by the HL-93 truck was "W" and the experimental cracking moment from the channel test was 115 kip*ft. The factored moment equal to 133% of 148 kip*ft. is greater than 115 kip*ft. Because 133% of W is greater than the theoretical cracking moment, the member behavior can't be extrapolated to 1.33W. It was determined that the channel behavior could not be extrapolated to 1.33W but the ratio of T/W = 0.85 which is greater 0.7 so K_b was taken as 0.5. These two factors, K_a and K_b, were taken into account when using the

results from the nondestructive and channel tests. The full calculations for the modified load rating can be found in Appendix C.

Table 5-31 below shows a comparison of the inventory and operating design load ratings and the legal load rating for both the modified and unmodified methods.

Table 5-31: Load Rating Comparison

	Inventory		Operating		Legal	
	Original	Modified	Original	Modified	Original	Modified
DFM	0.5	0.44	0.5	0.44	0.44	0.44
IM	0.33	0.33	0.33	0.33	0.33	0.33
Rating Factor	0.523	0.75	0.678	0.98	0.79	***1.14***

The table above displays all six load rating factors that can be calculated using the MBE. The table also provides the impact factor and distribution factor for moment that alter the calculations of the original and modified load rating factors. The IM of 0.33 was used because it is the value that AASHTO provides. Using the AASHTO provided IM of 0.33 provided conservative results. The original values for the inventory and operating load rating were both below one so further investigation was required.

The experimental strain in the girders was much less than the theoretical prediction which allowed for an increase in the modified load rating factor. The increase provided by the experimental results was not enough though, the modified ratings were still below one. The legal load rating process in the MBE was then followed. Table E6.A-1 in the MBE provides the maximum moment caused by the legal load trucks for a specific span length. The maximum moment was found for the 30 ft. span of the Five Forks Bridge. The evaluation live load factor is different for legal load rating compared to design load rating. The evaluation live load factor was calculated using the average

annual daily traffic (AADT) of 750 for the Five Forks Bridge. The AADT value was provided by the SCDOT. The unmodified legal load rating factor was less than one, but the modified factor was greater than one. The weights and dimensions of the trucks used for legal load rating can be found in Appendix C.

5.6.3 Bridge Posting

If the Five Forks Bridge was load rated without any modifications from a nondestructive test then it would have to be posted. The unmodified rating factors for the inventory, operating, and legal loads are 0.523, 0.75, and 0.79, respectively. These all fell short of the required load rating factor. To determine the rating of the bridge in tons the rating factor is multiplied by the weight in tons of the vehicle used for rating. The vehicle used for the design load rating is 36 tons and the vehicle used for the legal load rating is 25 tons. The unmodified design load ratings of 0.523 and 0.678 would result in a safe load capacity of 18.8 and 24.4 tons, respectively. The unmodified legal load rating of 0.79 would result in a safe load capacity of 19.8 tons. The operating load rating factor would be so the Five Forks Bridge would have to be posted with a weight limit of 24.4 tons if a nondestructive test had not been conducted.

Only one rating factor of the six calculated needed to be greater than one in order to satisfy current AASHTO LRFD standards and not require posting though. Using strain data from the nondestructive test resulted in a 44% increase in the legal load rating from 0.79 to 1.14. The final legal load rating factor for the Five Forks Bridge is 1.14. Any load rating factor greater than one is sufficient to satisfy the MBE legal load rating requirements. There is no need to post the bridge or calculate any further rating factors.

The bridge did not pass the inventory design load rating though, so all legal loads that cross the bridge must comply with the federal weight limits and Formula B (the FHWA bridge formula).

5.7 Channel Test Results

The channel girder test was covered in Section 2.6. The main purpose of the test was to find the moment vs. deflection behavior of a typical channel girder up to and including flexural failure. Failure was confirmed when the moment-deflection plot plateaued and it was noted that the concrete on top of the girder crushed. Compressive and tensile surface strain were recorded at mid-span as well as the mid-span deflection of the channel. Strain values from the nondestructive test were compared to the laboratory test moment-strain plots of the strain transducers on the bottom of the girder.

The same string pots used in the nondestructive test of the Five Forks Bridge were used in the channel test. No odd behavior was noticeable in the plots of the deflection so the deflection data for the channel tests was used. The moment-deflection plot from the channel test can be seen below in Figure 5-23.

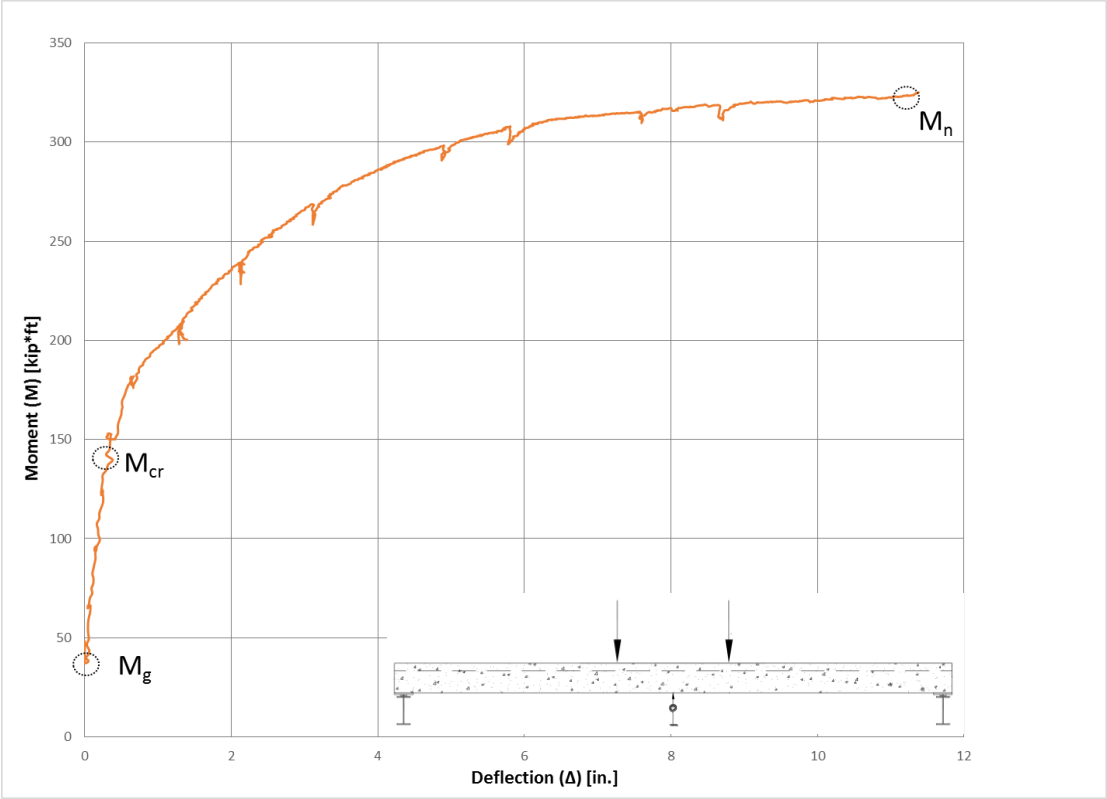

Figure 5-23: Moment-Deflection Plot

Three points are marked on the moment-deflection plot above. The moment caused by the self-weight of the channel is marked as M_g. This moment is present in the channel before the external moment is applied so the plot starts at this value of 40 kip*ft. The experimental cracking moment, M_{cr}, is marked at the 150 kip*ft. mark. This value is found by observing the point where the moment-deflection plot turns nonlinear and noting the point at which cracks started to form during the laboratory test. The last point marked is the nominal strength of the channel, M_n. The nominal strength of the channel is the point of highest moment resistance once the deflection data has levelled off. The nominal strength for the channel was 324 kip*ft.

5.7.1 Channel Test Strain Results

Strain values were recorded for the channel test and the nondestructive test of the Five Forks Bridge. A comparison of the surface strains are plotted in Figure 5-24 below.

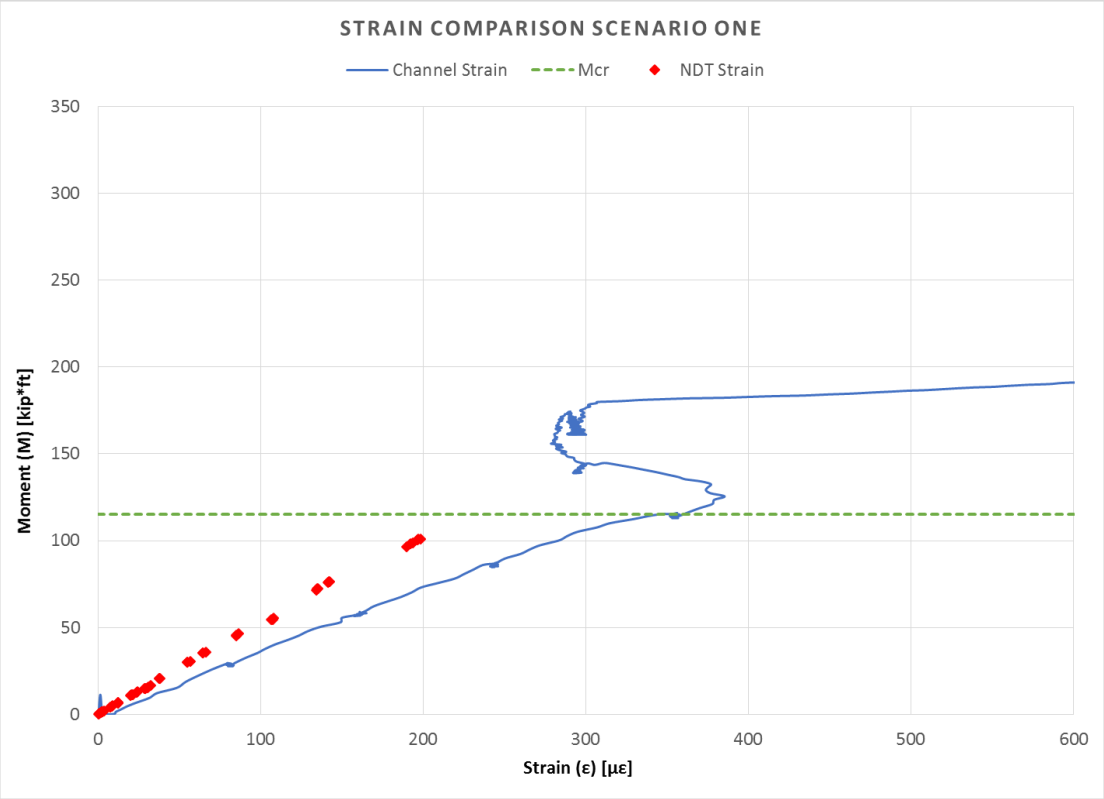

Figure 5-24: Comparison of NDT and Channel Strains

The solid blue line in the plot above is the tensile strain from the average of the two strain transducers attached to the bottom of the channel girder stems. The red diamonds are the maximum average strain points for girders 6 through 11 of the Five Forks Bridge under loading scenario one. The maximum strain for each girder for each run and under all three truck sizes was plotted against the moment it experienced. The moment each girder experienced was determined by taking the total moment caused by each truck size and multiplying it by the girder's DFM as determined using the strain

transducer results for the respective truck crossing. In total there were 9 data points for each girder, three per run for three truck sizes. The experimental cracking moment determined from the channel test is plotted above at 115 kip*ft.

The plot of the strain experienced during the nondestructive test shows the range of strain that the girders experience during typical service conditions. The plot of the strain from the channel test yields a good approximation of when the crack formed in the stems of the channel. The strain plot for the channel was linear until approximately 115 kip*ft. when the applied moment caused the strain to behave nonlinearly. In this comparison of strain it can be seen that no girder from the nondestructive test experienced a moment as large as 115 kip*ft. and therefore the Five Forks Bridge girders were within the linear elastic range. Linear elastic behavior indicates that the girders still have excess capacity beyond the demand from the truck load. The factor of safety against cracking for the 25 ton truck used in the nondestructive tests can be seen below in Table 5-32. A factor of safety was calculated for each scenarios one through three. The experimental cracking moment was divided by the maximum moment seen by a girder in each scenario to calculate the factor of safety.

Table 5-32: 25 Ton Truck Factor of Safety

Scenario One	1.14
Scenario Two	1.00
Scenario Three	1.27

The plot of the strain against the moment also shows the respective stiffness of the girders from each test. The channel test experienced larger strains for the same moment compared to the bridge test so the individual girder has less stiffness than the overall

bridge superstructure. Less stiffness means that the individual channel will deform more under the same load. The presence of the guardrail and the condition of the bearings may have increased the stiffness of the girders at the bridge. Similar strain comparison plots for scenarios two and three can be found in Appendix D.

5.7.2 Comparison of Theoretical and Experimental Strengths

The deflection data from the nondestructive test couldn't be used due to unexplained behavior in the data, but the deflection data from the channel test was usable. The deflection data was used to create moment-deflection plots that could be used to determine the approximate cracking moment and nominal strength of the channel. These experimental values could then be compared to the theoretical values. Figures 5-25 and 5-26 below shows moment-deflection plots from the channel test. Figure 5-25 below is a comparison of the experimentally and theoretically determined nominal strengths of the channel.

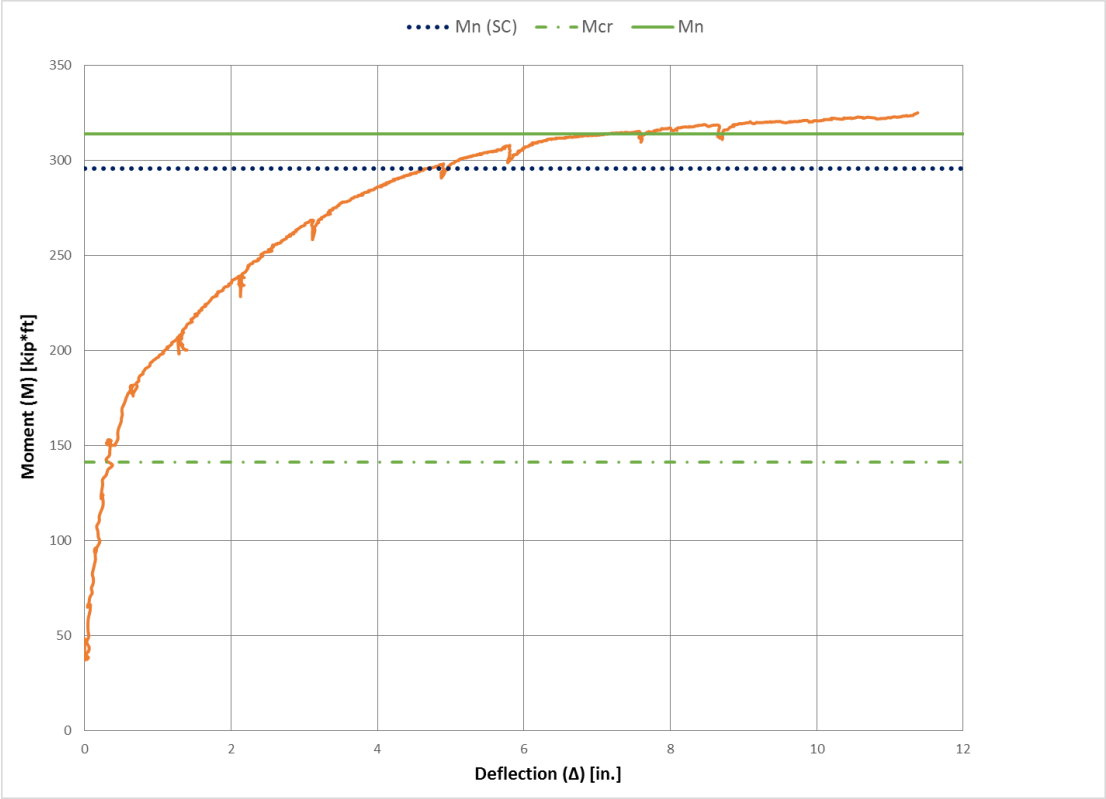

Figure 5-25: Moment vs. Deflection Behavior

The figure above shows the full moment-deflection plot from the channel test. There are three "benchmarks" plotted as well. These are the calculated cracking moment from AASHTO LRFD equation 5.7.3.3.2-1 (M_{cr}), the calculated nominal strength using the strain compatibility method (M_n SC), and the calculated nominal strength from AASHTO LRFD equation 5.7.3.2.2-1 (M_n). These equations were solved using the girder and strand properties determined in the investigation detailed in Section 5.1. The details of these calculations can be found in Appendix C.

The calculated cracking moment is 141 kip*ft. This moment appears to be slightly smaller than the experimental cracking moment from the plot. The deflection plot goes nonlinear around 150 kip*ft. This value of 150 kip*ft. includes the moment

caused by the self-weight of the girder. The strain plot from Figure 5-24 does not include the self-weight, so if the 40 kip*ft. of self-weight is subtracted from the experimental cracking moment in Figure 5-25 then this value is similar to the approximate cracking moment of 115 kip*ft. determined from the strain plot in Figure 5-24. Most design equations are conservative in nature so it would be expected for the experimental cracking moment to be slightly larger than the theoretical cracking moment.

Due to the uncertainty in the girder and strand properties, two different approaches were used to determine the calculated nominal strength of the channel. The current AASHTO LRFD equation for nominal capacity was used as well as the strain compatibility approach outlined in Nilson's *Design of Prestressed Concrete*. Nilson's strain compatibility value may be different from current methods due to the time period that the strain-stress curve in Nilson's textbook was created. Using a stress-strain curve that is similar in age to the bridge would ideally result in calculations similar to those used in design. This curve gives slightly different approximations to the stress-strain curve presented in the *PCI Design Handbook*. The AASHTO nominal strength is larger than the strain compatibility approach but both are conservative compared to the experimentally determined nominal strength. It is expected that a typical new design would have more reserve capacity than designed for so it's a good sign that these channels follow the same pattern. Table 5-33 below shows a summary of the experimental and theoretical cracking moments and nominal strengths. The theoretical nominal strengths from Design 1 and Design 2 are included as well.

Table 5-33: Comparison of Experimental and Theoretical Moments

	M_{cr} (kip*ft.)	M_n (kip*ft.)
Channel Experimental	150	324
Channel AASHTO	141	314
Channel Strain Comp.		296
Design 1 AASHTO		228
Design 2 AASHTO		350

The moment-deflection plot was also compared to the Service III and Strength I design moments. These moments were calculated using AASHTO LRFD Table 3.4.1-1. Figure 5-26 shows a comparison of the experimental nominal strength with the Service III and Strength I design moments.

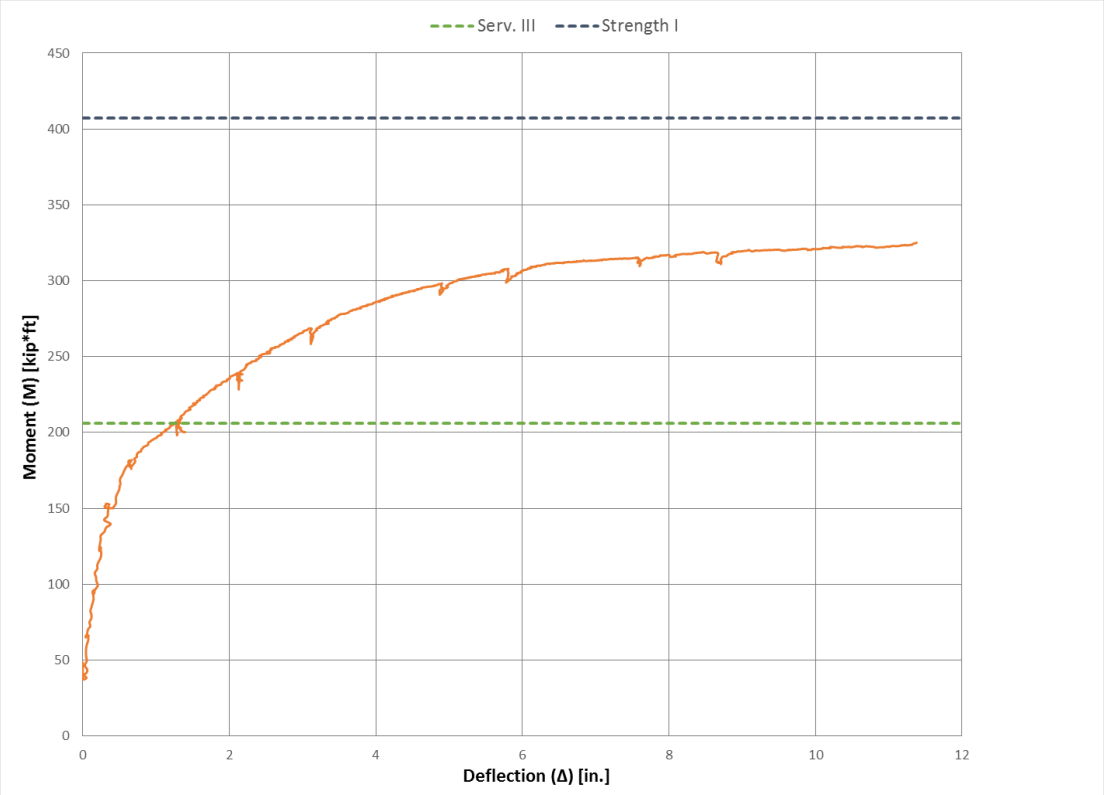

Figure 5-26: Moment vs. Deflection Behavior

The Service III design moment is of importance in new design because it is concerned with service tensile stresses. Strength I is calculated and met with strength and stability in mind. The design load rating factors presented in Table 5-31 show that the Five Forks Bridge does not have enough capacity to carry the load from the HL-93 design truck. The applied moment from the Service III design moment is 206 kip*ft., a value larger than the experimental and theoretical cracking moments. The difference between the girder cracking moment and the Service III design moment shows that the Five Forks Bridge would be expected to crack under service conditions. The nominal strength from the Strength I design moment is 407 kip*ft, approximately 100 kip*ft larger than the experimentally determined nominal strength. The Five Forks Bridge does not have enough capacity resist the factored load of the HL-93 truck. This deficit between the AASHTO-defined load demand and nominal capacity is corroborated by the bridge's insufficient design load rating factor.

The Five Forks Bridge is allowed to stay open though because it has a load rating greater than one for legal loads. The HL-93 set of design loads are greater in magnitude than the truck loads that must comply with federal weight limits and the FHWA Bridge Formula. The Five Forks Bridge may not be sufficient for these design loads but it has a safe load capacity that is greater than the demand caused by legal loads. The bridge can sustain legal loads set forth by AASHTO therefore it does not require posting. A flow chart provided in Appendix A6A of the MBE walks through the process of load rating and the actions taken for each step, this flow chart is provided in Appendix C of this paper.

Chapter 6: Conclusions and Recommendations

Multiple bridge and girder properties were tested in the nondestructive field test and channel test conducted for this project. A summary of the results found as well as the conclusion and recommendations for the SCDOT are presented below.

6.1 Summary of Results

- Two different girder cross-section drawings were provided by the SCDOT. An investigation into the properties of the channel provided by the SCDOT revealed a strand layout and strand properties different than the two drawings made available.
- An unexplained plateau-ing behavior occurred in all of the string pot data from the nondestructive test of the Five Forks Bridge. The deflection data was discarded due to this behavior.
- The largest strain recorded in the nondestructive test was 238.9 με found in girder 10 of scenario five.
- Girder 11 did experience the largest strain under the half-full loading of scenario three. The other two truck sizes didn't produce the largest strain in girder 11 though. No data suggests that the barrier rail increased the girder stiffness or the load seen in girder 11.
- The span showed a symmetrical strain response about girder 6, the middle girder.
- Under scenarios one and two, the strain in the girders exhibited a strong linear relationship with the size of the load. There was a weaker linear relationship

when the load was place right beside the barrier rail, although this could be influenced by a variability in the truck position between test runs.

- The lever rule could not be used to determine the exterior girder DFM so the AASHTO LRFD equation was used for all girders.
- All of the experimentally determined DFMs fell between the initial assumption for DFM and the theoretically calculated DFM from AASHTO LRFD.
- The AASHTO impact factor is typically a conservative value that estimates dynamic loading by amplifying the static load by a factor of 1.33. The experimental impact factor was found to be less than one in girders directly under the load.
- The design load rating factors, inventory and operating, were below one before and after the factors were modified using the experimental results from the nondestructive test. The modified legal load rating factor was greater than one (1.14).
- No moment experienced by girders in the nondestructive field test exceeded the experimental cracking moment determined in the channel test.
- The bridge girders in the nondestructive field test were stiffer than the individual girder in the channel test.
- The theoretical cracking moment was smaller than the experimentally determined cracking moment. Design equations are often conservative in nature so it was expected that the theoretical cracking moment would be smaller than the experimental cracking moment.

- Both the strain compatibility and AASHTO LRFD ultimate strengths were below the experimentally determined ultimate strength.
- The Strength I design moment was approximately 25% larger than the experimentally determined nominal strength.

6.2 Conclusions

- The maximum loading in the girders occurs in the outer edge of the design lanes (girder 10) directly under the load.
- Girders 10 and 11 of the west span (damaged side) saw more load than the east span, but the geometry of the bridge made it to where loading girder 11 is unfeasible if vehicles drive in the design lanes. Due to the difficulty in loading girder 11 the damage in girder 11 of the west span is not of concern.
- The experimentally determined DFM (0.44) is bound by the initial assumption for the DFM (0.50) and the AASHTO LRFD DFM (0.293). There is load sharing amongst the girders but not a significant amount.
- The experimentally determined IM was less than one but there are multiple factors outside the range of this project that may have influenced this value.
- A legal load rating factor greater than one was determined therefore no posting of the bridge is required. Vehicles crossing the Five Forks Bridge must comply with federal weight limits and Formula B (FHWA Bridge Formula).
- The individual girders have 3% more strength than the AASHTO LRFD equation provides.

6.3 Recommendations

- Based on results from the nondestructive test and the channel test the Five Forks Bridge should remain open and unposted. A legal load rating of 1.14 means that the bridge has sufficient strength for vehicles adhering to federal weight limits.
- When load rating channel bridges similar to the Five Forks Bridge, conservative values for the transverse load distribution (DFM) and dynamic allowance (IM) of 0.5 and 0.33, respectively, should be used unless other values are confirmed through testing. Experimental values for DFM and DLA for the Five Forks Bridge may not be representative of other channel bridges. Unless the strand size and layout are confirmed through observation, the strand detail from Figure 7-10 should be used to calculate the nominal strength. Load testing and nondestructive evaluation may justify load rating which support unrestricted used of the subject bridge.
- If the recommended conservative values for DFM and DLA result in a load rating factor less than one, then a nondestructive live load test should be considered. Similarly, to determine the strand pattern of in-place girders, methods such as ground penetrating radar can be used for a nondestructive forensic investigation.
- For the Five Forks Bridge the damage to the exterior girder of the west span does not warrant immediate closer or repair. The flexural stains at mid-span of the damaged exterior girder of the west span were similar to the exterior girder of the east span. Maximally loading the exterior girder proved difficult so the

magnitude of strain in the exterior girders was negligible when loading was located in the design lanes.

- If observed, damage similar to the Five Forks Bridge at an interior girder should be monitored and reviewed. A girder underneath a design lane would experience greater load effects compared to an exterior girder. A nondestructive live load test may be reasonable to determine the behavior of a damaged interior girder.
- The equations from AASHTO LRFD Table 4.6.2.2.2b-1 should not be used to determine the DFM for channel bridges similar to the Five Forks Bridge. These equations assume there is more load transfer between girders than was present in the Five Forks Bridge. As noted, the tie rods at the Five Forks Bridge were in poor condition which hurt the load distribution of the bridge. A bridge with tie rods in better condition would most likely have a lower DFM. The conservative assumption for DFM = 0.5 should be used unless a nondestructive test is conducted to determine the degree of load sharing and experimental DFM.

Chapter 7: Executive Summary

7.1 Project Motivation and Objectives

The Five Forks Bridge in Liberty, SC (Figure 7-1) is one of approximately 450 prestressed concrete channel bridges in the SCDOT inventory. Many of these channel bridges, such as the Five Forks Bridge, have unknown structural properties and flexural capacity. The Five Forks Bridge is a prestressed concrete channel bridge consisting of 33 girders that form three simple spans each 30 ft. in length.

Figure 7-1: Profile of Five Forks Bridge

It is understood that many of these bridges were built in the 1950's, 1960's, and 1970's. Their age as well as the uncertainty in physical properties provides a motivation to investigate the performance and capacity of these bridges. Some bridges such as the Five Forks Bridge also have damaged girders that may affect the capacity and posting recommendations for the bridges.

In addition to the reasons listed above, the SCDOT possesses two different sets of drawings that describe the girders in these types of bridges. Not knowing what strand layouts and properties are present in the bridges presents a challenge for rating these bridges. To address these problems, this project seeks to characterize the Five Forks Bridge and similar bridges through live load tests, laboratory channel tests, and analysis. Information from the project will guide SCDOT as they manage these bridges. Specific objectives include:

- Conduct a load rating of the Five Forks Bridge.
- Provide recommendations to the SCDOT for evaluation and testing of channel bridges similar to the Five Forks Bridge.
- Assess the impact on structural behavior due to the damaged exterior girder of the west span of the Five Forks Bridge.
- Evaluate the flexural capacity and cracking moment of an individual channel girder.
- Measure the structural behavior of the Five Forks Bridge including the transverse load distribution and dynamic load allowance.

7.2 Live Load Test

A nondestructive live load test was conducted on the Five Forks Bridge to determine how the bridge responded to truck loads. The Five Forks Bridge was subjected to varying magnitudes of load at different transverse locations under pseudo-static and dynamic conditions. The goal of the nondestructive tests was to determine the

distribution factor for moment, the impact factor for dynamic loading, and a comparison of how the healthy and damaged girders responded to load differently.

The bridge was instrumented with strain transducers, string pots, and linear variable differential transformers to measure strain and displacement of the girders (Figures 7-2 and 7-3).

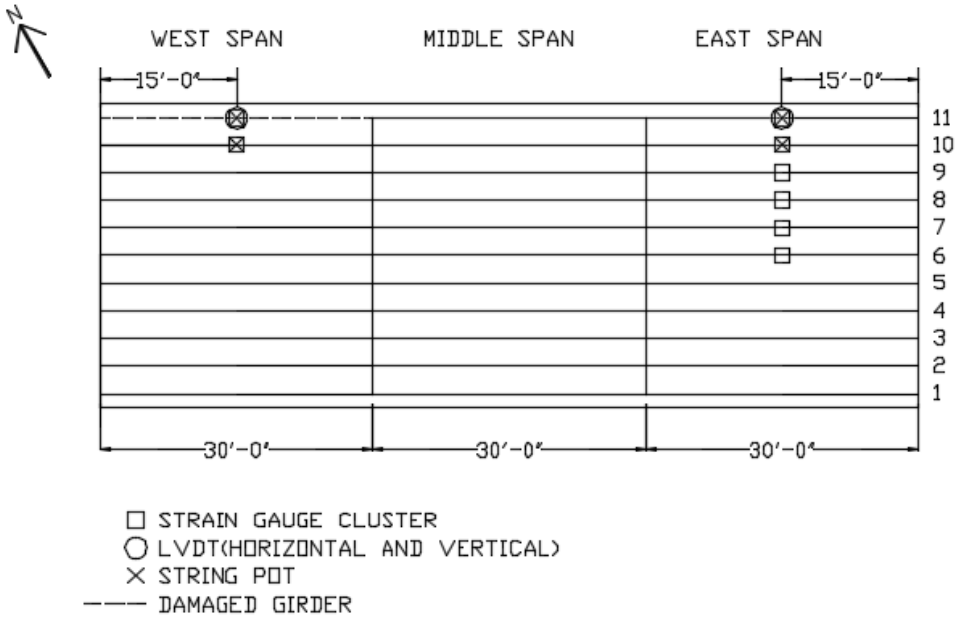

Figure 7-2: Plan View of Instrumentation Layout One

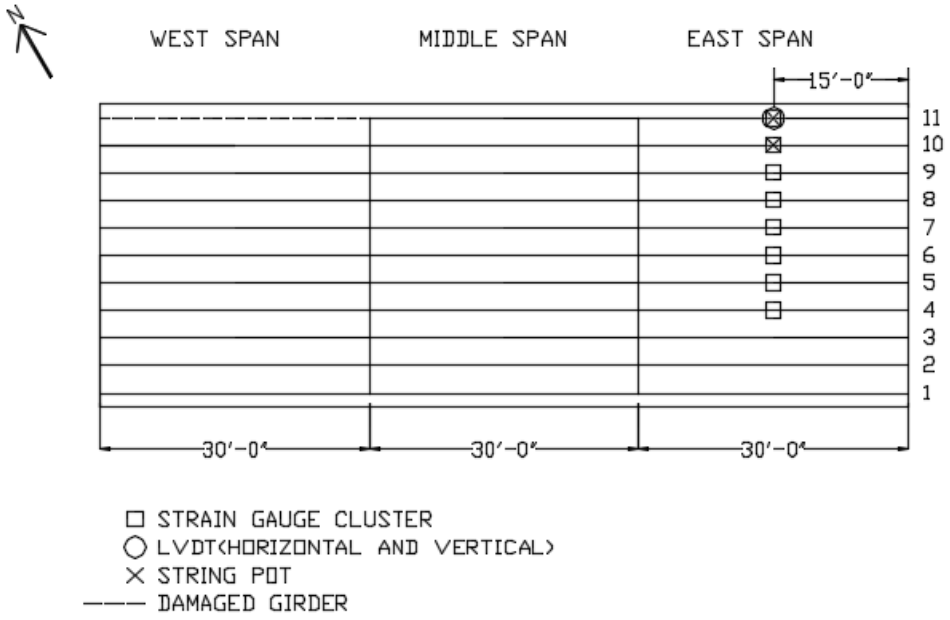

Figure 7-3: Plan View of Instrumentation Layout Two

The loading of the Five Forks Bridge was accomplished using three tandem axle dump trucks with variable loads of gravel. The trucks were designated as being empty (18.8 kips), half-full (36.6 kips), and full (48.7 kips). Six loading scenarios were tested as summarized in Table 7-1.

Table 7-1: Loading Scenario Summary

Loading Scenario	Trucks Used	Truck Speed (mph)	Repetitions	Instrumentation Plan	Primary Purpose
1	All	< 5	3	1	Damaged Girder Comparison
2	All	< 5	3	1	
3	All	< 5	3	1	
4	Full Only	< 5	3	2	Transverse Load Distribution
5	Full Only	< 5	3	2	
6	Full Only	45	3	2	Dynamic Load Allowance

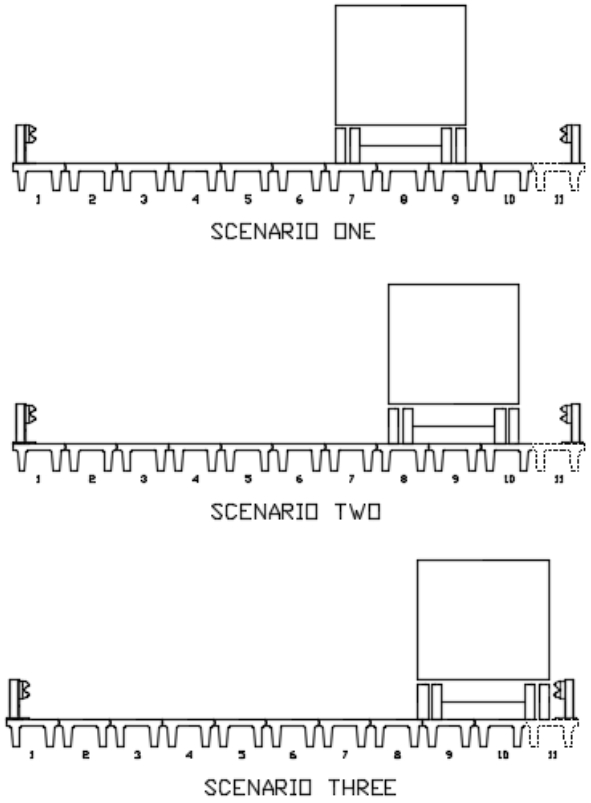

Figure 7-4: Truck Scenarios One through Three

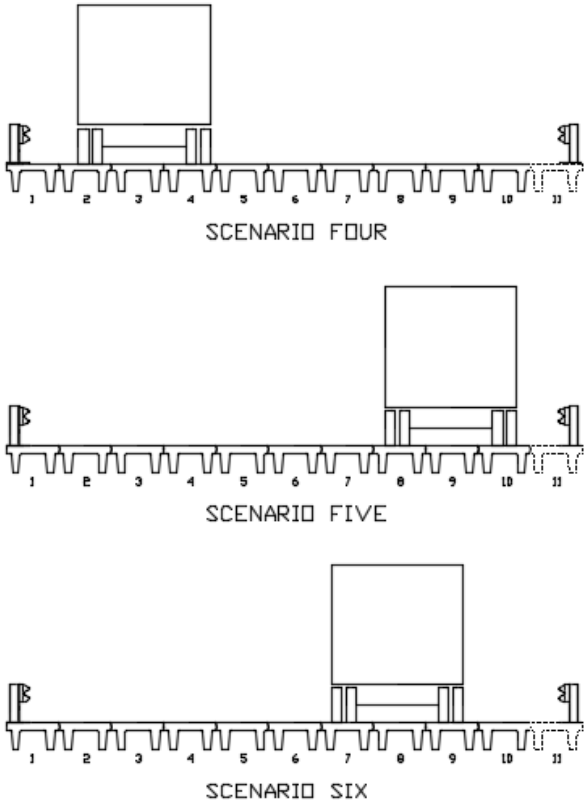

Figure 7-5: Truck Scenarios Four through Six

The truck location for each of the loading scenarios can be seen in Figures 7-4 and 7-5 above. The damaged girder 11 of the west span is shown as dashed lines in Figures 7-4 and 7-5. During loading of the exterior girders, girder 11 of the west span saw more load than girder 11 of the east span. Even though the damaged girder saw more load than the healthy girder, the magnitude of load that girder 11 saw for either span was less than the load that interior girders experienced. Also, the location of the design lanes made it so that vehicles would have to pass dangerously close to the guardrail to load girder 11 beyond a negligible amount. The magnitude of load seen by girder 11 and the difficulty in loading girder 11 means that the damage in girder 11 of the west span does not warrant immediate closure or repair.

Figure 7-6 below shows sample strain results from the dynamic loading superimposed over the strain results from the static loading. The difference between the two peaks is the experimental IM.

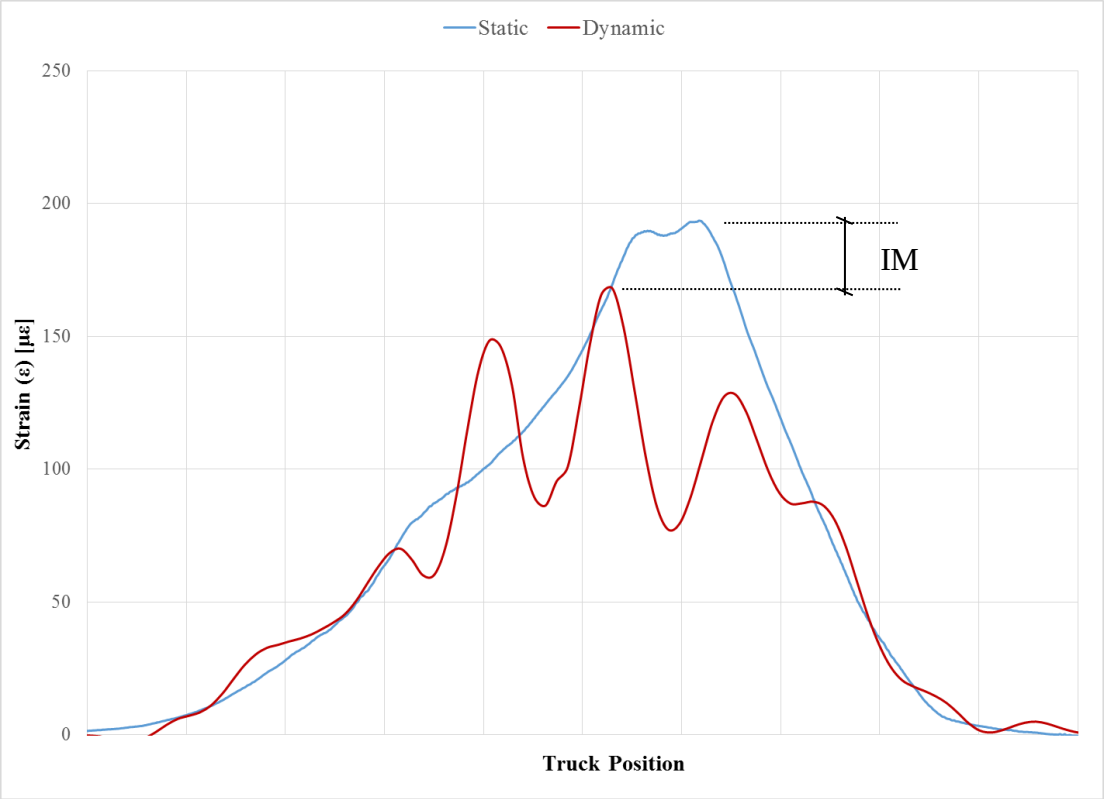

Figure 7-6: Dynamic Strain Superimposed over Static Strain

The results from the nondestructive test show that the strain response was less for the dynamic loading compared to the static loading. This difference results in a "negative" IM that reduces the static loading to account for the dynamic effects of moving traffic. Typically the IM is a positive value that amplifies the response from the static loading, but other tests have shown that the combination of a short span and contoured approach can result in a "negative" IM (STI 1998). The theoretical IM of 0.33 is given in AASHTO LRFD Table 3.6.2.1-1. The stiffness of the truck's suspension is a

factor that affects IM, but testing that parameter was not in the scope of this research. Because the "negative" IM can't be extrapolated for all vehicle types and suspensions, the conservative AASHTO value of 0.33 was used for all further calculations.

Experimental DFMs were calculated for every loading scenario except the dynamic loading of scenario six. The maximum DFM from each scenario can be found in Table 7-2. Before the live load test was conducted the DFM for the Five Forks Bridge was assumed to be 0.5. The width of the girders allowed there to be one wheel line over a single girder therefore an individual girder was conservatively assumed to support one wheel line. The assumed DFM of 0.5 for the Five Forks Bridge was conservative compared to the experimental values. The experimental values all fell between 0.37 and 0.44. The DFMs were lower than the assumed value so the girders possessed more load sharing ability than expected.

Table 7-2: DFM Summary

Distribution Factor for Moment	
Scenario	**Experimental**
One	0.374
Two	0.418
Three	0.394
Four	0.438
Five	0.414

7.3 Channel Test

The nondestructive test of the Five Forks Bridge revealed the bridge system behavior and response. A laboratory load test was conducted to assess structural behavior of individual channel members, in particular at nominal capacity. A channel similar in cross-sectional geometry and span length to those found in the Five Forks

Bridge was provided by the SCDOT for laboratory testing. The specimen was salvaged from a bridge demolition project in the SC upstate.

The channel was instrumented with strain gauges on the bottom and top of the channel at mid-span (Figure 7-7). String pots were attached at the mid-span of the bridge to measure deflection throughout the test. A dial gage was setup over top of the support to measure the bearing pad compression.

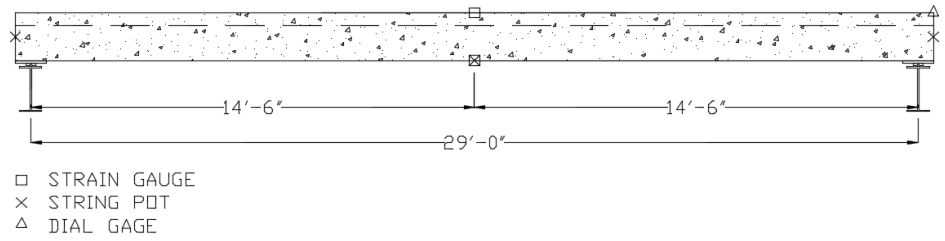

Figure 7-7: Elevation of Instrumentation

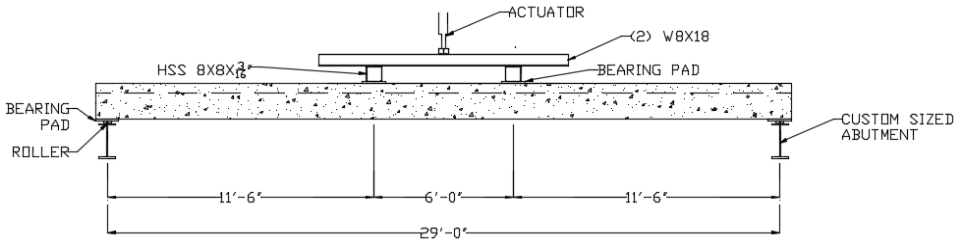

Figure 7-8: Elevation of Channel Test Loading

The channel was loaded in a four-point bending arrangement as seen in Figure 7-8. The actuator applied load to the spreader beam and down through the two transverse tubes. The load was applied in 5 kip increments until the first cracks formed. Figure 7-9 below shows the moment-deflection plot from the test with the dead load moment (M_g), cracking moment (M_{cr}), and nominal strength (M_n) labeled. The girder failed when it was loaded past its flexural capacity. Cracks formed at the bottom of the girder within the constant moment region in the middle of the span and extended into the flange of the

girder. At failure the concrete on top of the girder was crushed from the compressive stresses. The ductility of the girder was notable with the deflection at failure reaching almost 12 in.

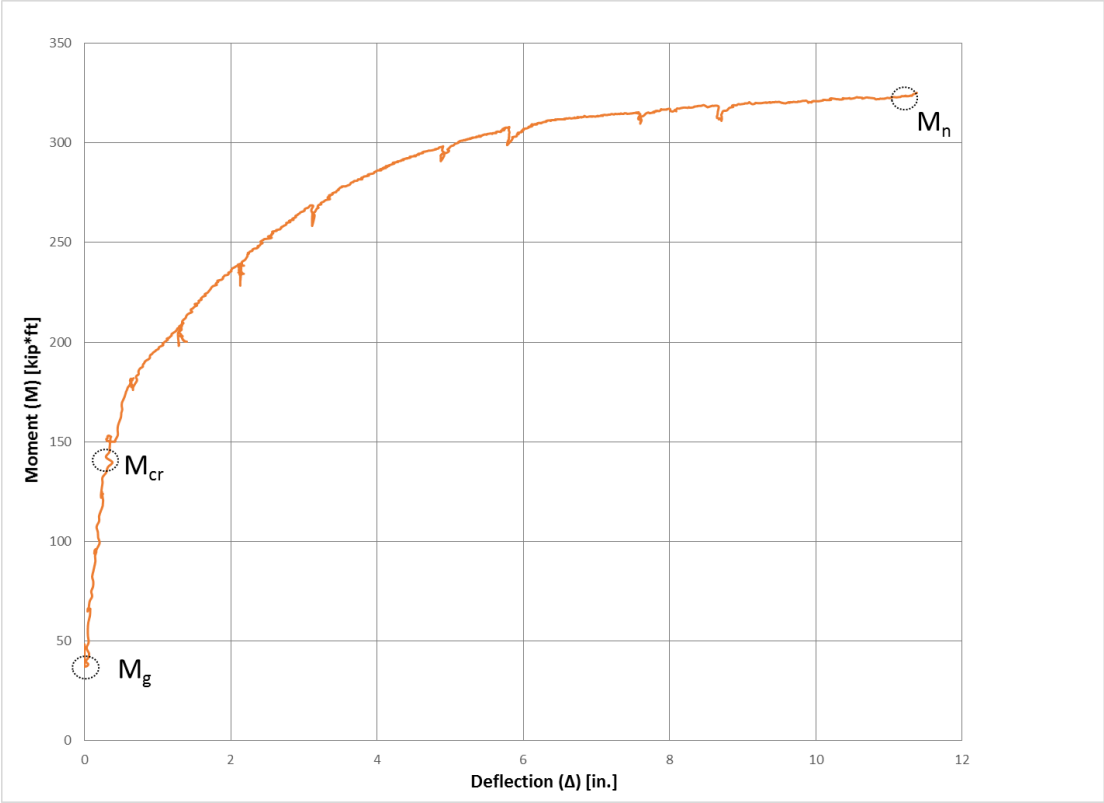

Figure 7-9: Moment-Deflection Plot

7.4 Forensic Investigation

After completion of the channel test, the specimen was compared to the two cross section drawings provided by the SCDOT (Figures 7-10 and 7-11). Design 1 uses a strand with a nominal diameter of 3/8" and an ultimate stress of 250 ksi. Design 2 uses a strand with a nominal diameter of 7/16" and an ultimate stress of 270 ksi. The girder geometry from the Five Forks Bridge matched the girder geometry from the channel test

and the girder in Design 2. The load rating calculations include the nominal strength of the bridge girders therefore an accurate nominal strength was needed for the girder in the channel test.

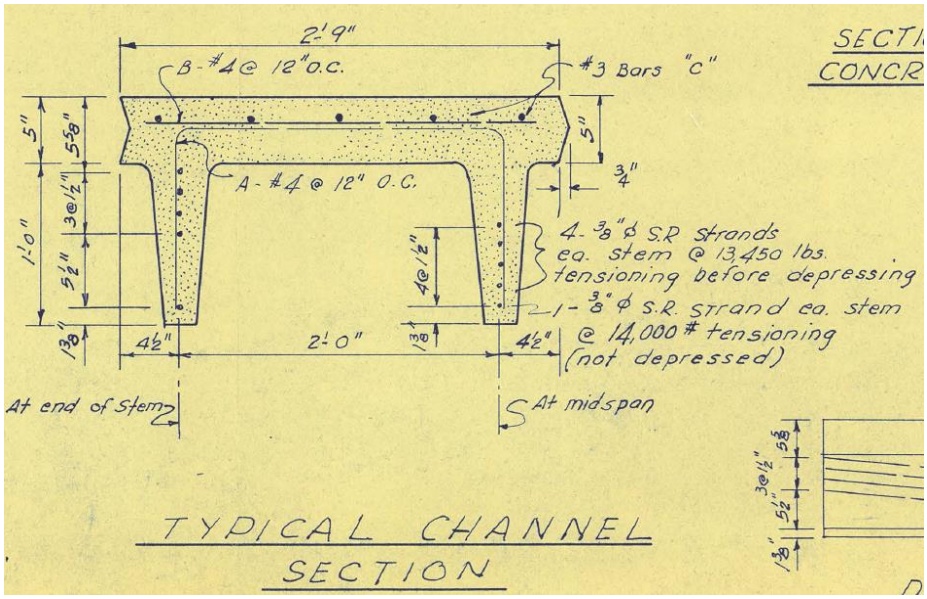

Figure 7-10: Design 1 Girder Cross Section

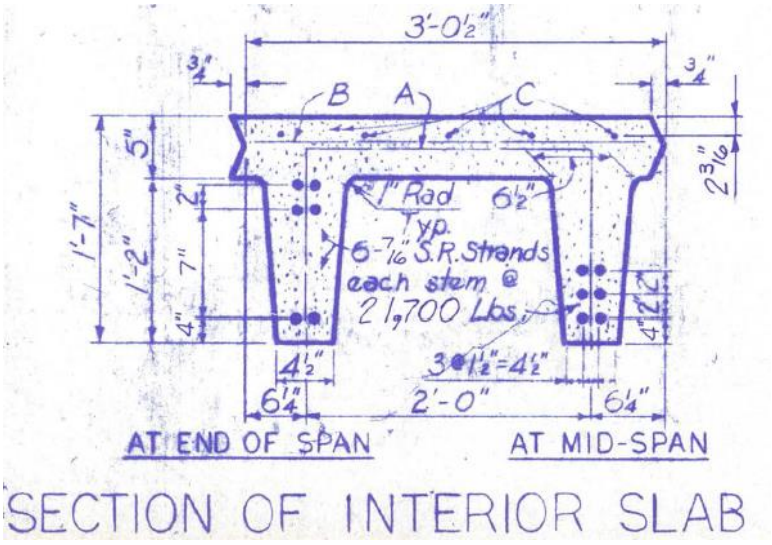

Figure 7-11: Design 2 Girder Cross Section

To determine the strand properties and layout for the provided channel, the concrete at the end of the beam was excavated with a jack hammer to expose the

prestressing strands. The layout of the strands was noted and the diameter and area of each strand was measured. The strands are outlined in red circles below in Figure 7-12. It was observed that the strand pattern did not match either Design 1 or Design 2.

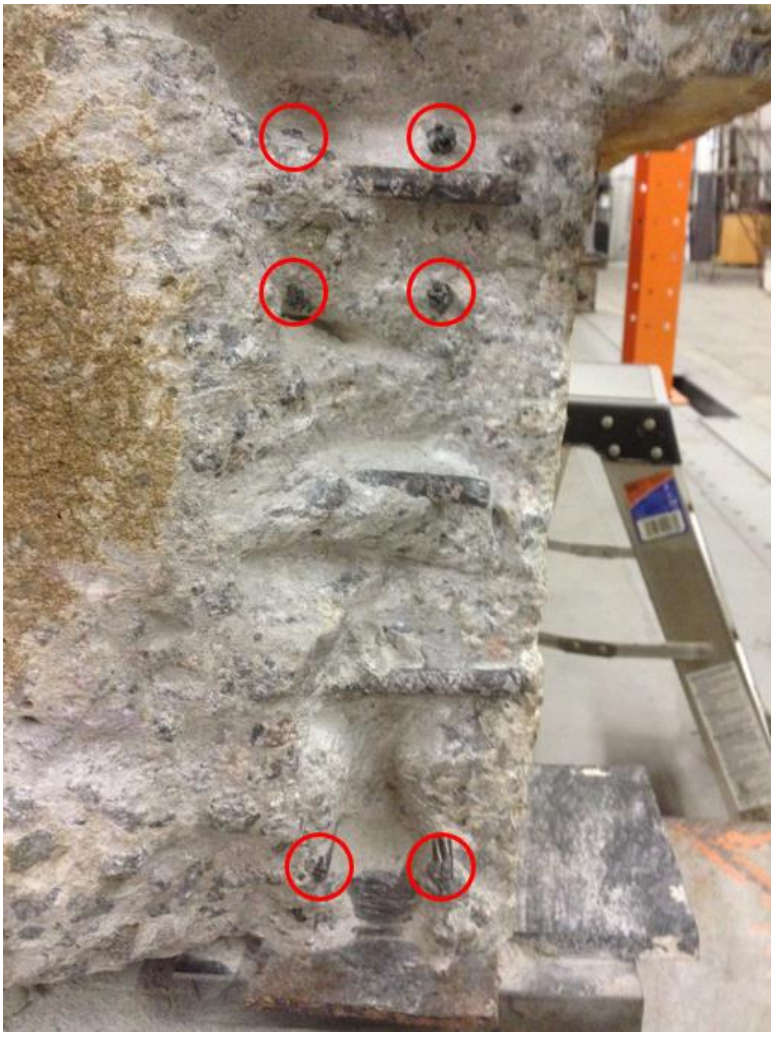

Figure 7-12: Exposed Strands of Channel

Measurements were taken to evaluate the strand size and grade. Prestressing strands have a unique cross-sectional area associated with different combinations of nominal diameter and ultimate stress (PCI 1971). The measurement of the strand

diameters and areas revealed that the strands in the channel girder had a diameter of 3/8 in. and an ultimate stress of 270 ksi.

Thus the tested beam was a hybrid between the provided drawings. The strand diameter matched Design 1, and the strand grade matched Design 2. However, the strand layout was different than Designs 1 and 2. The bottom layer of prestressing was 2 in. from the bottom of the beam instead of the 4 in. as in Design 2 shows. The observed strand properties found in the forensic investigation resulted in a smaller nominal strength than the nominal strength calculated from the strand properties in Design 2. Because the strand properties from the forensic investigation resulted in a more conservative nominal strength, these properties were used for all subsequent calculations.

7.5 Analysis

The experimental value for the distribution factor for moment (DFM) was calculated using the strain results from the nondestructive live load test of the Five Forks Bridge. These values were compared to the theoretical DFM found in AASHTO LRFD Table 4.6.2.2.1-1. Figure 7-13 presents a comparison of the experimental DFMs for each loading scenario with the AASHTO LRFD DFM of 0.293 and the initially assumed DFM of 0.5 (one wheel line per girder) plotted as well. The experimental results were bounded by the assumed DFM of 0.5 and the AASHTO DFM of 0.293. The girders in the Five Forks Bridge did not take on the entire weight from one wheel line as assumed, but they possess less load sharing ability than the AASHTO equations dictate. The Five Forks Bridge has tie rods at the quarter points of each span to provide facilitate transverse load distribution, but it was noted during the live load test that the tie rods were partially

corroded and the bolts were loose enough to turn by hand. The derelict condition of the tie rods reduces the bridges ability to share load.

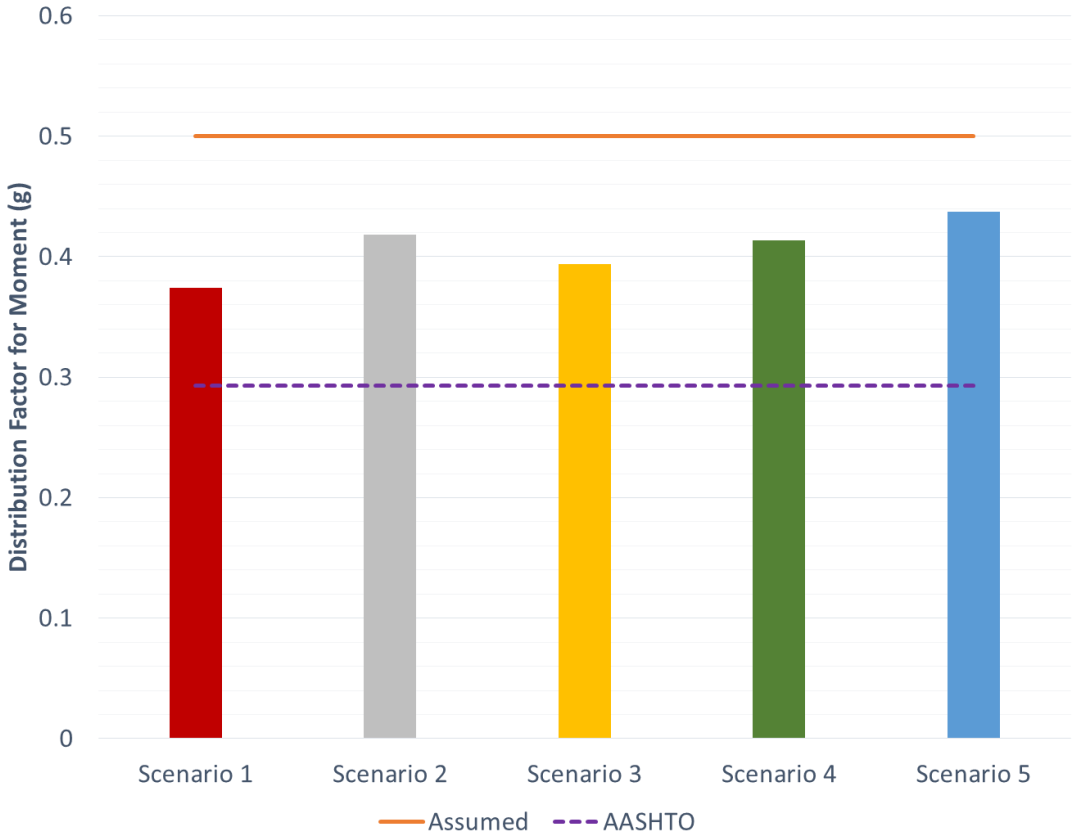

Figure 7-13: DFM Comparison

Strand properties determined from the forensic investigation were used to calculate theoretical values for the nominal strength and cracking moment of the channel from AASHTO LRFD Section 5.7.3. Nominal strength for the channel was also calculated using the strain compatibility method. Table 7-3 displays a comparison of the experimental and theoretical values for the nominal strength and cracking moment of the girder from the channel test. The theoretical nominal strengths are included for the girder properties from Design 1 and Design 2.

Table 7-3: Comparison of Experimental and Theoretical Moments

	M_{cr} (kip*ft.)	M_n (kip*ft.)
Channel Experimental	150	324
Channel AASHTO	141	314
Channel Strain Comp.		296
Design 1 AASHTO		228
Design 2 AASHTO		350

The experimental values for nominal strength and cracking moment were greater than the theoretically calculated values. The experimental cracking moment was 6% greater than the theoretical cracking moment, and the experimental nominal strength was 3% greater than the theoretical value from AASHTO LRFD. Figure 7-14 shows the theoretical values plotted as "benchmarks" against the moment-deflection plot from the channel test. This plot shows that the moment-deflection plot exhibited linear behavior past the theoretical cracking moment and that the experimental nominal strength was greater than both theoretically calculated values.

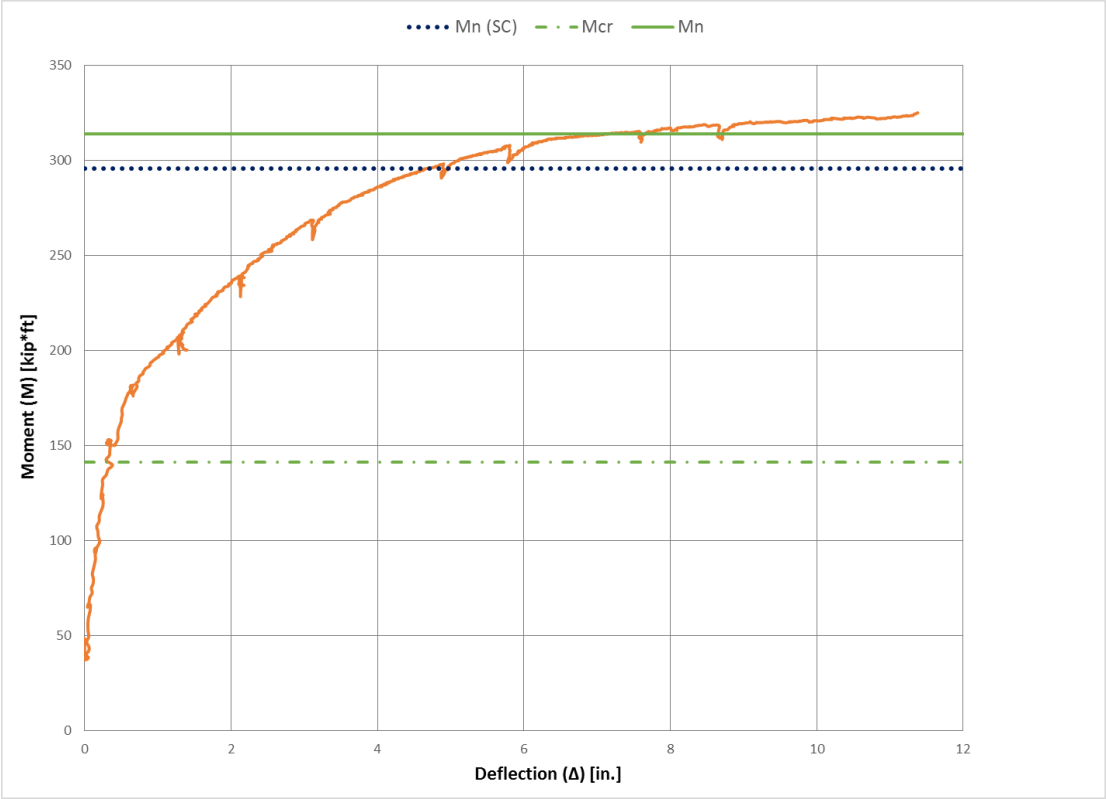

Figure 7-14: Moment vs. Deflection Behavior

The original and modified load rating factors for the Five Forks Bridge were calculated following the steps laid out in Sections 6 and 8 of the Manual for Bridge Evaluation (MBE). The original design load rating was calculated using the nominal strength associated with the strand properties found in Section 7.4, the assumed values for DFM and IM, and the load effects from an HL-93 truck. The modified design load rating was calculated using the same nominal strength and HL-93 load effects but the experimental DFM was used as well as results from the experimental service strains. The legal load rating was carried out using a Type 3 truck instead of an HL-93 truck and the experimental DFM was used. Table 7-4 shows the rating factor for the design and legal load rating levels. The original and modified factors are shown as well as the DFM and

IM used to calculate each factor. The AASHTO IM of 0.33 was used for all load rating. The assumed DFM of 0.5 was used for the original design load rating factors, but the largest experimental DFM of 0.44 was used for the modified load ratings and the legal load rating. Only the modified legal load rating factor was greater than one and therefore sufficient. Thus, a load rating greater than one means that the Five Forks Bridge does not need to be posted.

Table 7-4: Load Rating Factors

	Inventory		Operating		Legal	
	Original	Modified	Original	Modified	Original	Modified
DFM	0.5	0.44	0.5	0.44	0.44	0.44
IM	0.33	0.33	0.33	0.33	0.33	0.33
Rating Factor	0.523	0.75	0.678	0.98	0.79	***1.14***

7.6 Recommendations for SCDOT

- Based on results from the nondestructive test and the channel test the Five Forks Bridge should remain open and unposted. A legal load rating of 1.14 means that the bridge has sufficient strength for vehicles adhering to federal weight limits.
- When load rating channel bridges similar to the Five Forks Bridge, conservative values for the transverse load distribution (DFM) and dynamic allowance (IM) of 0.5 and 0.33, respectively, should be used unless other values are confirmed through testing. Experimental values for DFM and DLA for the Five Forks Bridge may not be representative of other channel bridges.
- Unless the strand size and layout are confirmed through observation or non-destructive testing (e.g. ground penetrating radar), the strand detail from Figure 7-

10 should be used to calculate the nominal strength. To the extent possible, cross-section dimensions should also be verified for us in calculating nominal strength.

- If the recommended conservative values for DFM and DLA result in a load rating factor less than one, then a nondestructive live load test should be considered as a means to avoid posting the bridge. Load testing and nondestructive evaluation may justify section properties and load calculations which support higher load rating.
- For the Five Forks Bridge the damage to the exterior girder of the west span does not warrant immediate closer or repair. The flexural stains at mid-span of the damaged girder were similar to the strains in undamaged exterior girders. Negligible load was transmitted to the exterior girder when loading was located in the design lanes.
- If observed, damage similar to the Five Forks Bridge at an interior girder should be monitored and reviewed. A girder underneath a design lane would experience greater load effects compared to an exterior girder. A nondestructive live load test likely warranted to determine the behavior of a damaged interior girder. Repair or replacement is also likely warranted.
- The equations from AASHTO LRFD Table 4.6.2.2.2b-1 should not be used to determine the DFM for channel bridges similar to the Five Forks Bridge. These equations assume there is more load transfer between girders than was present in the Five Forks Bridge. As noted, the tie rods at the Five Forks Bridge were in poor condition which hurt the load distribution of the bridge. A bridge with tie

rods in better condition would most likely have a lower DFM. The conservative assumption for DFM = 0.5 should be used unless a nondestructive test is conducted to determine the degree of load sharing and experimental DFM.

References

AASHTO (1993). Standard Specification for Highway Bridges. 15th ed. Washington DC

American Association of State Highway and Transportation Officials (2011a), "Manual for Bridge Evaluation, 2nd Edition" Washington, D.C.

American Association of State Highway and Transportation Officials (2010), "LRFD Bridge Design Specifications, 5th Edition" Washington, D.C.

ARCHES-D16 (2009). *Recommendations on the use of soft, diagnostic and proof load testing*, Deliverable D16 [On line]. ARCHES Project. VI EU Framework Program. Brussels. [cited 16 Feb, 2010],Available from Internet: <http://arches.fehrl.org >

Barker, R. M. and Puckett, J. A. (2007). *Design of Highway Bridges: An LRFD Approach*, John Wiley & Sons, Inc., Hoboken, New Jersey, pp. 178-184, 302-317.

Barnes, R. W., Stallings, J. M., and Porter, P. W. (2003). "Live-Load Response of Alabama's High-Performance Concrete Bridge." *Transportation Research Board: Journal of the Transportation Research Board*, No. 1845, 115-124.

Barr, P. J., Eberhard, M. O., and Stanton, J. F. (2001). "Live-Load Distribution Factors in

California Department of Transportation (2015). *Bridge Design Practice*. 9 Nov. 2015. Web. 24 May 2016.

Casas, Joan R., and Juan D. Gomez. "Load Rating of Highway Bridges by Proof-loading." KSCE Journal of Civil Engineering 17.3 (2013). Apr. 2013. Web. 24 May 2016.

Chajes, M. J., Shenton, H. W., and O'Shea, D. (2000). "Bridge-condition Assessment and Load Rating Using Nondestructive Evaluation Methods." *Transportation Research Board: Journal of the Transportation Research Board*, Vol. 2, No. 1696, 83-91.

Collins, William. “Live Load Testing and Analysis of the Southbound Span of U.S. Route 15 over Interstate-66.” Virginia Polytechnic Institute and State University, 2010.

Cross, B., Vaughan, B., Panahshahi, N., Petermeier, D., Siow, Y., and Domagalski, T. (2009). "Analytical and Experimental Investigation of Bridge Girder Shear Distribution Factors." *Journal of Bridge Engineering***,** Vol. 14, No. 3, 154-163.

Durham, Stephan, Ernest Heymsfield, and John Schemmel. "Structural Evaluation of Precast Concrete Channel Beams in Bridge Superstructures."*Transportation Research Record: Journal of the Transportation Research Board* 1845 (2003): 79-87. Web.

Fu, C. C., Elhelbawey, M., Sahin, M. A., and Schelling, D. R. (1996). "Lateral Distribution Factor from Bridge Field Testing." *Journal of Structural Engineering*, Vol. 122, No. 9, 1106-1109.

Gunasekaran, Umarani, Kanchanadevi Ashokkumar, and Rose Enid Teresa Amaladosson. "Load rating of bridges--current practices and issues." Applied Technologies and Innovations 2.2 (2010): 9+. Academic OneFile. Web. 24 May 2016.

Halbe, Kedar. “New Approach to Connections between Members of Adjacent Box Beam Bridges.” Virginia Polytechnic Institute and State University, 2014.

Harris, D. K., Cousins, T., Murray, T. M., and Sotelino, E. D. (2008). "Field Investigation of a Sandwich Plate System Bridge Deck." *Journal of Performance of Constructed Facilities***,** Vol. 22, No. 5, 305-315.

Hwang, E. S. and A. S. Nowak (1991a). “Simulation of Dynamic Load for Bridges,” *Journal of Structural Engineering,* ASCE, Vol. 117, No. 5, May, pp. 1413-1434.

Iplikcioglu, M. (2012). *Nondestructive load testing and comparison of approaches for bridge load rating using ASD, LFD, and LRFD methods* (Order No. 1512899). Available from ProQuest Dissertations & Theses Global. (1023805126). Retrieved from http://libproxy.clemson.edu/login?url=http://search.proquest.com.libproxy.clemson.edu/docview/1023805126?accountid=6167

Issa, M. and Shahawy, M. (1993). “Dynamic and Static Tests of Prestressed Concrete Girder Bridges in Florida.” Structural Research Center, MS 80. Florida DOT.

Kassner, B. L. (2004). “Long-Term In-Service Evaluation of Two Bridges Designed with Fiber-Reinforced Polymer Girders.” Master’s Thesis, Virginia Polytechnic Institute and State University, Blacksburg, VA.

Klaiber, F.W., et al. “Field and Laboratory Evaluation of Precast Concrete Bridges.” Iowa DOT Project TR-440. 2001

National Bridge Inventory. Federal Highway Administration. 2015. Accessed from: https://www.fhwa.dot.gov/bridge/nbi/2015/delimited/SC15.txt. Accessed on 11/29/16.

Nilson, Arthur H. *Design of Prestressed Concrete.* 2nd ed. New York: Wiley, 1978. Print.

Paultre, P., Chaallal, O., and Proulx, J. (1992). "Bridge Dynamics Amplification Factors – A Review of Analytical and Experimental Finding." *Canadian Journal of Civil Engineering.* Vol. 19, 260-278

PCI Design Handbook: Precast and Prestressed Concrete. Chicago, 1971. Print.PennState Eberly College of Science (2016). "(Pearson) Correlation Coefficient R." https://onlinecourses.science.psu.edu/stat501/node/30. Web.

Phelps, John E. "Instrumentation, Non Destructive Testing, and Finite Element Model Updating for Bridge Evaluation." Order No. 1481051 Tufts University, 2010. Ann Arbor: *ProQuest.* Web. 24 May 2016.

Prestressed Concrete Girder Bridges." *Journal of Bridge Engineering*, Vol. 6, No. 5, 298-306.

Restrepo, E., Cousins, T., and Lesko, J. (2005). "Determination of Bridge Design Parameters through Field Evaluation of the Route 601 Bridge Utilizing Fiber-Reinforced Polymer Girders." *Journal of Performance of Constructed Facilities*, Vol. 19, No. 1, 17-27.

Rogers, B. and Jauregui, D. (2005). "Load Rating of Prestressed Concrete Girder Bridges: A Comparative Analysis of LFR and LRF." New Mexico State University. Report NM02STR-01.

Structural Testing Incorporated (STI).(1998). Field Test of Washington Schoolhouse Lane Bridge. Report to HardCore Composites, Dec. 7, 1998.

Wipf, Terry, et al. "Field and Laboratory Testing of Precast Concrete Channel Bridges."*Transportation Research Record: Journal of the Transportation Research Board* 1976 (2006): 88-94. Web.

Yang, Y. and Meyers, J. J. (2003). "Live-Load Test Results of Missouri's First High-Performance Concrete Superstructure Bridge." *Transportation Research Board: Journal of the Transportation Research Board*, No. 1845, 96-103.

Zhang, J., Peng, H., and Cai, C. (2013). "Destructive Testing of a Decommissioned Reinforced Concrete Bridge." J. Bridge Eng., 10.1061/(ASCE)BE.1943-5592.0000408, 564-569.

Appendices

Appendix A: National Bridge Inventory Filtering

To estimate the number of bridges similar to the Five Forks Bridge in South Carolina, the National Bridge Inventory was filtered based on information about the Five Forks Bridge. The date of construction was filtered based on plans from SCDOT dated as early as 1959 and as late as 1979. The angle of skew of zero was based on the skew specified in the plans provided by SCDOT. The structure kind and structure type was filtered as "prestressed" and "multi-girder" based on the bridges of interest being prestressed concrete channel bridges. The span length and number of spans were filtered based on the span length and number of spans in the Five Forks Bridge and the plans provided by SCDOT.

Table A 1: National Bridge Inventory Filter

Filter Level	Item Description	Item Number	Number of Bridges
1	2015 SC NBI		9344
2	Year Built: 1955-1985	27	4885
3	Skew = 0^{o}	34	3850
4	Structure Kind: Prestressed	43a	669
5	Number of Spans: 1-4	45	569
6	Span Length: 9.1 m	48	460
7	Structure Type: Multi-girder	43b	449

Appendix B: Strain Data from Nondestructive Test

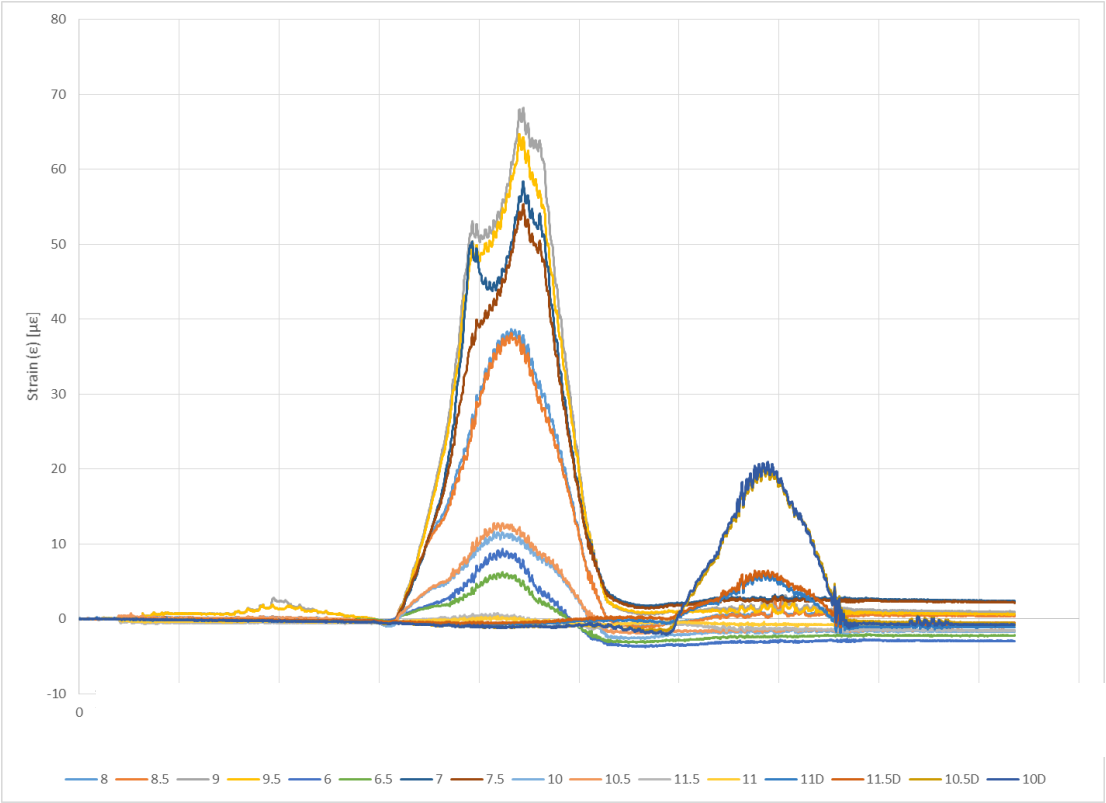

Figure B 1: Empty Truck, Scenario One, Run One

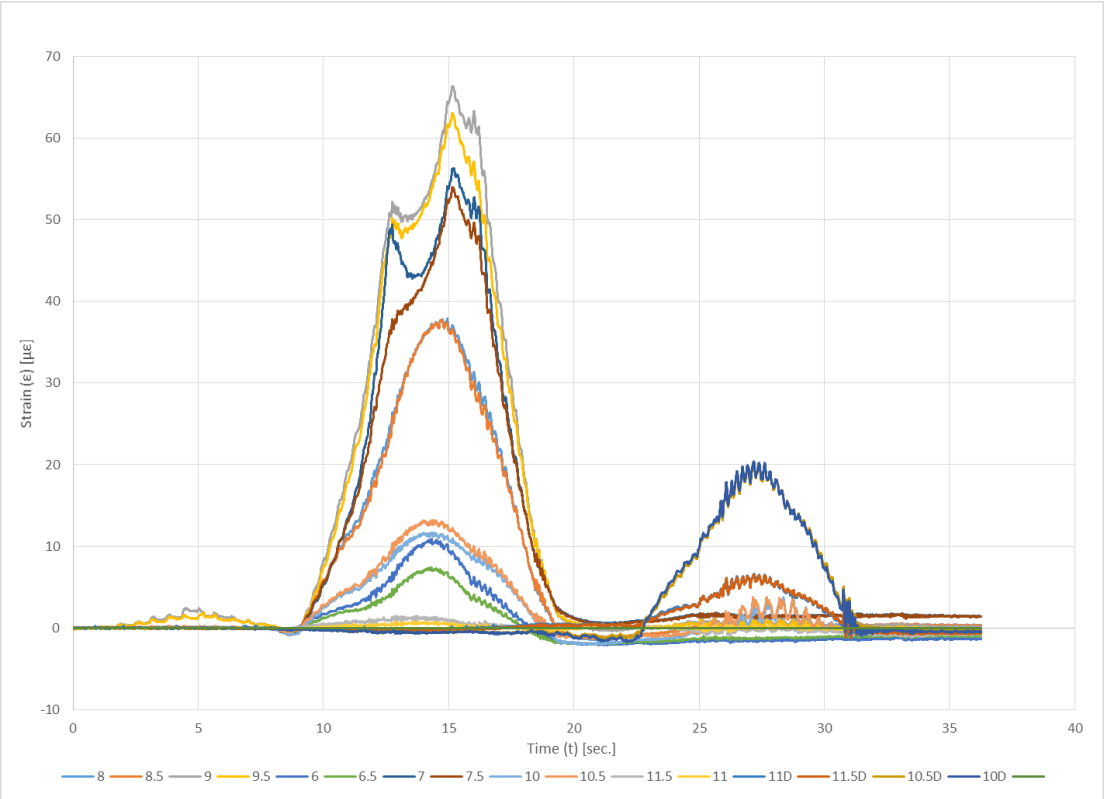

Figure B 2: Empty Truck, Scenario One, Run Two

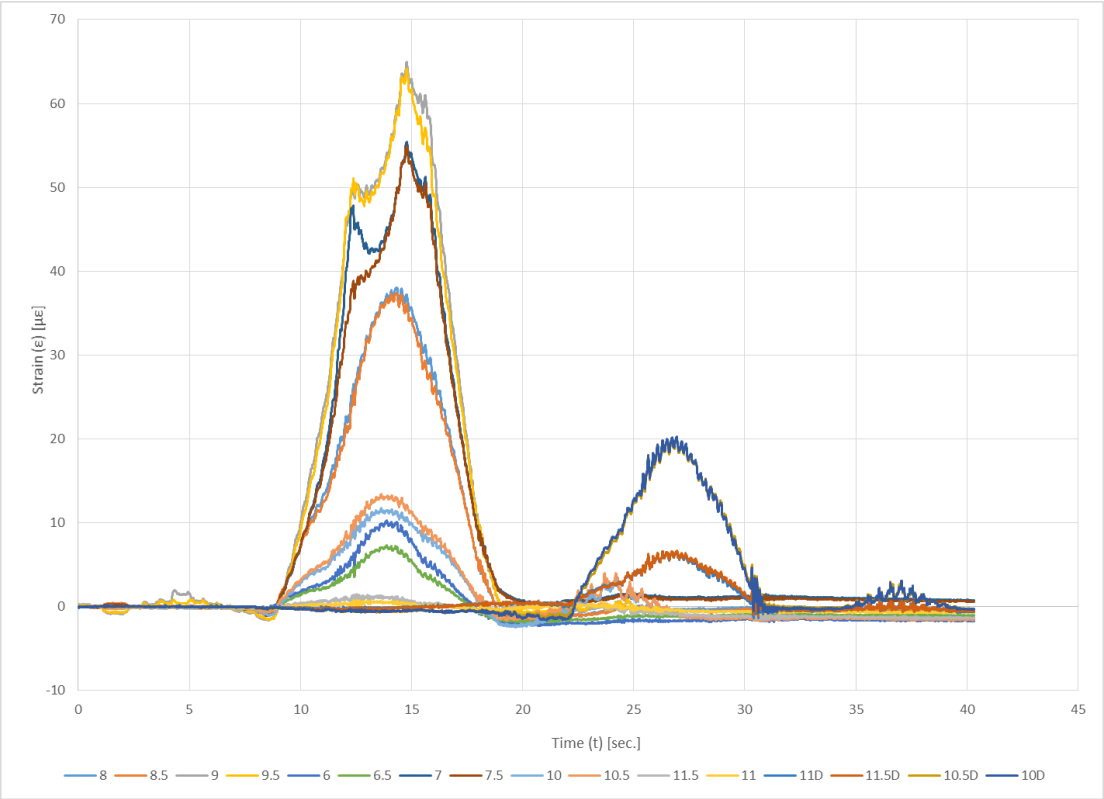

Figure B 3: Empty Truck, Scenario One, Run Three

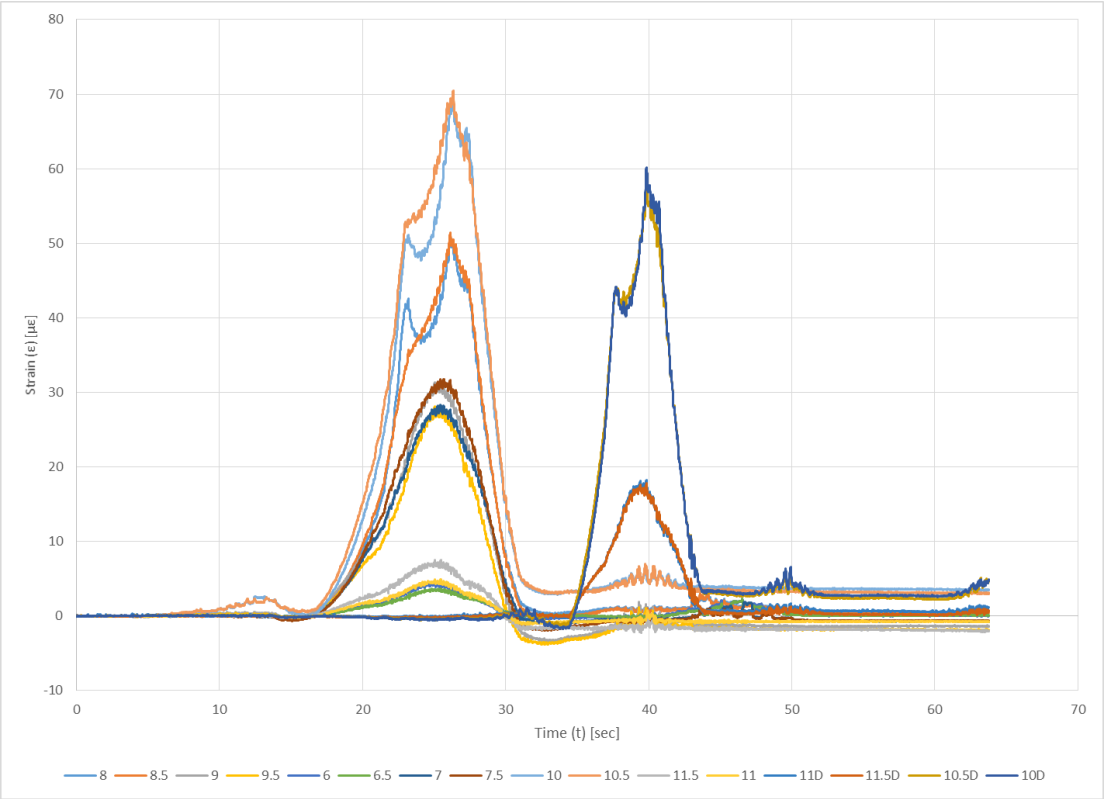

Figure B 4:Empty Truck, Scenario Two, Run One

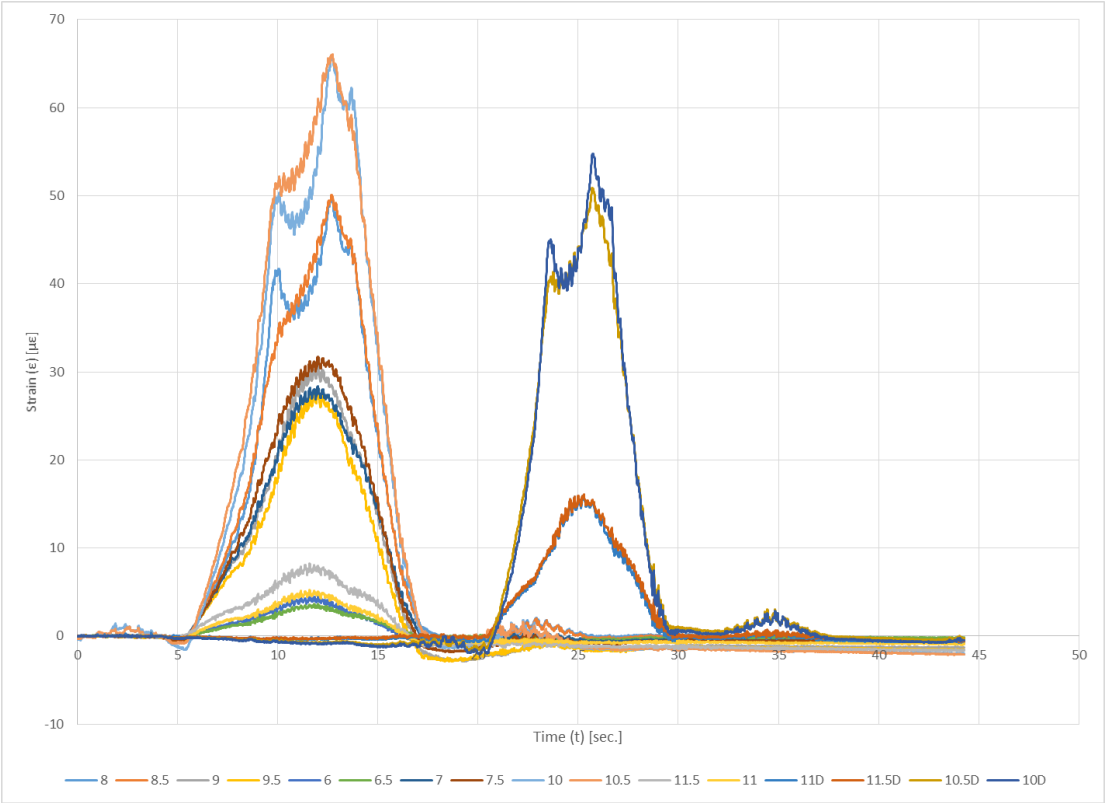

Figure B 5: Empty Truck, Scenario Two, Run Two

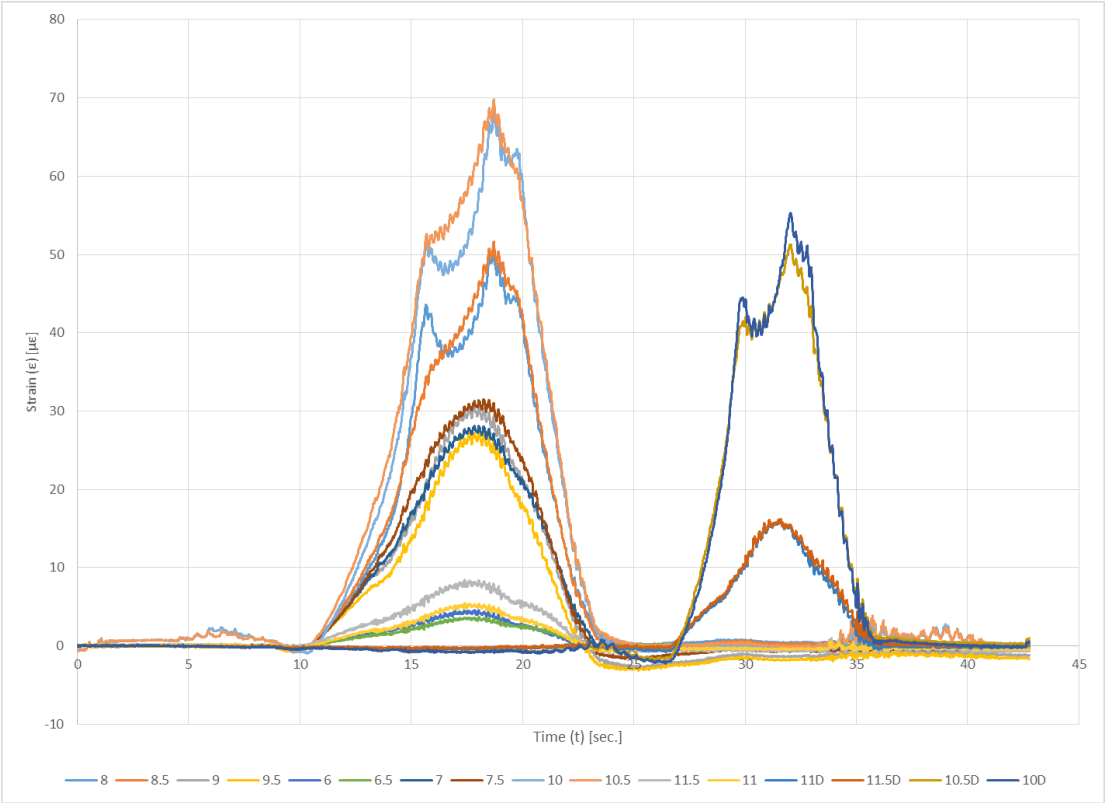

Figure B 6: Empty Truck, Scenario Two, Run Three

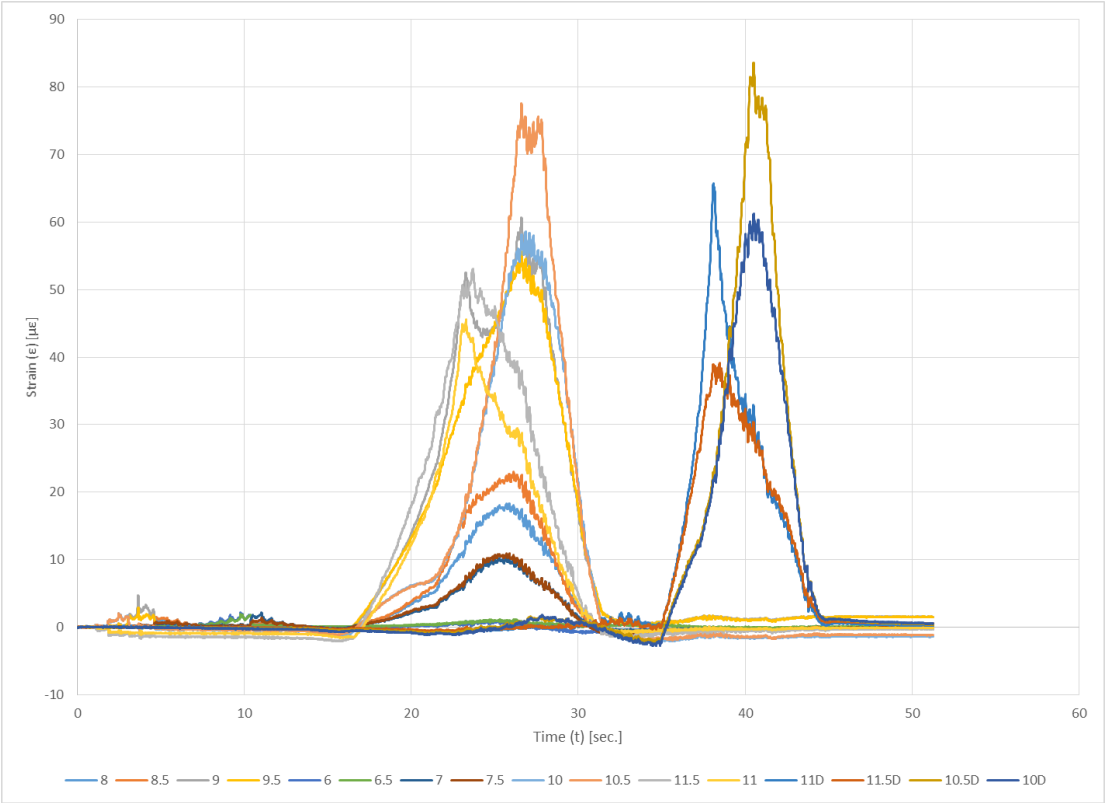

Figure B 7: Empty Truck, Scenario Three, Run One

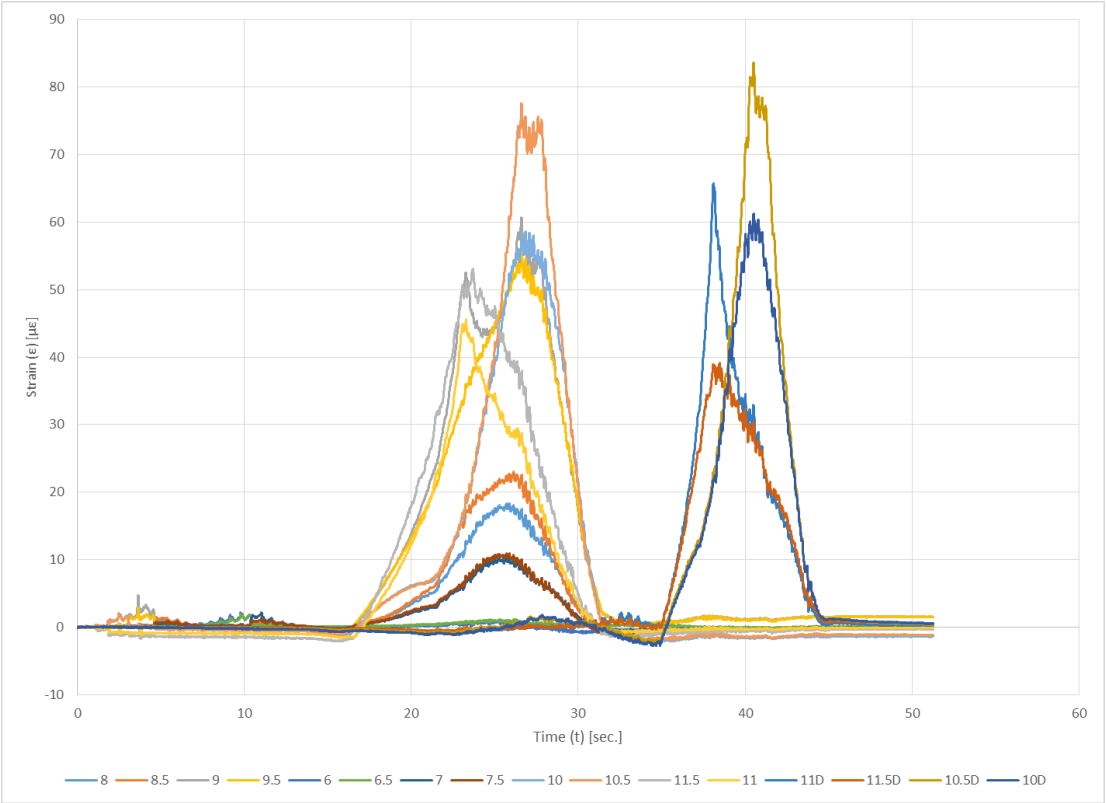

Figure B 8: Empty Truck, Scenario Three, Run Two

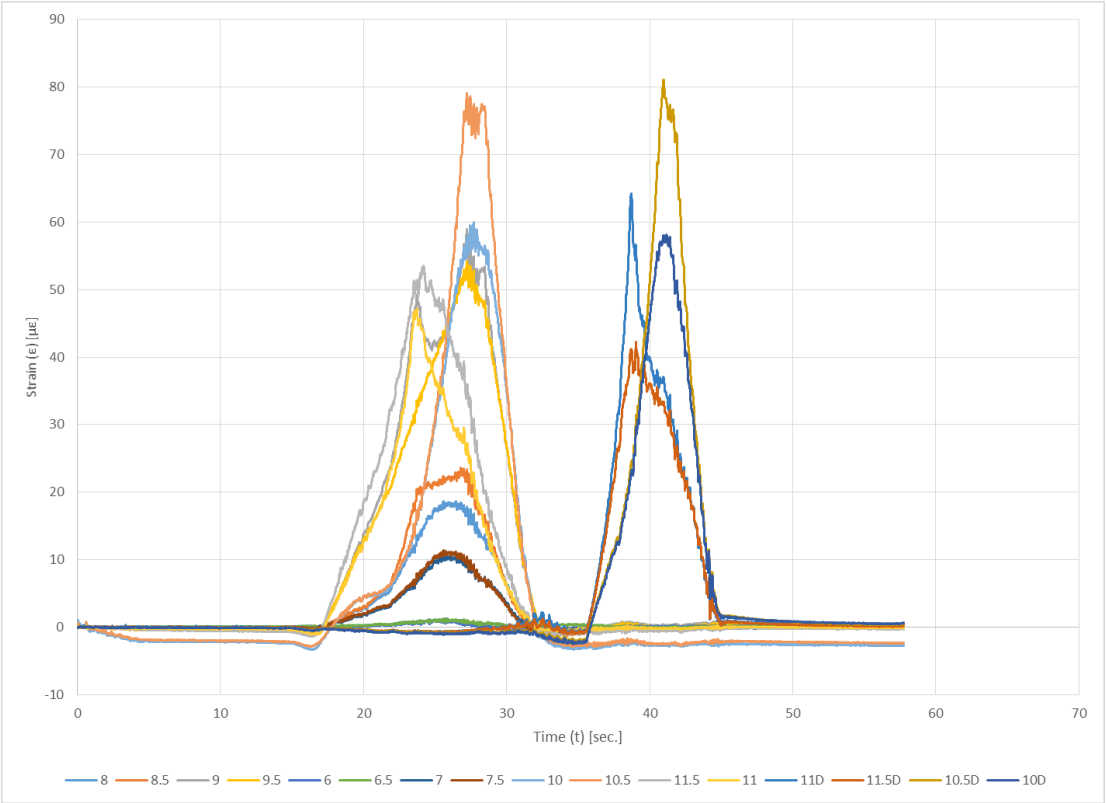

Figure B 9: Empty Truck, Scenario Three, Run Three

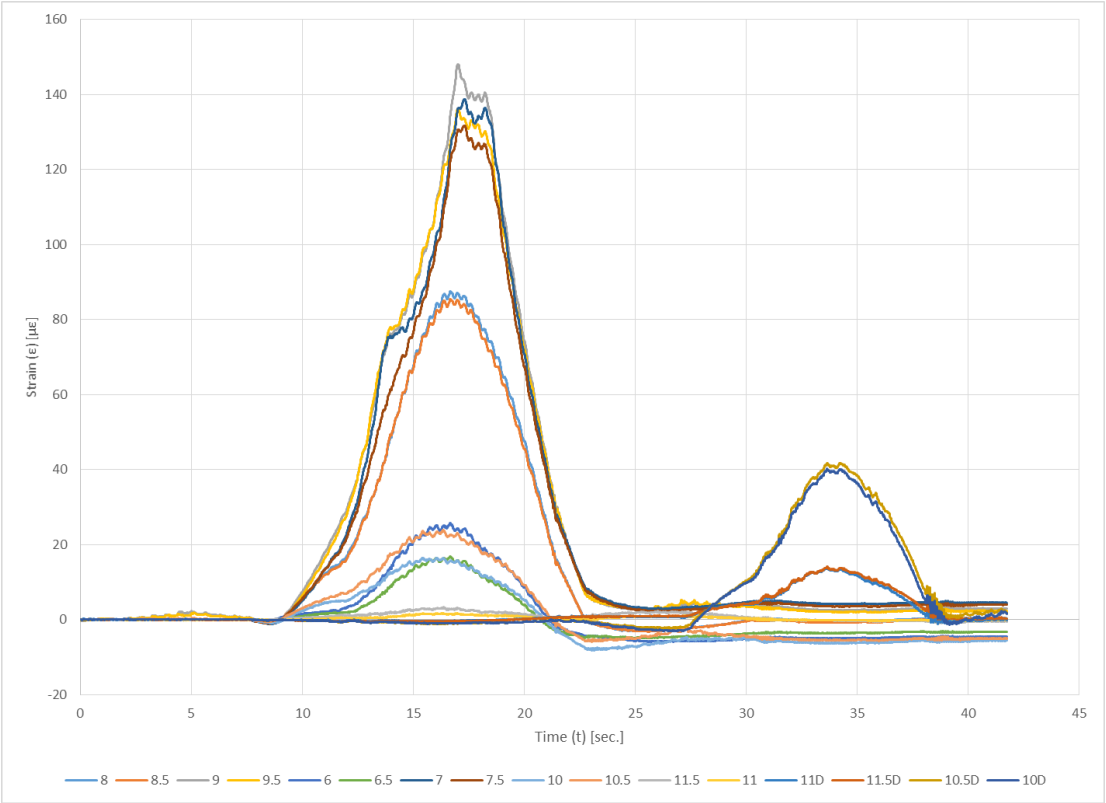

Figure B 10: Half Truck, Scenario One, Run One

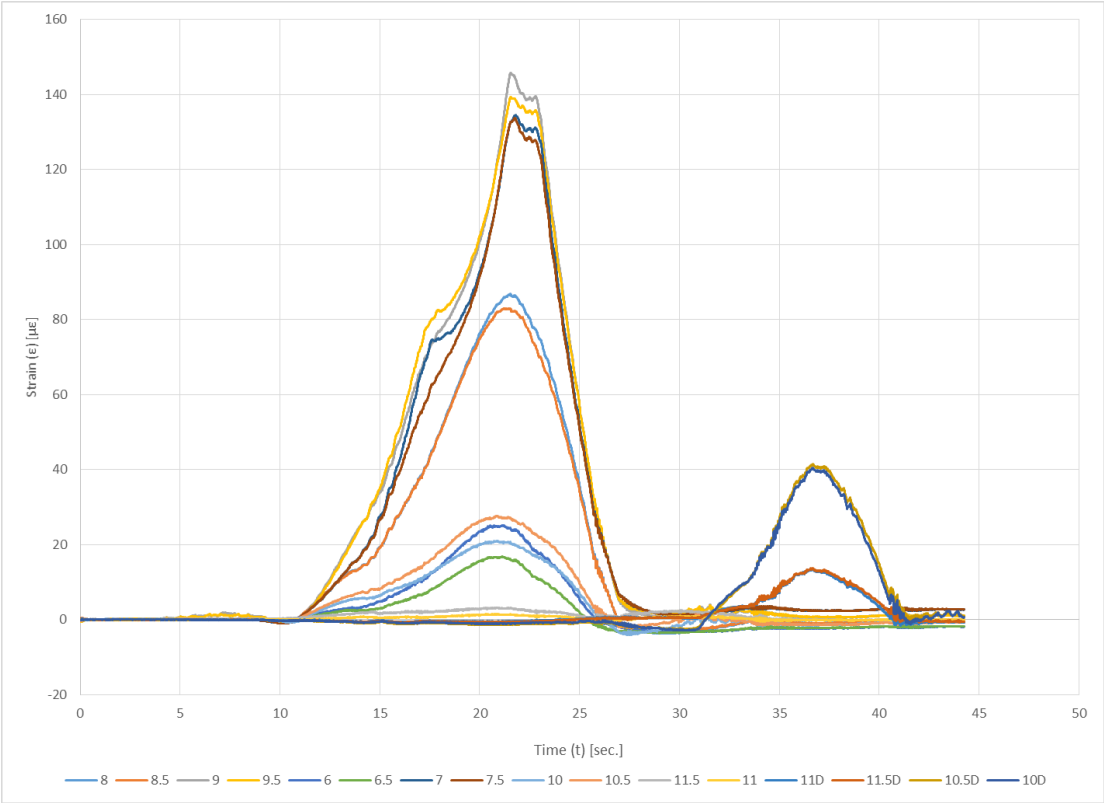

Figure B 11: Half Truck, Scenario One, Run Two

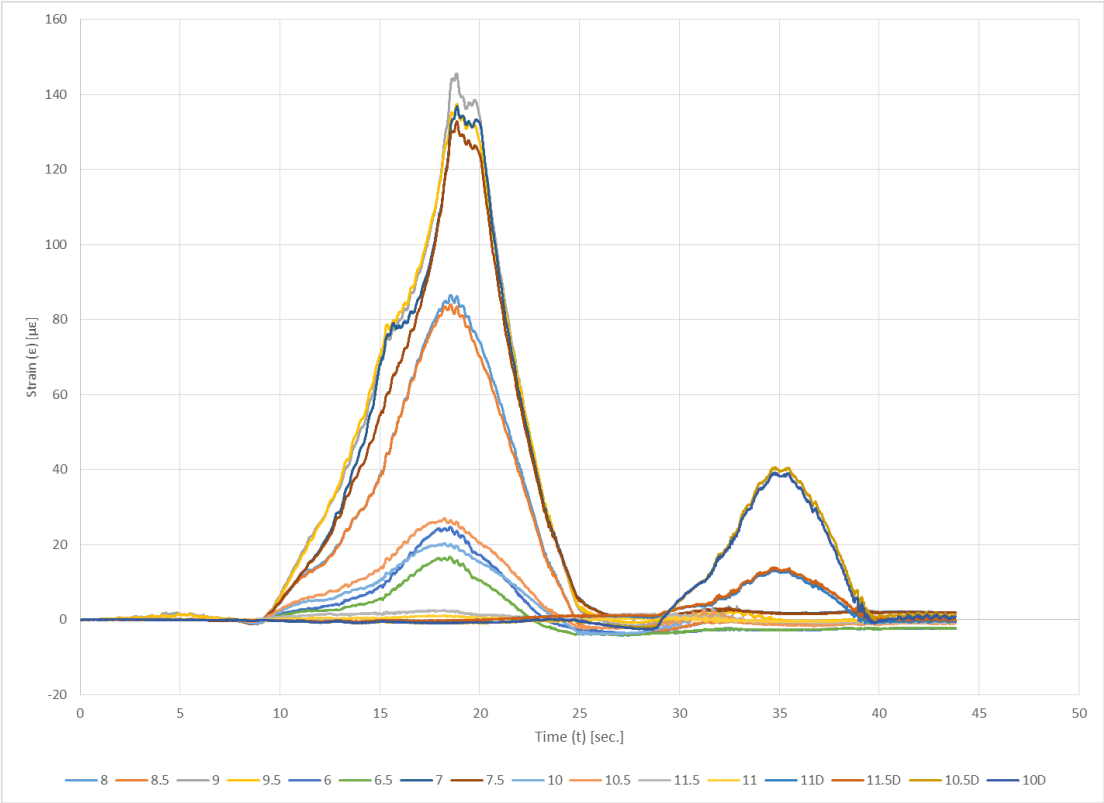

Figure B 12: Half Truck, Scenario One, Run Three

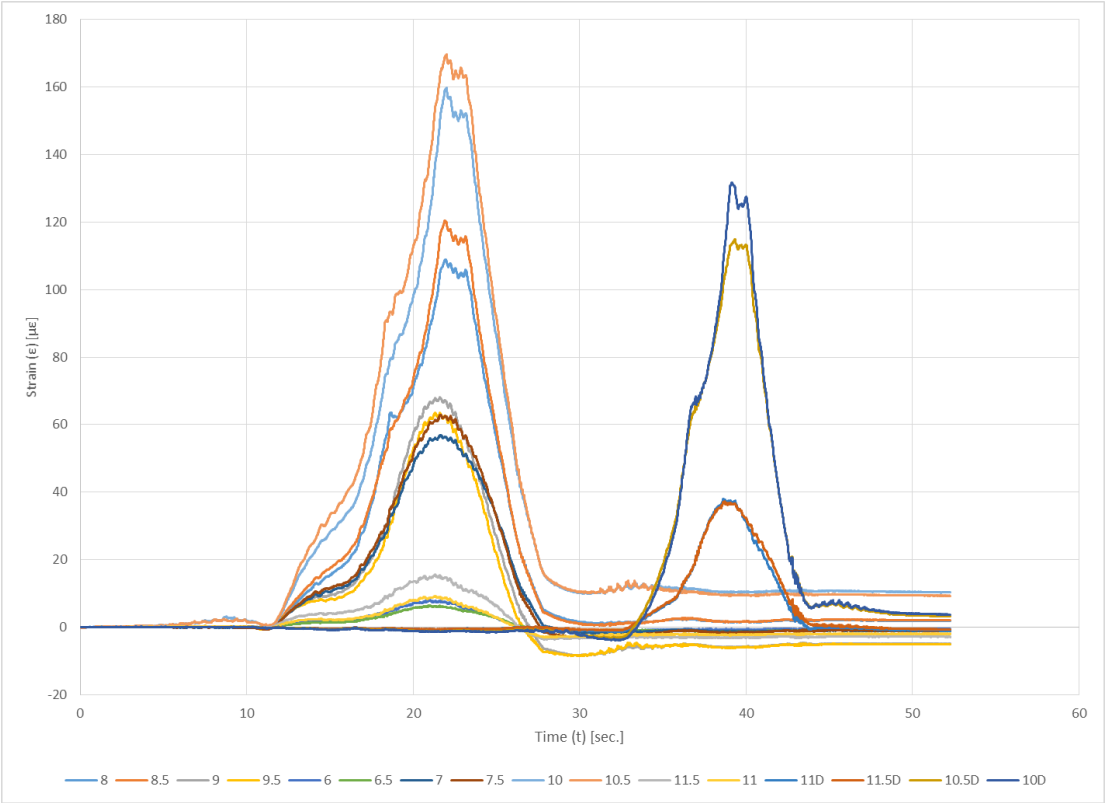

Figure B 13: Half Truck, Scenario Two, Run One

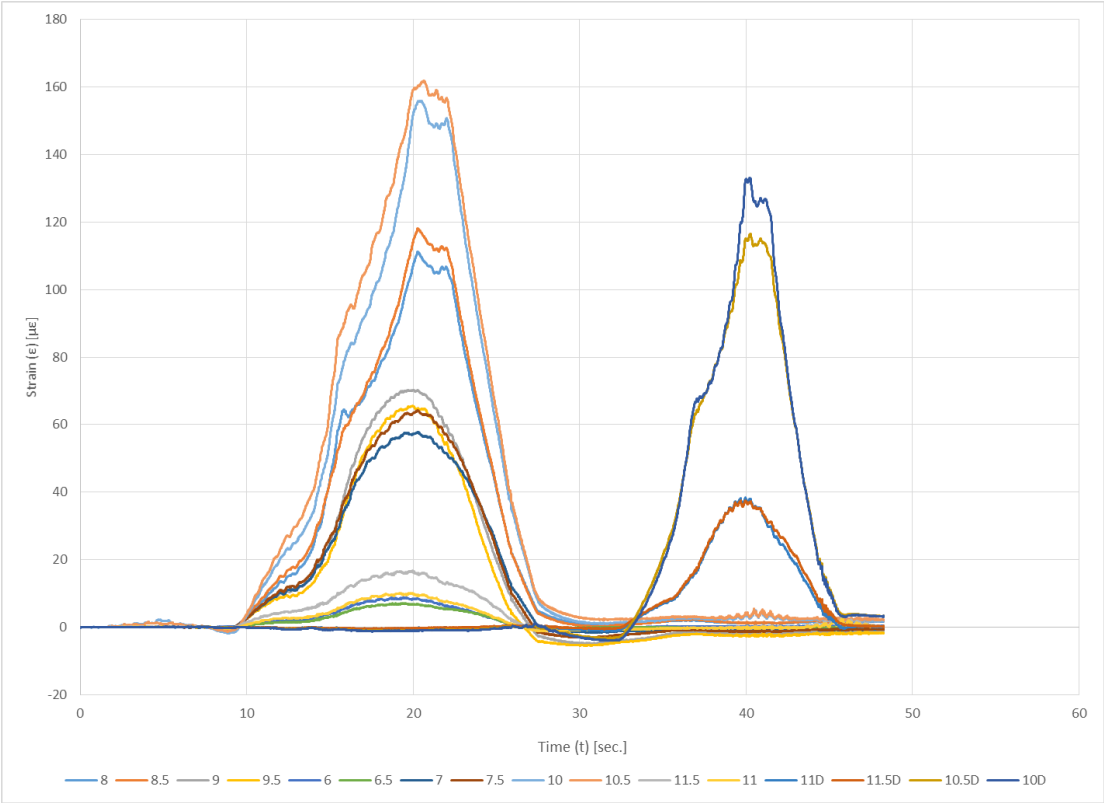

Figure B 14: Half Truck, Scenario Two, Run Two

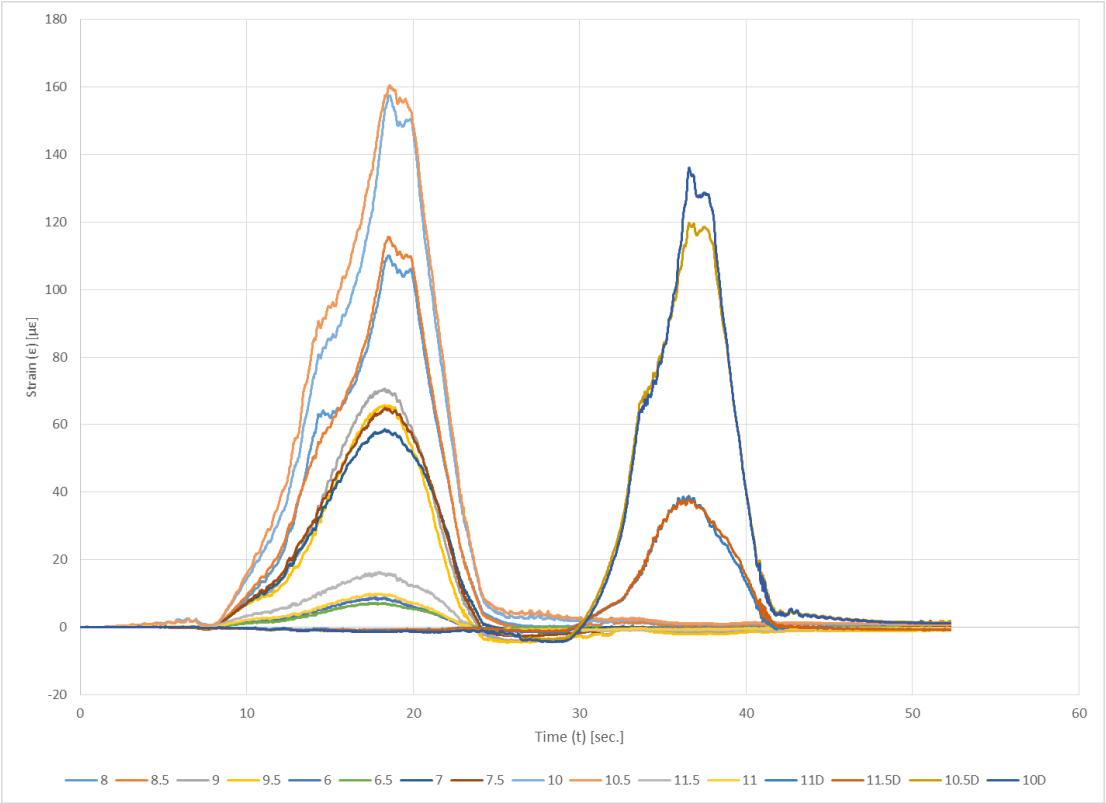

Figure B 15: Half Truck, Scenario Two, Run Three

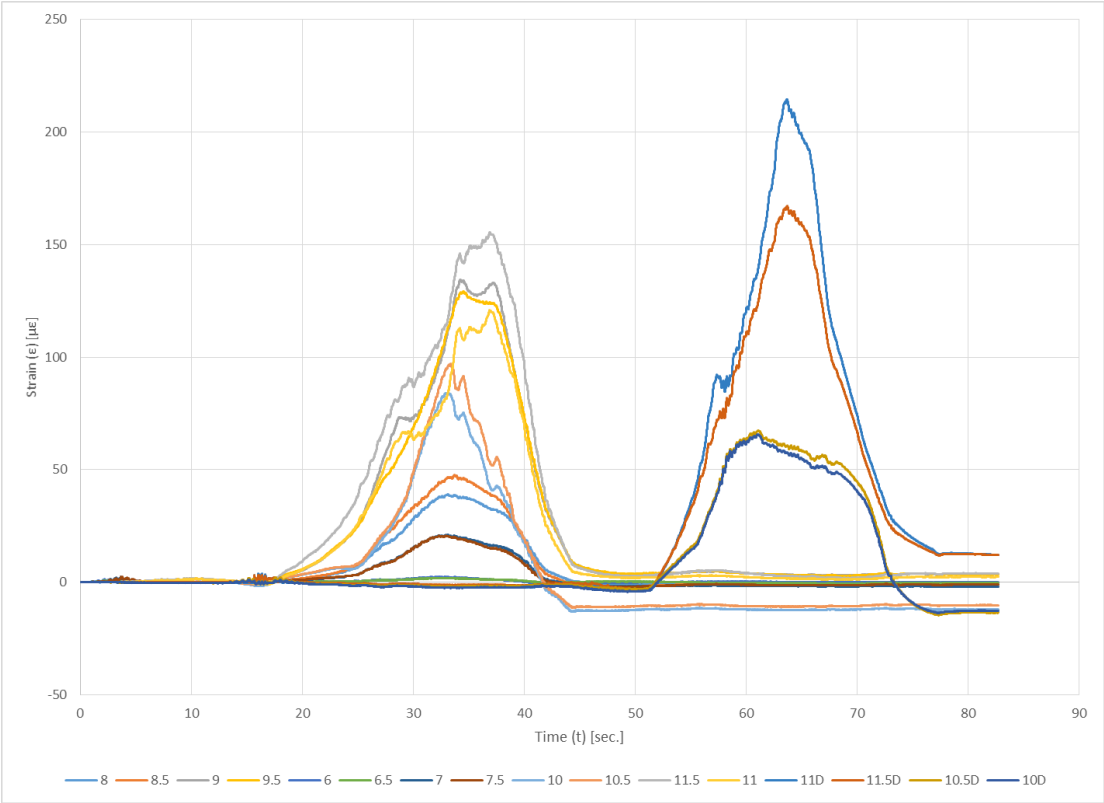

Figure B 16: Half Truck, Scenario Three, Run One

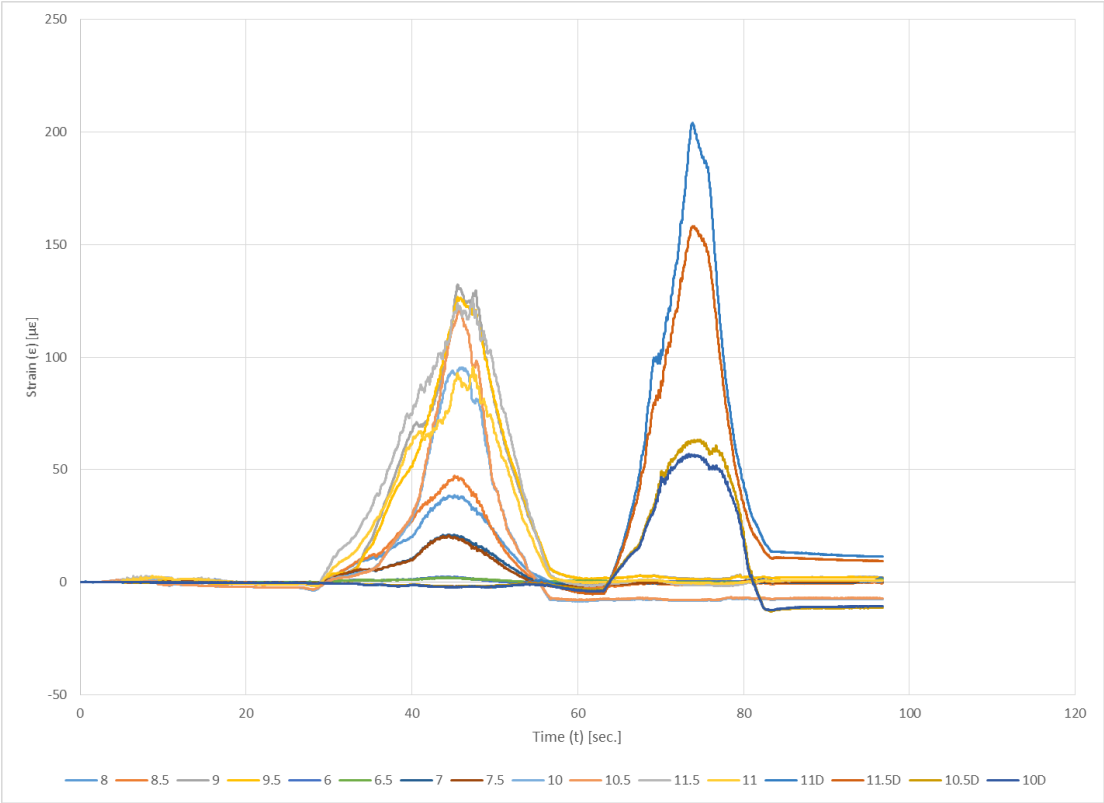

Figure B 17: Half Truck, Scenario Three, Run Two

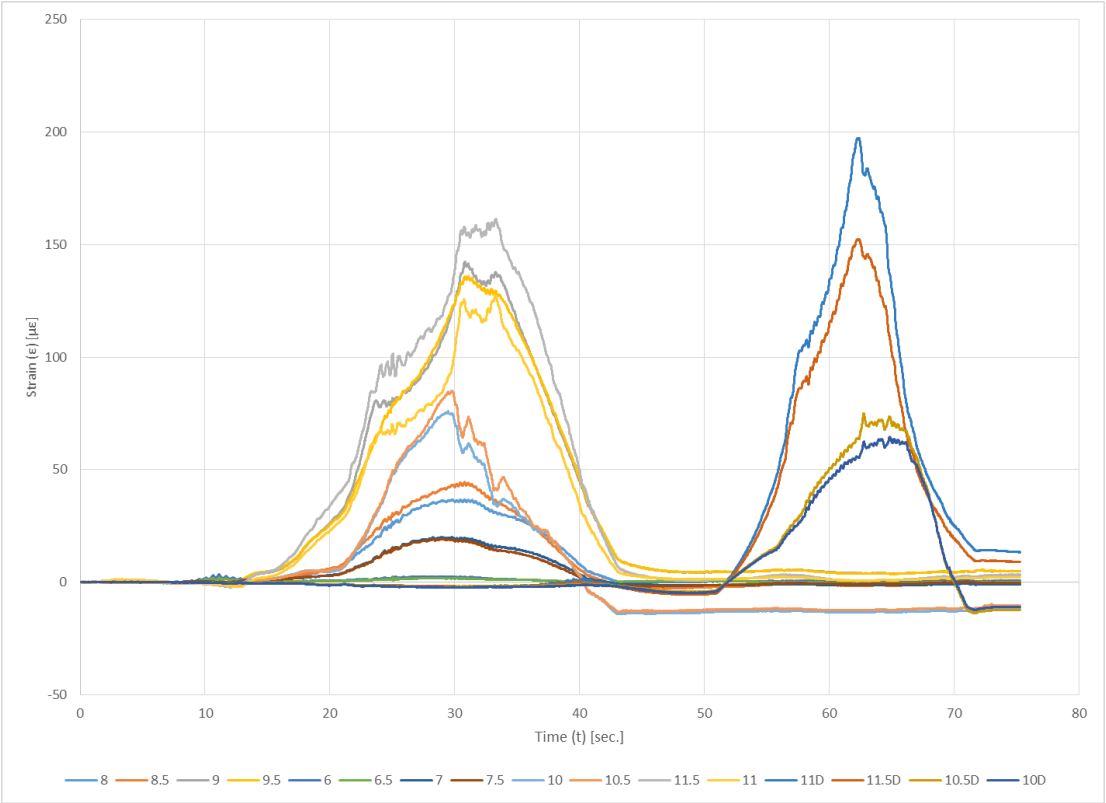

Figure B 18: Half Truck, Scenario Three, Run Three

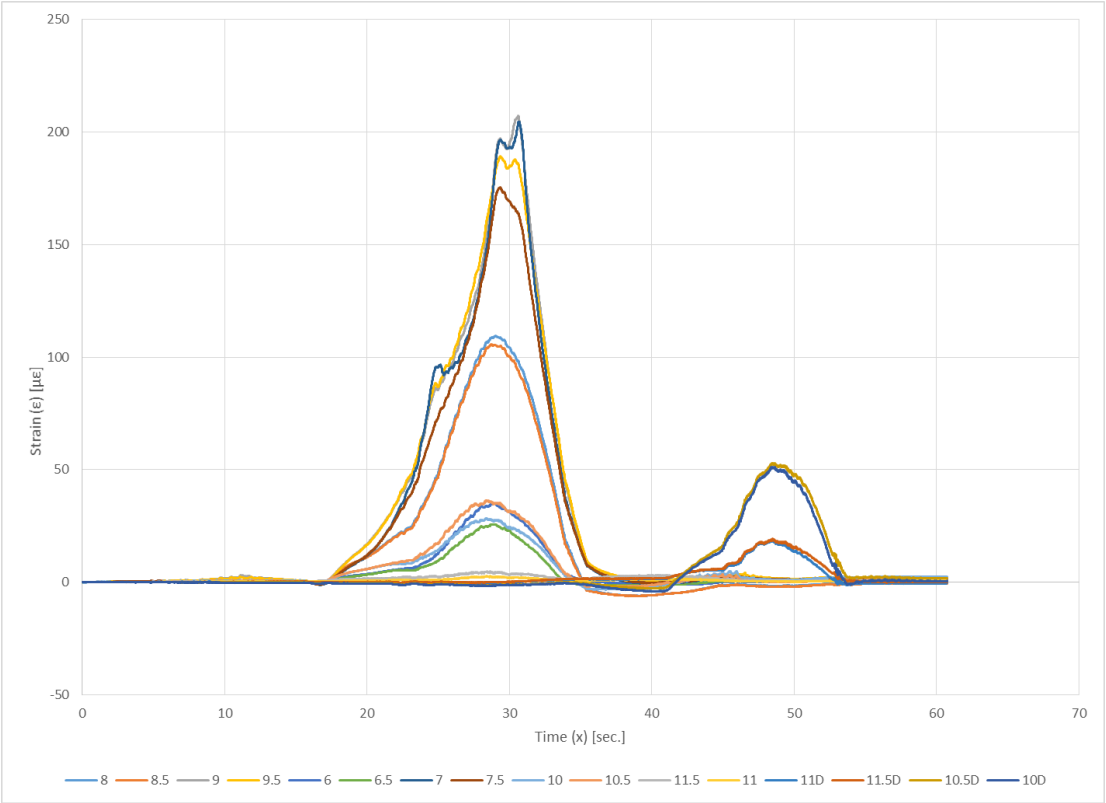

Figure B 19: Full Truck, Scenario One, Run One

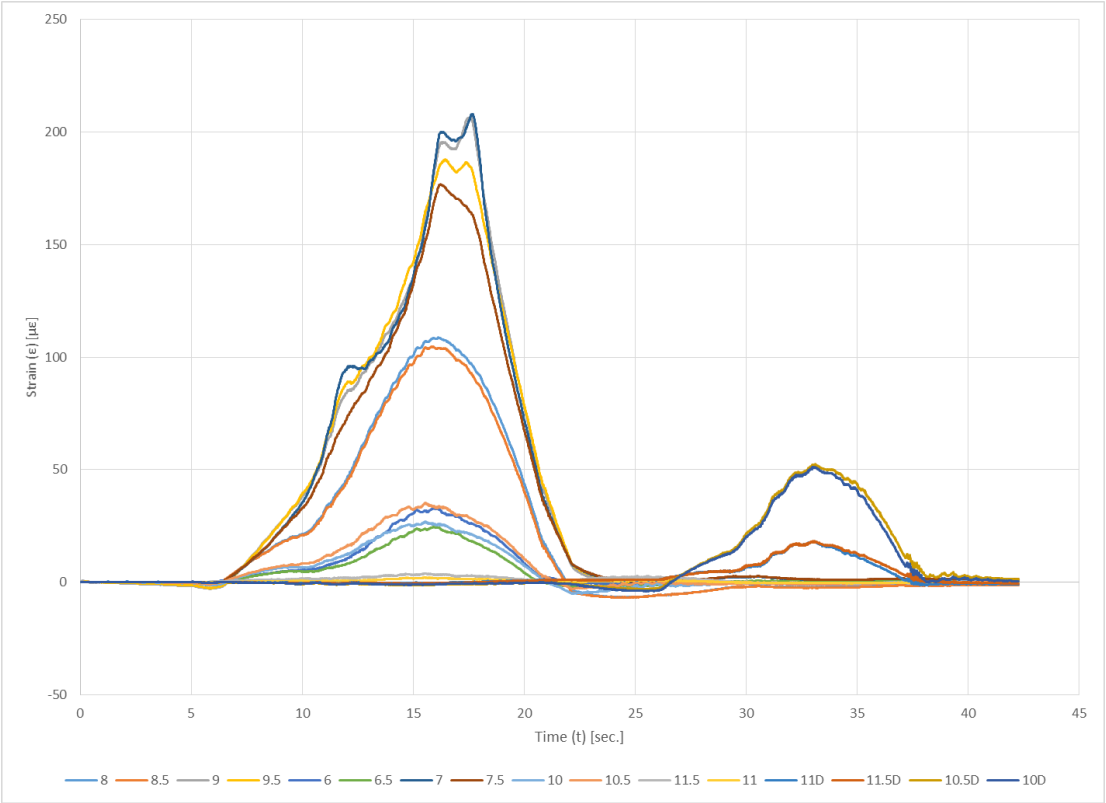

Figure B 20: Full Truck, Scenario One, Run Two

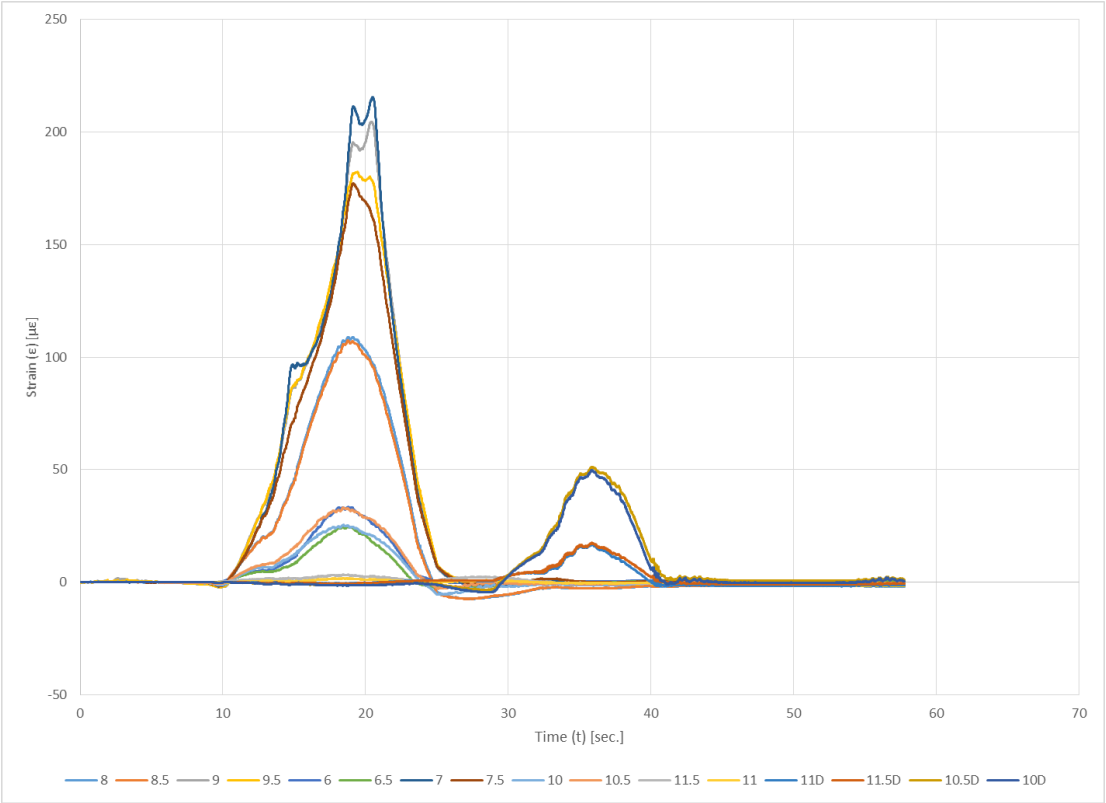

Figure B 21: Full Truck, Scenario One, Run Three

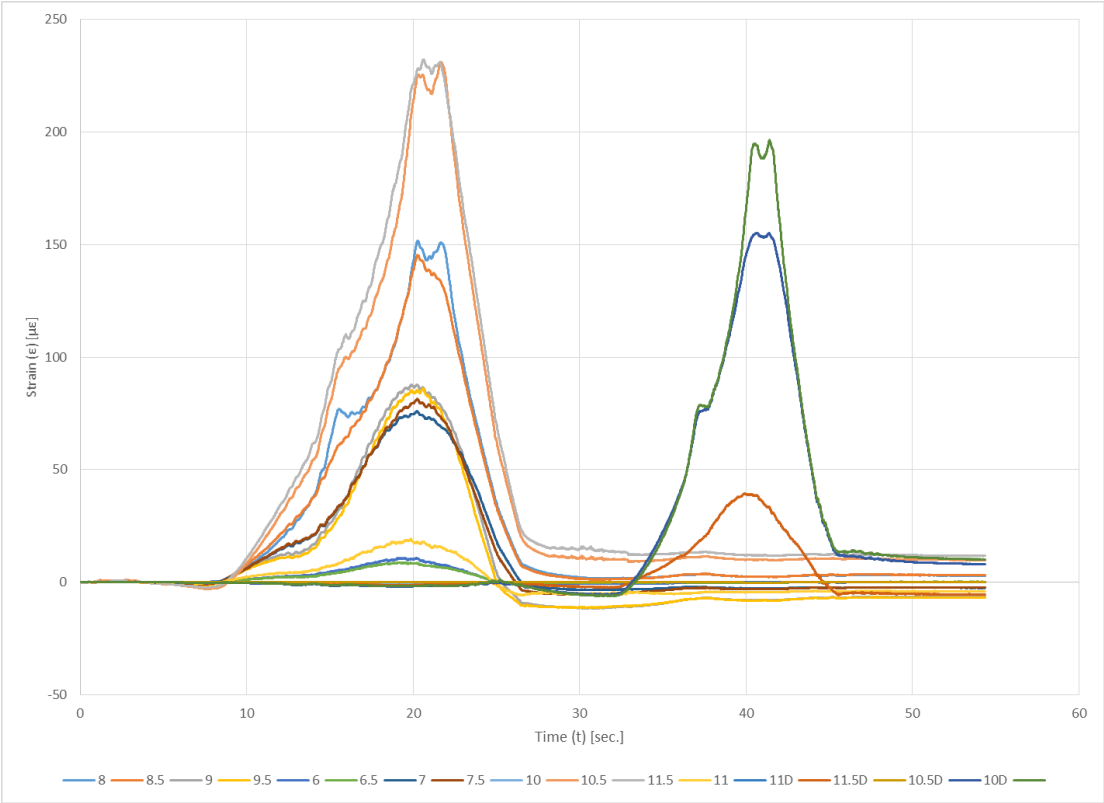

Figure B 22: Full Truck, Scenario Two, Run One

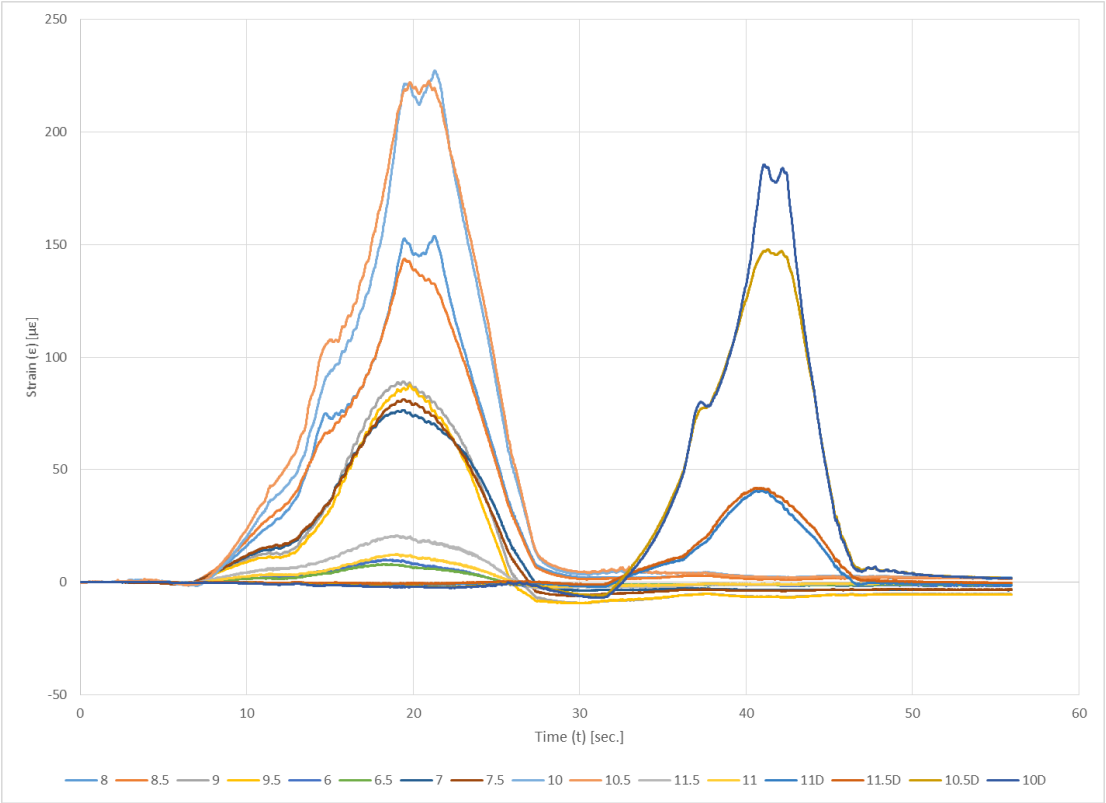

Figure B 23: Full Truck, Scenario Two, Run Two

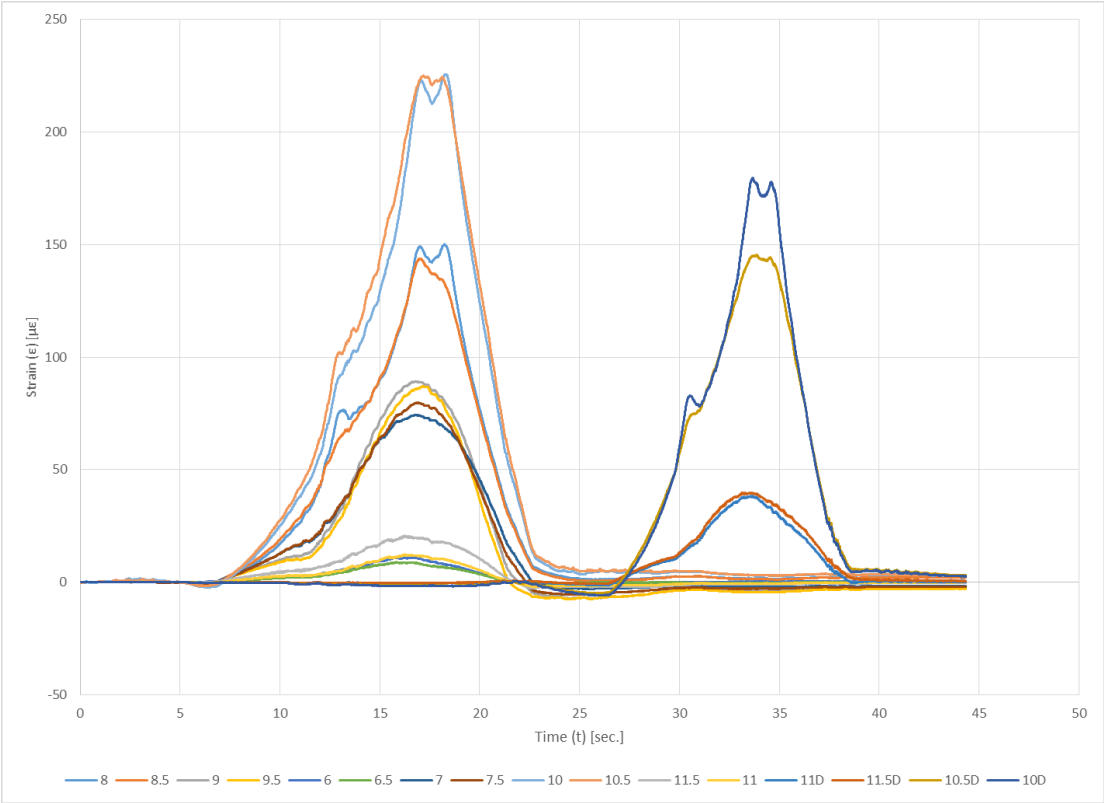

Figure B 24: Full Truck, Scenario Two, Run Three

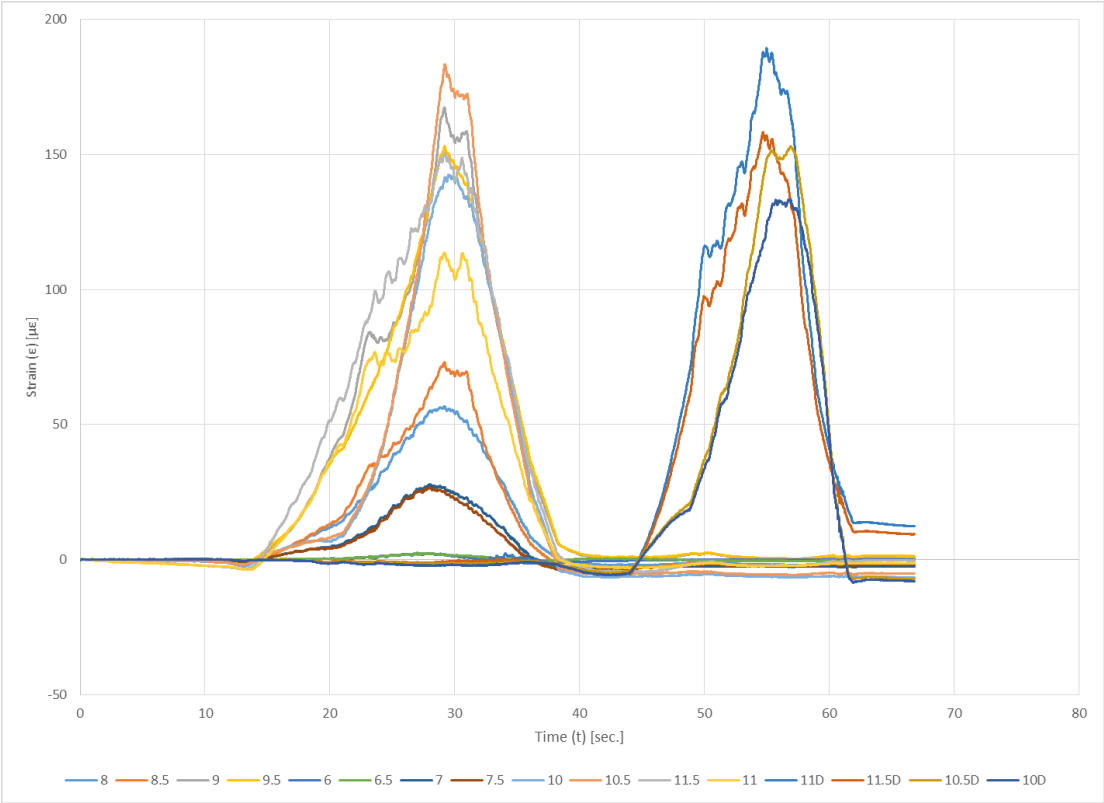

Figure B 25: Full Truck, Scenario Three, Run One

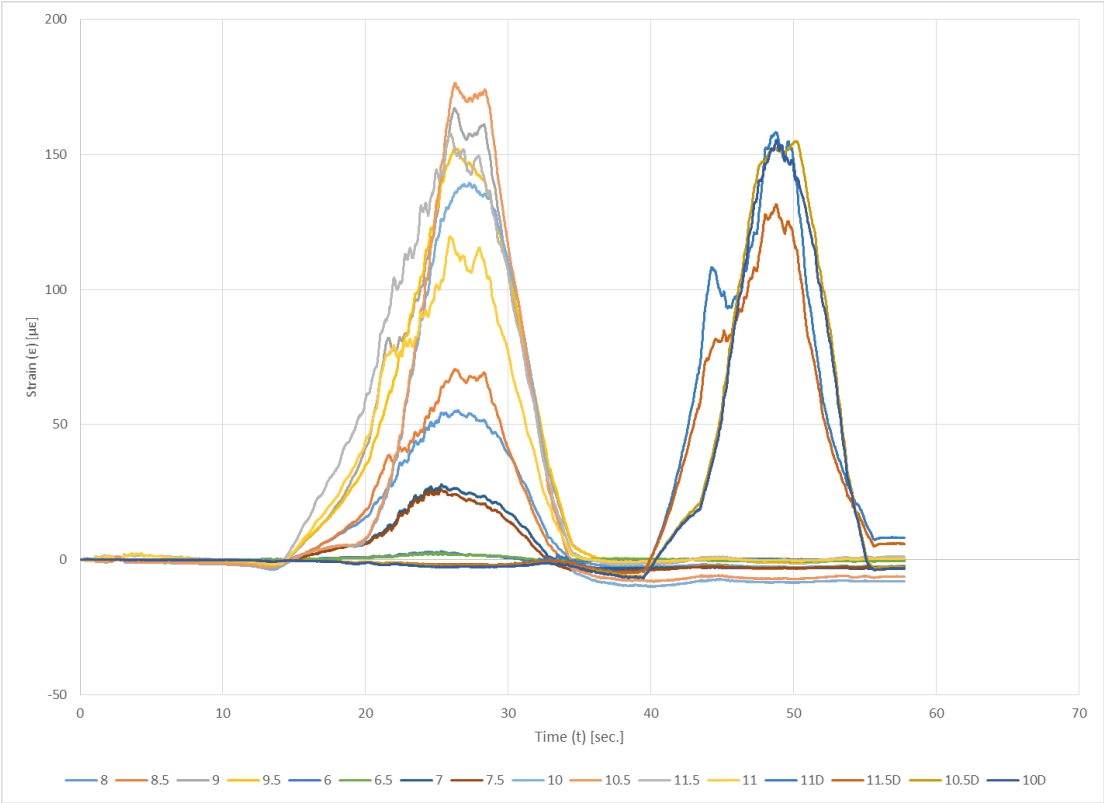

Figure B 26: Full Truck, Scenario Three, Run Two

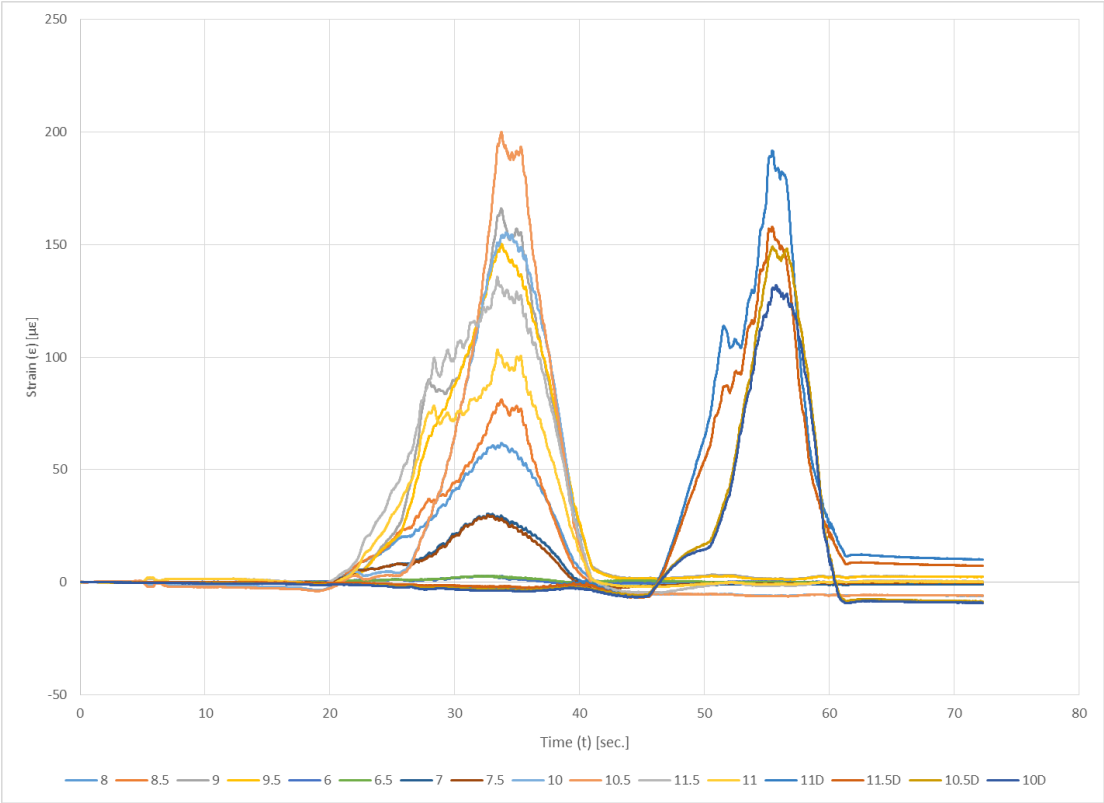

Figure B 27: Full Truck, Scenario Three, Run Three

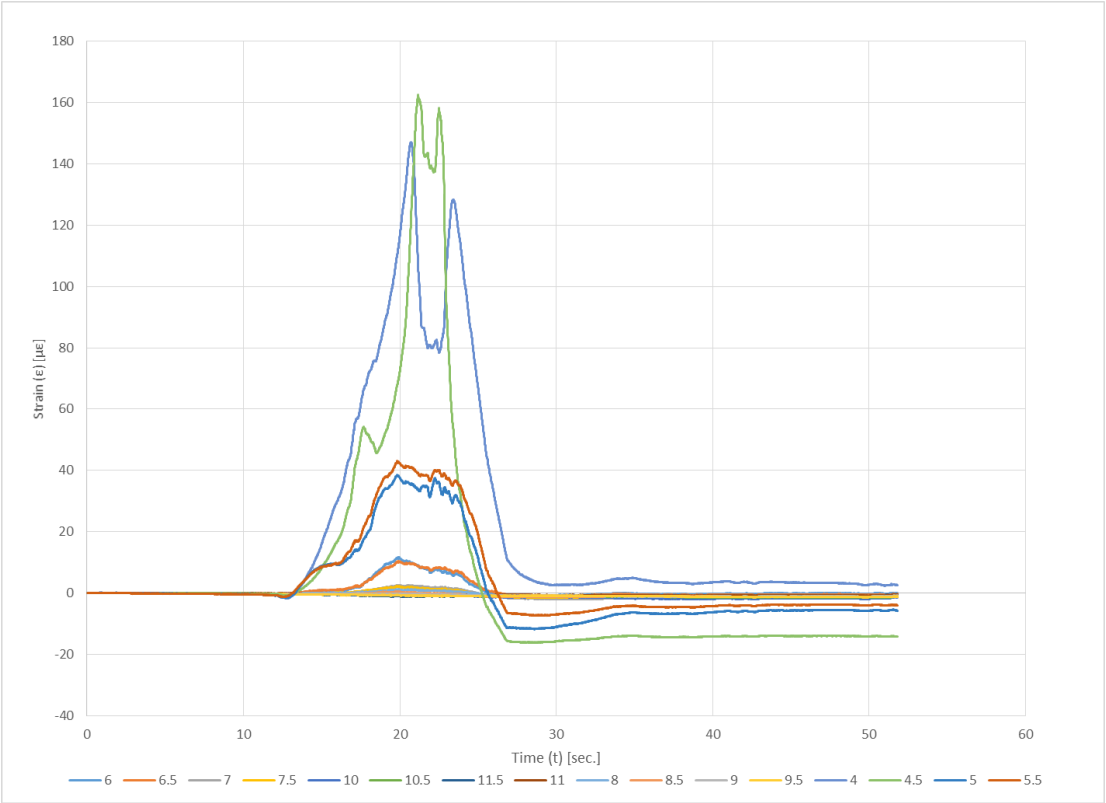

Figure B 28: Full Truck, Scenario Four, Run Two

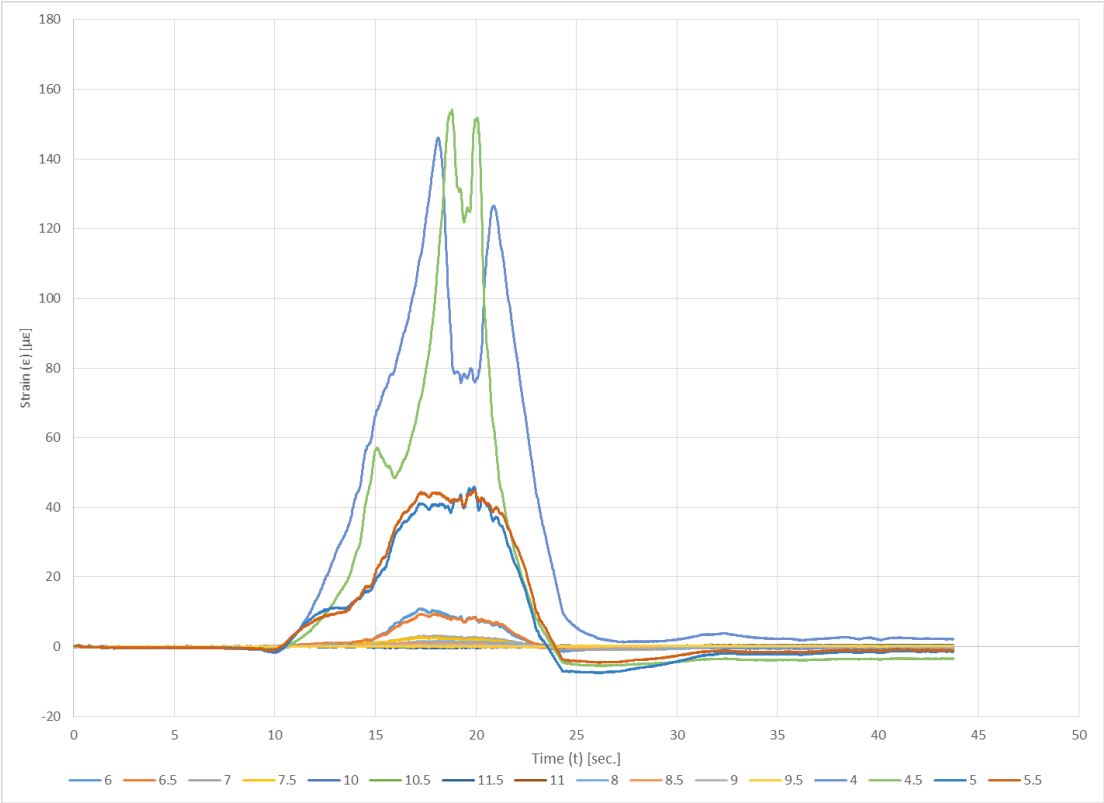

Figure B 29: Full Truck, Scenario Four, Run Three

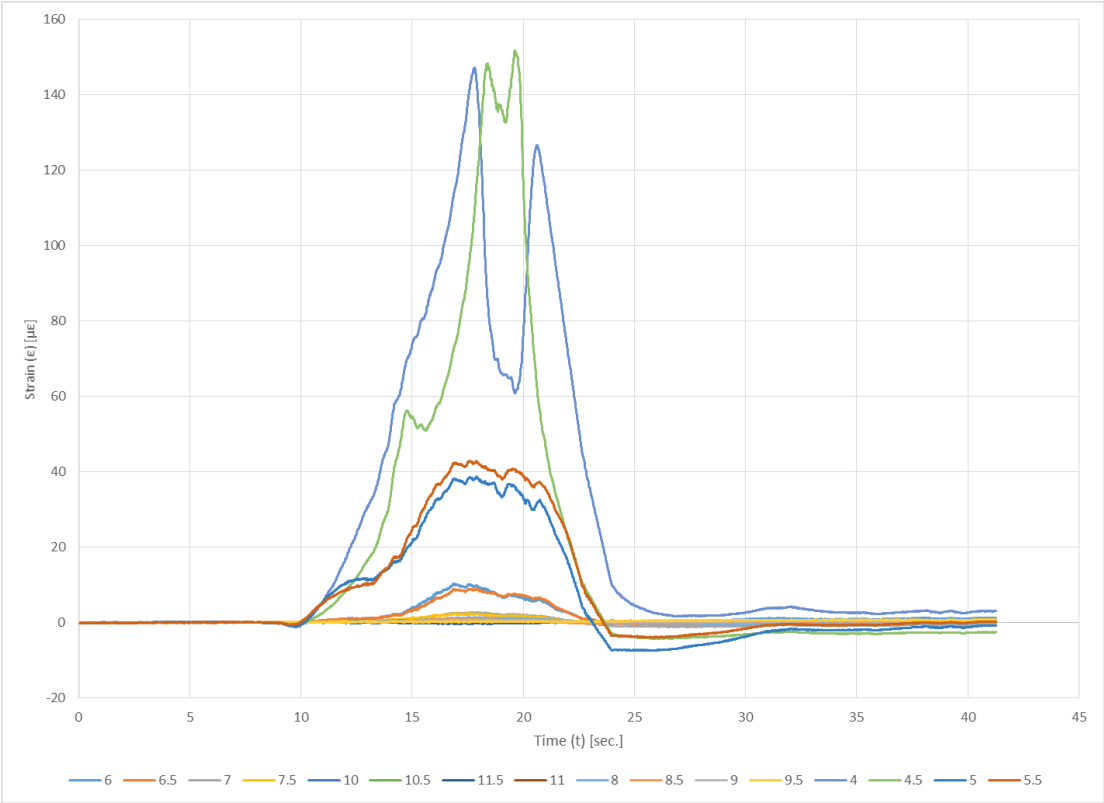

Figure B 30: Full Truck, Scenario Four, Run Four

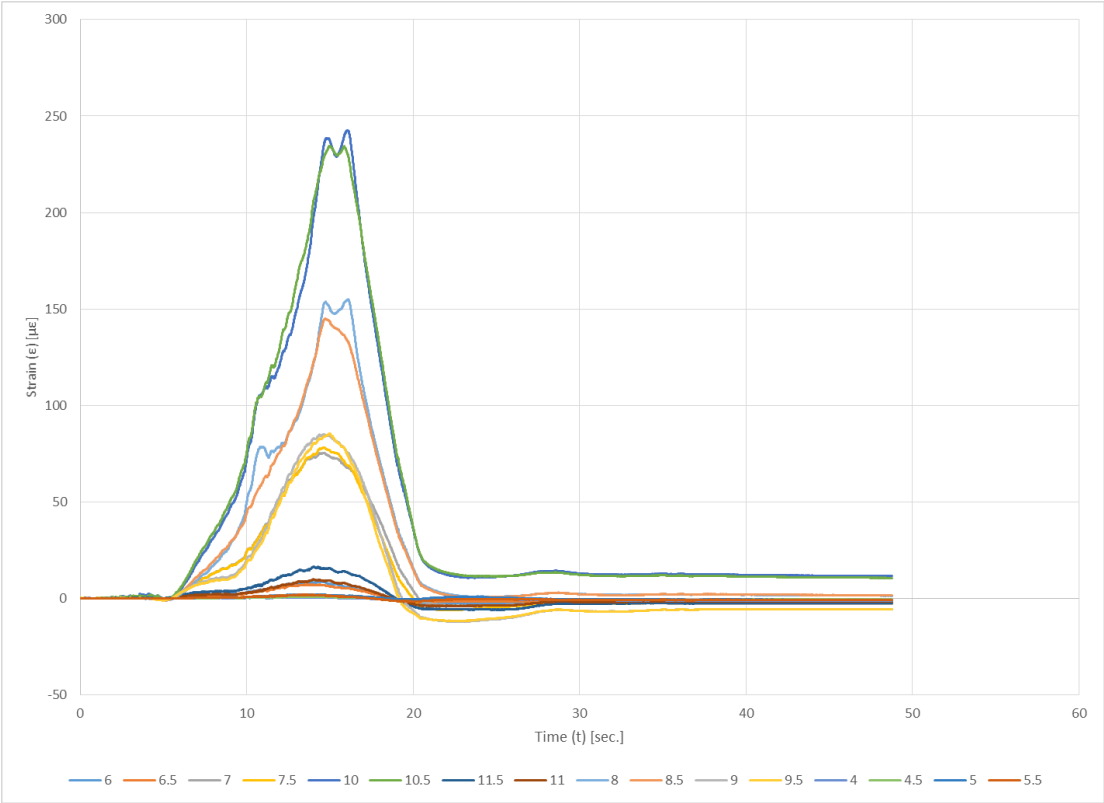

Figure B 31: Full Truck, Scenario Five, Run One

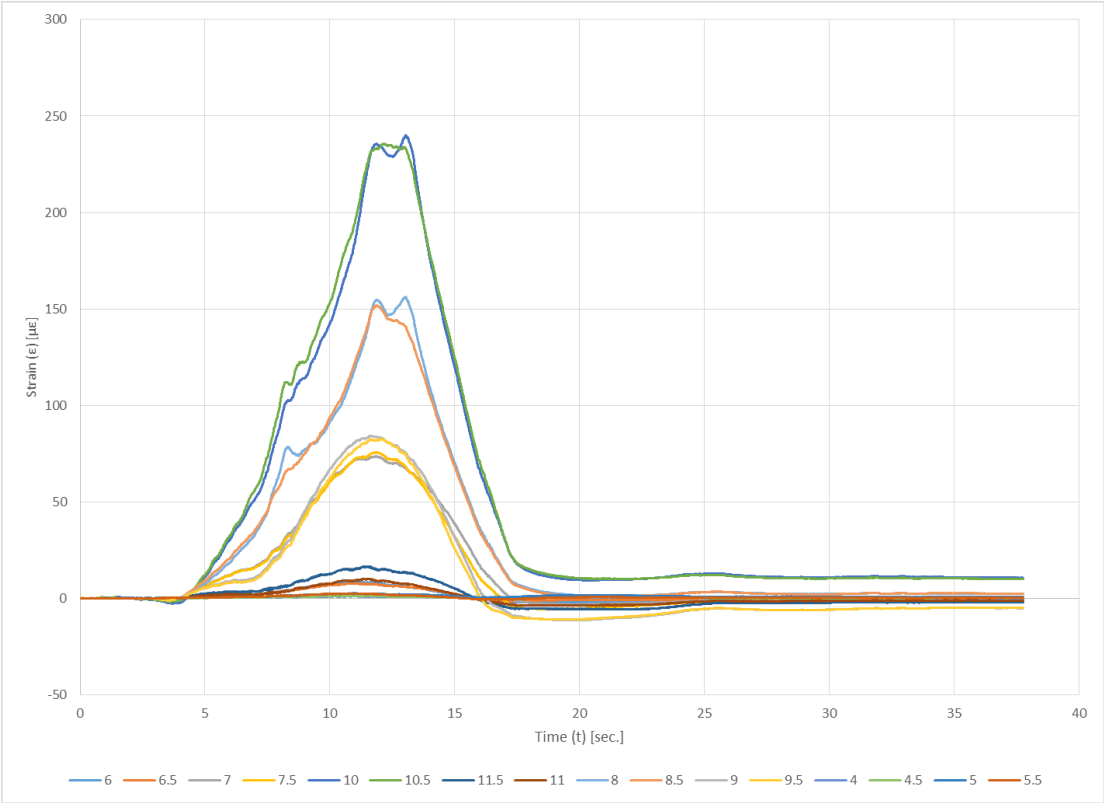

Figure B 32: Full Truck, Scenario Five, Run Two

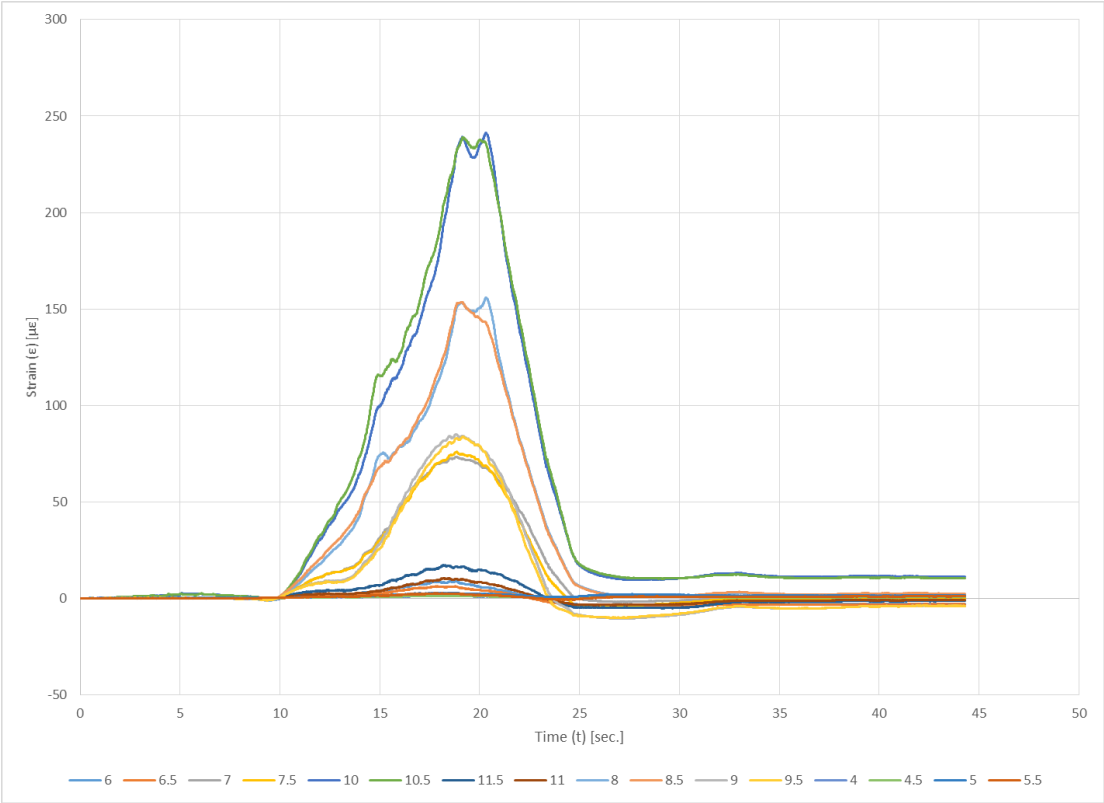

Figure B 33: Full Truck, Scenario Five, Run Three

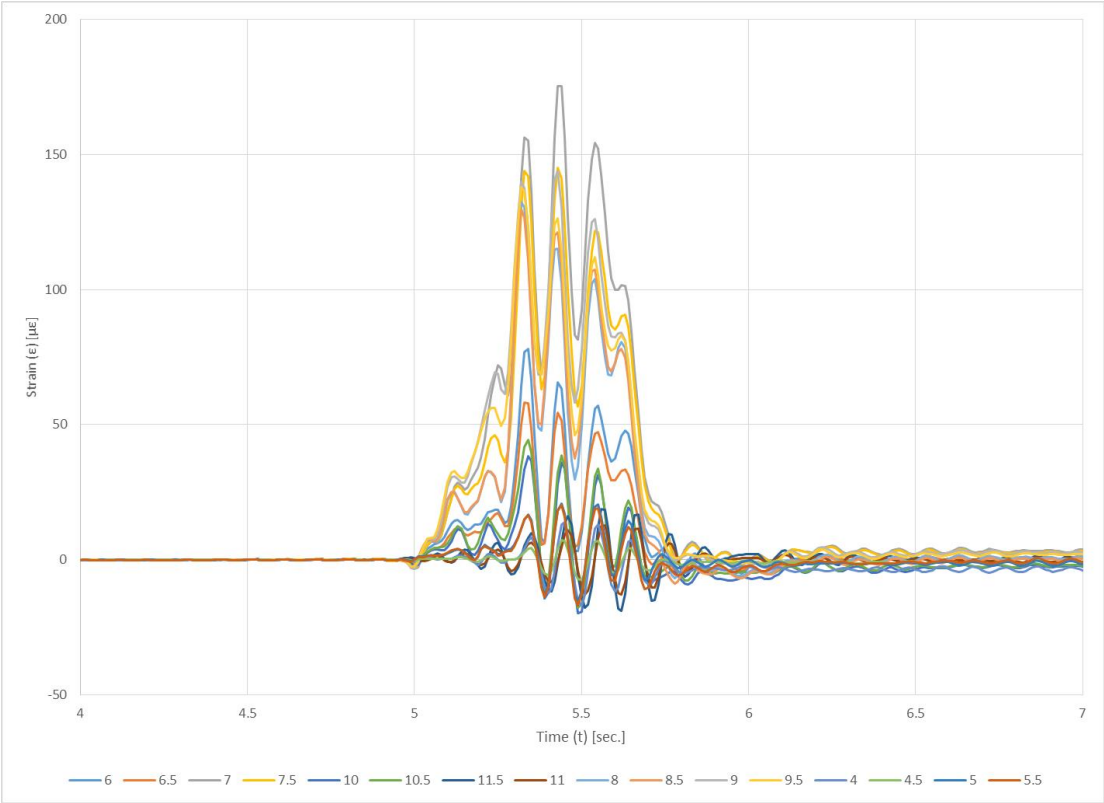

Figure B 34: Full Truck, Scenario Six, Run One

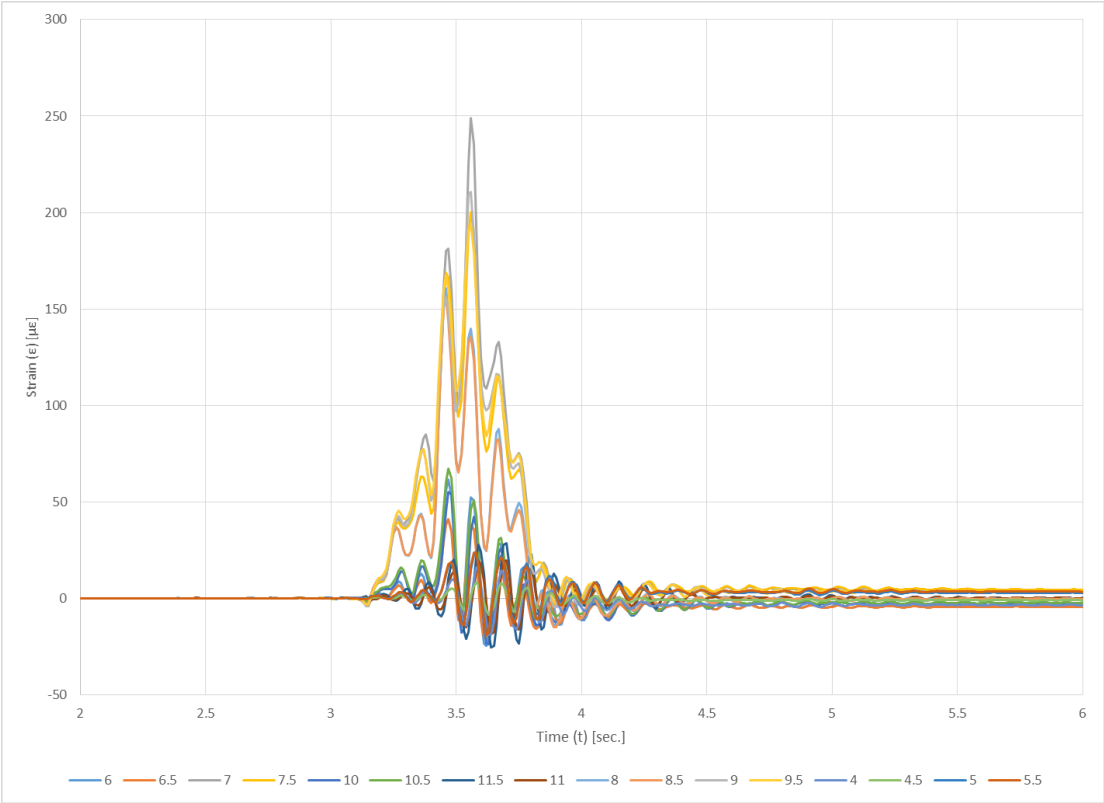

Figure B 35: Full Truck, Scenario Six, Run Two

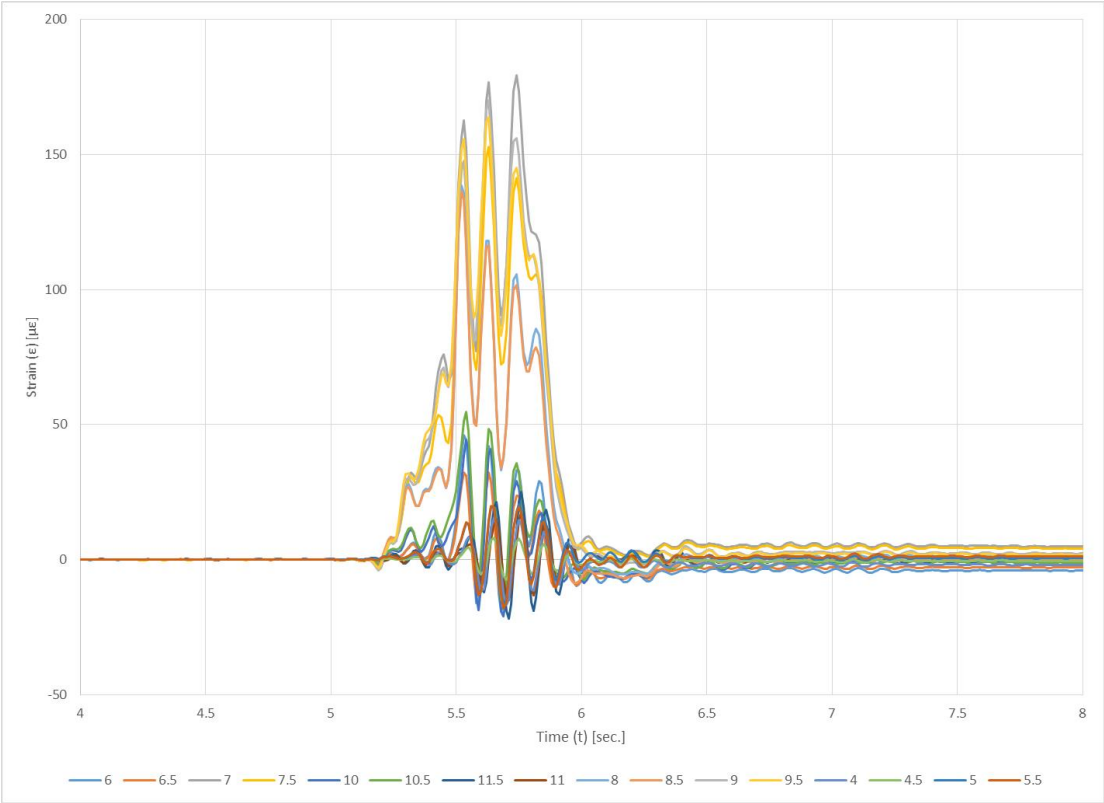

Figure B 36: Full Truck, Scenario Six, Run Three

Appendix C: Calculations

Table 4.6.2.2.2b-1 (continued)—Distribution of Live Loads for Moment in Interior Beams

Type of Superstructure	Applicable Cross-Section from Table 4.6.2.2.1-1	Distribution Factors	Range of Applicability
	h	Regardless of Number of Loaded Lanes: S/D where: $C = K(W/L) \le K$ $D = 11.5 - N_L + 1.4N_L(1-0.2C)^2$ when $C \le 5$ $D = 11.5 - N_L$ when $C > 5$ $K = \sqrt{\frac{(1+\mu)I}{J}}$ for preliminary design, the following values of K may be used: Beam Type — K Nonvoided rectangular beams — 0.7 Rectangular beams with circular voids: — 0.8 Box section beams — 1.0 Channel beams — 2.2 T-beam — 2.0 Double T-beam — 2.0	Skew $\le 45°$ $N_L \le 6$
	g, i, j if connected only enough to prevent relative vertical displacement at the interface		

Figure C 1: DFM Excerpt from AASHTO LRFD Table 4.6.2.2.2b-1

Beam Capacity and Demand

Precast Beam Info:

Required Compressive Strength for use in Design $f'_c := 5ksi$

Required Compressive Strength Before Transfer $f'_{ci} := 4ksi$

Concrete Unit Weight $w_c := .150\frac{kip}{ft^3}$

Design Span $l := 30ft$

Prestressing Strands:

Area of Strands $A_s := 0.085in^2$

Ultimate Strength of Strands $f_{pu} := 270ksi$

Yield Strength $f_{py} := .9 \cdot f_{pu} = 243 \cdot ksi$

Before Transfer $f_{pi} := 0.75 f_{pu} = 202.5\,ksi$

At Service Limit State $f_{pe} := 0.8 f_{pi} = 162 \cdot ksi$

Modulus of Elasticity $E_p := 28500ksi$

Channel Properties:

Bituminous Surfacing, 1.5 in. thick $w_s := 0.140\frac{kip}{ft^3}$

Cross Section Properties

Area of Channel

$A_g := 36.5in \cdot 5in + .75in \cdot 2.5in + 2 \cdot (4.5in \cdot 14in) + 4 \cdot .5 \cdot 1in \cdot 14in = 338.375in^2$ $A_g = 338.375in^2$

Depth of Beam $h := 19in$

Moment of Inertia

$$y_t := \frac{36.5in \cdot 5in \cdot 2.5in + .75in \cdot 2.5in \cdot 2.5in + 2 \cdot (4.5in \cdot 14in \cdot 12in) + 4 \cdot \left[.5 \cdot 1in \cdot 14in \cdot \left(5in + \frac{14}{3}in \right) \right]}{36.5in \cdot 5in + .75in \cdot 2.5in + 2 \cdot (4.5in \cdot 14in) + 4 \cdot (.5 \cdot 1in \cdot 14in)} = 6.631 \cdot in$$

$y_t = 6.631 \cdot in$

$y_b := h - y_t = 12.369in$ $y_b = 12.369in$

$$I_g := \frac{1}{12}\cdot 36.5in\cdot(5in)^3 + 36.5in\cdot 5in\cdot\left(y_t - 2.5in\right)^2 + 2\left[\frac{1}{36}\cdot .75in\cdot(2.5in)^3\right] \ldots = 9.588\times 10^3\cdot in^4$$
$$+ .5\cdot .75in\cdot 2.5in\cdot\left(y_t - 2.5in\cdot\frac{2}{3}\right)^2 + .5\cdot 2.5in.75in\cdot\left[y_t - \left(2.5in + 2.5in\cdot\frac{1}{3}\right)\right]^2 \ldots$$
$$+ 2\cdot\left[\frac{1}{12}\cdot 4.5in\cdot(14in)^3 + 4.5in\cdot 14in\cdot\left(y_b - 7in\right)^2\right] \ldots$$
$$+ 4\cdot\frac{1}{36}\cdot 1in\cdot(14in)^3 + \frac{1}{2}\cdot 1in\cdot 14in\cdot\left(y_b - 14in\cdot\frac{2}{3}\right)^2$$

$I_g = 9.588\times 10^3\cdot in^4$

Section Modulus for bottom fiber

$S_b := \frac{I_g}{y_b} = 775.133in^3$ $S_b = 775.133in^3$

Section Modulus for top fiber

$S_t := \frac{I_g}{y_t} = 1.446\times 10^3\cdot in^3$ $S_t = 1.446\times 10^3\cdot in^3$

Beam Weight per unit length

$w_g := \frac{A_g}{144in^2}\cdot 1ft^2\cdot w_c = 0.352\frac{kip}{ft}$ $w_g = 0.352\frac{kip}{ft}$

Modulus of Elasticity of Concrete

At Service Loads:

$E_{c'} := 330000.15^{1.5}\cdot 5^{.5} = 4.287\times 10^3$ $E_{c'} := E_{c'}\cdot ksi = 4.287\times 10^3\cdot ksi$

Distance between center of gravity of bottom fiber and strands

$y_{bs} := \frac{4\cdot 2in + 4\cdot 4in + 4\cdot 6in}{12} = 4\cdot in$ $y_{bs} = 4\cdot in$

Strand eccentricity at midspan

$e_c := y_b - y_{bs} = 8.369\,in$ $e_c = 8.369\,in$

Bending Moments:

DC $w_g = 0.352\,\frac{kip}{ft}$

DW

$w_{ws} := \left(\frac{1.5in}{12in}\,1ft \cdot w_s \cdot 37.25in\right) = 0.054\,\frac{kip}{ft}$ $w_{ws} = 0.054\,\frac{kip}{ft}$

barrier weight $w_b := .022\,\frac{kip}{ft}$

Bending Moments at Mid-Span due to Dead Load

Beam Weight

$M_g := 0.5 \cdot w_g \cdot 15ft \cdot (30ft - 15ft) = 39.653\,kip \cdot ft$ $M_g = 39.653\,kip \cdot ft$

Wearing Surface

$M_{ws} := 0.5 \cdot w_{ws} \cdot 15ft \cdot (30ft - 15ft) = 6.111\,kip \cdot ft$ $M_{ws} = 6.111\,kip \cdot ft$

Barrier

$M_b := 0.5 \cdot w_b \cdot 15ft \cdot (30ft - 15ft) = 2.475\,kip \cdot ft$ $M_b = 2.475\,kip \cdot ft$

Bending Moments due to Live Load

Assumed DFM $DFM_1 := 0.5$

Experimental DFM $DFM_2 := 0.44$

Dynamic Load Allowance

All Other Limit States $IM := .33$

Moment from Tandem Axle of HL-93 Truck:

$l := 30ft$

$P_1 := 32kip$ $P_2 := 32kip$

$x_1 := 14ft$ $x_2 := 0ft$

$y_{bar} := \frac{P_1 \cdot x_1 + P_2 \cdot x_2}{P_1 + P_2} = 7ft$

$x := \frac{y_{bar}}{2} = 3.5ft$

$x' := \frac{l}{2} - x = 11.5ft$

$R_R := \frac{x' \cdot P_2 + (x' + x_1) \cdot P_1}{l} = 39.467kip$

$R_L := P_1 + P_2 - R_R = 24.533kip$

$M_{93} := R_L \cdot x' = 282.133kip \cdot ft$

$M_{LT} := M_{93} \cdot (1 + IM) = 375.237kip \cdot ft$ $M_{LT} = 375.237kip \cdot ft$

Moment from Design Lane Load

$M_{LL} := .5 \cdot .64\frac{kip}{ft} \cdot 15ft \cdot (30ft - 15ft) = 72 \cdot kip \cdot ft$ $M_{LL} = 72 \cdot kip \cdot ft$

AASHTO Limit States:

$DC := M_g = 39.653kip \cdot ft$

$DW := M_{ws} + M_b = 8.586kip \cdot ft$

$LL := M_{LT} + M_{LL} = 447.237kip \cdot ft$

Strength I with assumed DFM=0.5

$M_{u1} := 1.25 \cdot DC + 1.5 \cdot DW + 1.75 \cdot DFM_1 \cdot (LL) = 453.779kip \cdot ft$ $M_{u1} = 453.779kip \cdot ft$

Strength I with experimental DFM=0.44

$M_{u2} := 1.25 \cdot DC + 1.5 \cdot DW + 1.75 \cdot DFM_2 \cdot (LL) = 406.819kip \cdot ft$ $M_{u2} = 406.819kip \cdot ft$

Service III with assumed DFM=0.5

$$M_{applied1} := 1 \cdot DC + 1 \cdot DW + 0.8 \cdot DFM_1 \cdot (LL) = 227.135\,kip \cdot ft$$

$M_{applied1} = 227.135\,kip \cdot ft$

Service III with experimental DFM=0.44

$$M_{applied2} := 1 \cdot DC + 1 \cdot DW + .8 \cdot DFM_2 \cdot (LL) = 205.667\,kip \cdot ft$$

$M_{applied2} = 205.667\,kip \cdot ft$

AASHTO-defined Nominal Strength:

$$k_1 := 2 \cdot \left(1.04 - \frac{f_{py}}{f_{pu}}\right) = 0.28$$

$k_1 = 0.28$

Area of prestressing strands

$$A_{ps} := A_s \cdot 12 = 1.02\,in^2$$

$A_{ps} = 1.02\,in^2$

Area of nonprestressed tension reinforcement

$A' := 0\,in^2$

Yield strength of tension reinforcement

$f_y := 40\,ksi$

Area of compression reinforcement

$$A'_s := 5\left(\frac{3}{8}\,in\right)^2 \cdot \frac{\pi}{4} = 0.552\,in^2$$

$A'_s = 0.552\,in^2$

Yield strength of compression reinforcement

$f'_y := 40\,ksi$

$$\beta_1 := 0.85 - .05 \cdot \left(\frac{f'_c}{ksi} - 4\right) = 0.8$$

$\beta_1 = 0.8$

Width of compression flange

$b := 36.5\,in$

Distance from extreme compression fiber to centroid of prestress strands

$$d_p := h - y_{bs} = 15\,in$$

$d_p = 15\,in$

Distance from extreme compression fiber to N.A.

For 270 ksi steel:

$$c := \frac{A_{ps}\cdot f_{pu} + A'\cdot f_y - A'_s\cdot f'_y}{0.85\cdot f'_c\cdot \beta_1\cdot b + k_1\cdot A_{ps}\cdot \frac{f_{pu}}{d_p}} = 1.96\,in$$

$c = 1.96\,in$

Depth of equivalent stress block

$$a := \beta_1\cdot c = 1.568\,in$$

$a = 1.568\,in$

Compression flange depth

$t_s := 5in$

The depth of the equivalent stress block is less than the depth of the compression flange so these calculations are good.
a = 1.568" < t_s = 5"

Average stress in prestressing strand

$$f_{ps} := f_{pu}\cdot\left(1 - k_1\cdot\frac{c}{d_p}\right) = 260.122\,ksi$$

$f_{ps} = 260.122\,ksi$

Depth to compression reinforcement

$$d'_s := 2in + \frac{3}{16}in = 2.188\,in$$

$d'_s = 2.188\,in$

Check if compression steel yields

$$\varepsilon'_s := .003\cdot\frac{\left(c - d'_s\right)}{c} = -3.482\times 10^{-4} \qquad \varepsilon_s := \frac{40}{29000} = 1.379\times 10^{-3}$$

$\varepsilon'_s < \varepsilon_s$ So compression steel does not yield

Nominal flexural resistance

$$M_{na} := A_{ps}\cdot f_{ps}\cdot\left(d_p - \frac{a}{2}\right) = 314.321\,kip\cdot ft$$

$M_{na} = 314.321\,kip\cdot ft$

$M_{na} = 314.321 kip \cdot ft$ $M_{u1} = 453.779 kip \cdot ft$

$M_{u2} = 406.819 kip \cdot ft$ $M_n < M_u$

The capacity of the beam is less than the ultimate moment for both DFM values.

LIMITS OF REINFORCEMENT

Minimum Reinforcement

The amount of tensile reinforcement must be adequate to be equal to or greater than the minimum of 1.2*M_{cr} or 1.33*M_u

Modulus of rupture of concrete

$f_r := 7.5 \cdot \sqrt{f'_c \cdot psi} = 0.53 \cdot ksi$ $f_r = 0.53 \cdot ksi$

Cracking Moment

Compressive stress due to effective prestress force only

$P_{pe} := A_{ps} \cdot f_{pe} = 165.24 kip$

$f_{cpe} := \frac{P_{pe}}{A_g} + \frac{P_{pe} \cdot e_c}{S_b} = 2.273 ksi$ $f_{cpe} = 2.273 ksi$

$M_{cr} := \left(f_r + f_{cpe}\right) \cdot S_b - M_g = 141.394 kip \cdot ft$ $M_{cr} = 141.394 kip \cdot ft$

Strain Compatibility Approach for Nominal Strength:

$$r := \sqrt{\frac{I_g}{A_g}} = 5.323\,in$$

$$(r) = 5.323\,in$$

$$(f'_c := 5ksi)$$

$$(E_c := 330000.15^{1.5}\cdot\sqrt{5}\cdot ksi = 4.287\times 10^{3}\cdot ksi)$$

$$(\varepsilon_{cu} := .003)$$

The stress and strain in the tendons resulting from the effective prestress force:

$$\left(\varepsilon_{pe} := \frac{f_{pe}}{E_p} = 5.684\times 10^{-3}\right)$$
$$(\varepsilon_1 := \varepsilon_{pe} = 5.684\times 10^{-3})$$

The increase in steel strain as the concrete at its level is decompressed:

$$\varepsilon_2 := \frac{P_{pe}}{A_g\cdot E_{c'}}\cdot\left(1+\frac{y_b^{\,2}}{r^2}\right) = 7.29\times 10^{-4}$$

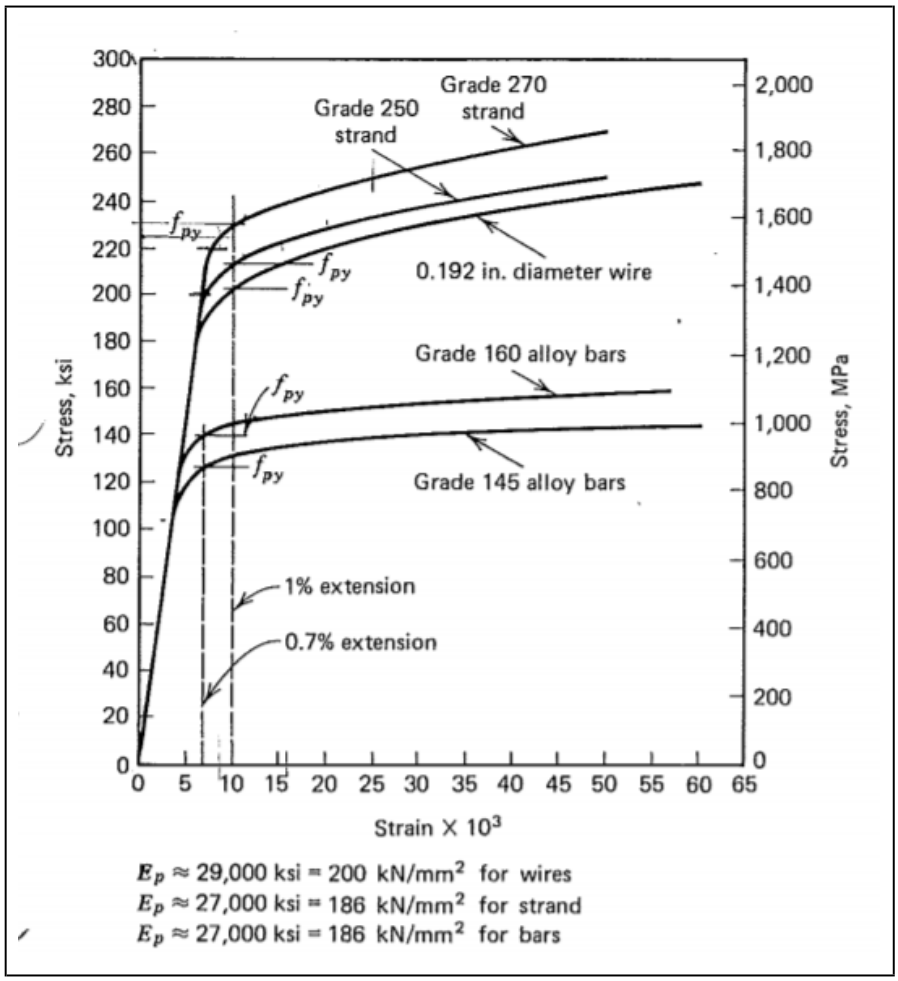

Assume initial steel stress at failure to be 200 ksi, this results in a strain of 0.007. (strain values determined from figure above)

$\left(f_{ps} := 200\text{ksi}\right)$

$\left(\varepsilon_{ps} := .007\right)$

$$a := \frac{A_{ps} \cdot f_{ps}}{0.85 \cdot f'_c \cdot b} = 1.315\,\text{in}$$

a is less than the flange depth of 5" so this equation was valid to use

$$\left(\beta_1 := 0.85 - .05 \cdot \left(\frac{f'_c}{\text{ksi}} - 4\right) = 0.8\right)$$

$$c := \frac{a}{\beta_1} = 1.644\,in$$

The increment of steel strain as the beam passes from decompression to failure:

$$\varepsilon_3 := \varepsilon_{cu} \cdot \frac{d_p - c}{c} = 0.024$$

Sum of strains results in strain at failure:

$$\left(\varepsilon_{ps} := \varepsilon_1 + \varepsilon_2 + \varepsilon_3 = 0.031\right)$$

This value is not close enough to the .007 strain first assumed so a new stress must be assumed, a stress of 245 will be chosen this time:

$$\left(f_{ps} := 245\,ksi\right)$$

$$\left(\varepsilon_{ps} := .02\right)$$

$$a := \frac{A_{ps} \cdot f_{ps}}{0.85 \cdot f'_c \cdot b} = 1.611\,in$$

a is less than the flange depth of 5" so this equation was valid to use

$$\left(\beta_1 := 0.85 - .05\left(\frac{f'_c}{ksi} - 4\right) = 0.8\right)$$

$$c := \frac{a}{\beta_1} = 2.014\,in$$

The increment of steel strain as the beam passes from decompression to failure:

$$\varepsilon_3 := \varepsilon_{cu} \cdot \frac{d_p - c}{c} = 0.01935$$

Sum of strains results in strain at failure:

$$\left(\varepsilon_{ps} := \varepsilon_1 + \varepsilon_2 + \varepsilon_3 = 0.02576\right)$$

The assumed strain of .02 and final strain of .02031 are equivalent (the initial strain was roughly estimated from a stress-strain curve so there are no claims for this to be an exact match). The stress of 245 ksi will be used to determine the capacity of the channel:

Nominal Moment at Mid-Span:

$$M_{ns} := A_{ps} \cdot f_{ps} \cdot \left(d_p - \frac{a}{2} \right) = 295.601 \text{kip} \cdot \text{ft}$$

Load Rating for Five Forks Bridge

Mid-Span Design Load Rating with HL-93 Tandem Axle

General Load Rating Equation *Eq. 6A.4.2.1-1*

$(\varphi_c := .85)$ Condition Factor

$(\varphi_s := 1)$ System Factor for Flexural and Axial Effects

$(\varphi_c \cdot \varphi_s) = 0.85$ >= 0.85 Factor product equals lower limit

$(\varphi := 1)$ Typical LRFD Resistance Factor for Prestressed Concrete

$R_n := M_{na} = 314.321 kip \cdot ft$ Nominal Resistance from AASHTO-defined Nominal Moment

$(C := \varphi_c \cdot \varphi_s \cdot \varphi \cdot R_n = 267.173 kip \cdot ft)$ Strength Limit State Value

$(x := 15ft)$ Location of Mid-Span

$(L := 30ft)$ Span Length

$DW = 8.586 kip \cdot ft$ Dead Load Effect from 1.5" Wearing Surface

$DC = 39.653 kip \cdot ft$ Dead Load Effect from Self-Weight and Barrier Rail

$(P := 0kip \cdot ft)$ Permanent Loads other than Dead

$LL = 447.237 kip \cdot ft$ Live load effect from HL-93 and design lane load

$(\gamma_{DC} := 1.25)$ Dead Load Factor for Strength I

$(\gamma_{DW} := 1.5)$ Dead Load Factor for Strength I

$(\gamma_{LL} := 1.75)$ Evaluation Live Load Factor for Inventory Strength I

$(\gamma_P := 1)$ Dead Load Factor for Strength I

$(DFM := .5)$ Initial Estimate of Distribution Factor for Moment

$$RF_i := \frac{C - \gamma_{DC}\cdot DC - \gamma_{DW}\cdot DW + \gamma_P\cdot P}{DFM\cdot\gamma_{LL}\cdot(LL)}$$

$(RF_i) = 0.523$

The Rating Factor at the inventory level for the design load rating is less than one so the load rating must be checked at the operating level

$(\gamma_{LL} := 1.35)$ Evaluation Live Load Factor for Operating Strength I

$$RF_o := \frac{C - \gamma_{DC}\cdot DC - \gamma_{DW}\cdot DW + \gamma_P\cdot P}{DFM\cdot\gamma_{LL}\cdot(LL)}$$

$(RF_o) = 0.678$

The Rating Factor at the operating level for the design load rating is less than one so the adjusted load rating will be calculated from section 8 of the MBE to see if the bridge has any reserve capacity.

Load Rating through Load Testing ***Eq. 8.8.2.3.1***

$(RF_{co} := RF_o = 0.678)$

$(RF_{ci} := RF_i = 0.523)$

The Ka factor for the modified load rating equation requires the theoretical strain a girder would experience under the live load test (full truck weight 25 tons) with the experimental DFM = 0.41

Moment from 25 ton truck:

$l := 30ft$

$P_1 := 11.76kip$ $P_2 := 36.92kip$

$x_1 := 14.33\text{ft}$ $x_2 := 0\text{ft}$

$y_{bar} := \frac{P_1 \cdot x_1 + P_2 \cdot x_2}{P_1 + P_2} = 3.462\text{ft}$

$x := \frac{y_{bar}}{2} = 1.731\text{ft}$

$x' := \frac{l}{2} - x = 13.269\text{ft}$

$R_R := \frac{x' \cdot P_2 + (x' + x_1) \cdot P_1}{l} = 27.149\text{kip}$

$R_L := P_1 + P_2 - R_R = 21.531\text{kip}$

$M_{25} := R_L \cdot x' = 285.701\text{kip} \cdot \text{ft}$

$\varepsilon_c := \frac{M_{25} \cdot DFM_2}{S_b \cdot E_c'} \cdot 10^6 = 453.977$ Theoretical microstrain from 25T truck with experimentally determined DFM

$(\varepsilon_T := 241)$ Experimental maximum microstrain from 25T truck at girder 10 in scenario 5

$\left(K_a := \frac{\varepsilon_c}{\varepsilon_T} - 1 = 0.884\right)$

$W := \frac{LL}{1 + IM} \cdot DFM_2 = 147.958\text{kip} \cdot \text{ft}$ Load effect at design level load rating

$T := M_{25} \cdot DFM_2 = 125.709\text{kip} \cdot \text{ft}$ Load effect from unfactored test vehicle (25 T truck)

The moment caused by W (HL-93 truck) is 148 kip*ft after the experimental DFM of 0.44 is taken into account, the laboratory test shows that individual girders can take load up to 115 kip*ft and still exhibit linear behavior. 115 < 148*1.33 therefore no, the member behavior cannot be extrapolated to 1.33W

$\left(\frac{T}{W}\right) = 0.85$ > .7 so K_b = .5 Table 8.8.2.3.1-1 (MBE)

$(K_b := .5)$

$\left(K := 1 + K_a \cdot K_b = 1.442\right)$ Adjustment Factor

$\left(RF_{To} := RF_{co} \cdot K = 0.978\right)$ Adjusted Load Rating Factor for Strength I at Operating Level

$\left(RF_{Ti} := RF_{ci} \cdot K = 0.754\right)$ Adjusted Load Rating Factor for Strength I at Inventory Level

RF_{To} <= 1.0 therefore the Five Forks Bridge needs to undergo legal load rating.

Mid-Span Legal Load Rating with Type 3 Truck

The AASHTO Legal Load Trucks are shown in the figure below:

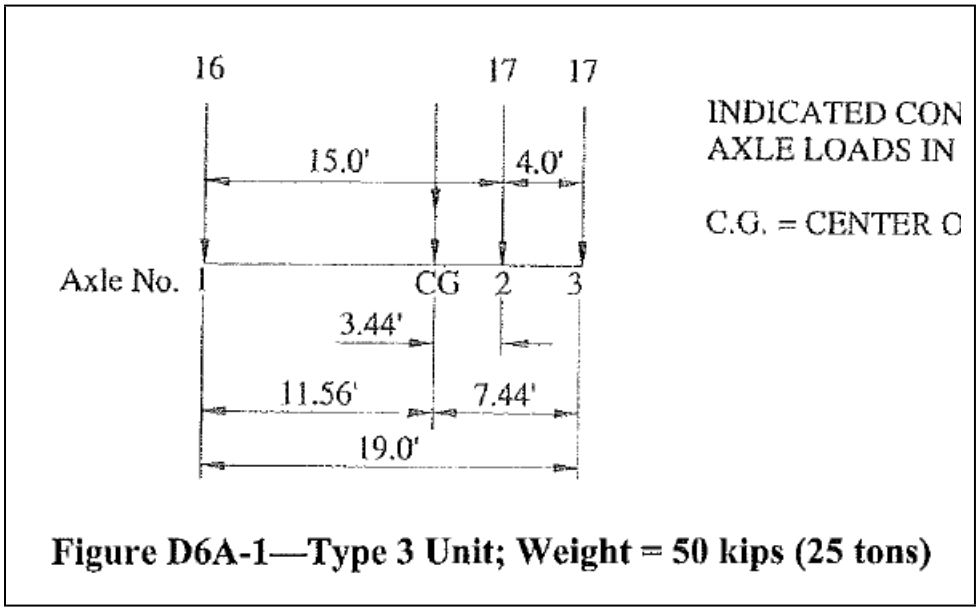

Figure D6A-1—Type 3 Unit; Weight = 50 kips (25 tons)

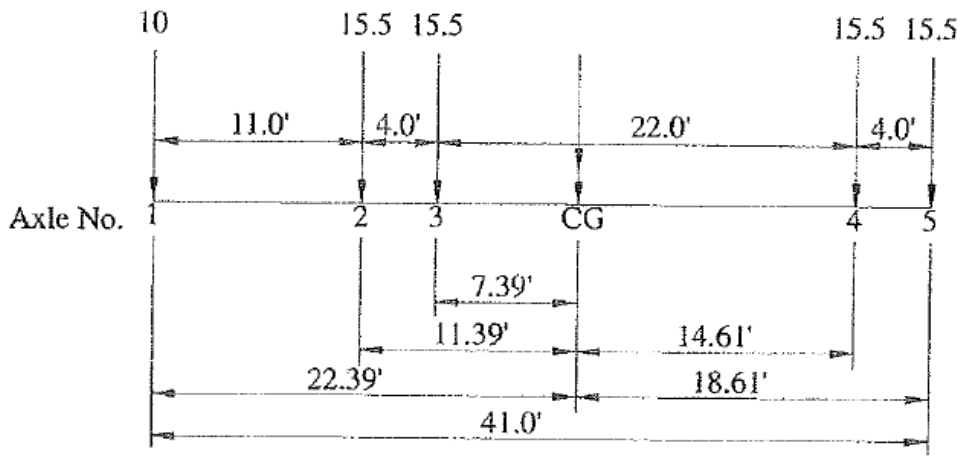

Figure D6A-2—Type 3S2 Unit; Weight = 72 kips (36 tons)

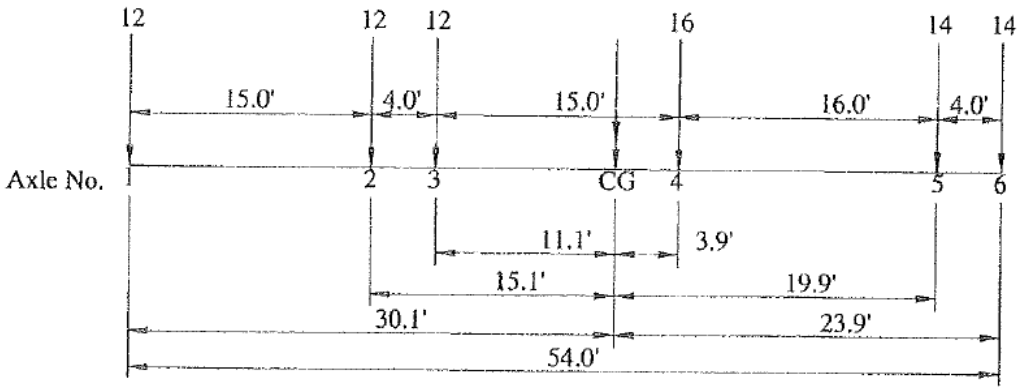

Figure D6A-3—Type 3-3 Unit; Weight = 80 kips (40 tons)

Only the truck from Figure D6A-1 is of interest because the other two trucks have lengths greater than the span length of the Five Forks Bridge. Table E6.A-1 backs up this statement by providing a list of the maximum moments caused by the three trucks at a span of 30 ft.

MAXIMUM MOMENT FROM WHEEL LINE LOAD

AASHTO Legal Load Truck Type 3

$L := 30ft$

$P_1 := 16kip$ $x_1 := 19ft$

$P_2 := 17\,kip$ $x_2 := 4\,ft$

$P_3 := 17\,kip$ $x_3 := 0\,ft$

$P_R := P_1 + P_2 + P_3 = 50\,kip$

$$y_{bar} := \frac{P_1 \cdot x_1 + P_2 \cdot x_2 + P_3 \cdot x_3}{P_R} = 7.44\,ft$$

$l_1 := x_2 - y_{bar} = -3.44\,ft$ l_1 is the distance from the resultant location to the nearest load

$$x := \frac{L}{2} - \frac{l_1}{2} = 16.72\,ft$$ x equals the distance to the resultant for the largest moment

$x' := x + l_1 = 13.28\,ft$

$$R_R := \frac{(x' - x_2) \cdot P_3 + x' \cdot P_2 + [x' + (x_1 - x_2)] \cdot P_1}{L} = 27.867\,kip$$

$R_L := P_R - R_R = 22.133\,kip$

$LL_1 := R_L \cdot (x' - x_2) + (R_L - P_3) \cdot (x_2) = 225.931\,kip \cdot ft$ Live Load Effect from Type 3 Truck at Mid-Span

$LL_2 := 0.64\,klf \cdot x \cdot .5 \cdot (L - x) = 71.053\,kip \cdot ft$ Live Load Effect from Design Lane

$\gamma_{DC} := 1.25$ Dead Load Factor for Strength I

$\gamma_{DW} := 1.5$ Dead Load Factor for Strength I

The Five Forks Bridge has an ADTT of 750, this value is reflected in the equation for the live load factor

$$\gamma_{LL} := 1.4 + \frac{750 - 100}{1000 - 100} \cdot .25 = 1.581$$ Evaluation Live Load Factor for Legal Load Rating

$\gamma_P := 1$ Dead Load Factor for Strength I

$DFM := .4$ Experimental Distribution Factor for Moment

$$RF_L := \frac{C - \gamma_{DC} \cdot DC - \gamma_{DW} \cdot DW + \gamma_P \cdot P}{DFM \cdot \gamma_{LL} \cdot [LL_1 \cdot (1 + IM) + LL_2]}$$

$RF_L = 0.792$ Single Factor for Legal Load Rating

The moment caused by W (Type 3 truck) is 93 kip*ft after the experimental DFM of 0.41 is taken into account, the laboratory test shows that indiviual girders can take load up to 115 kip*ft and still exhibit linear behavior. 115 < 93*1.33 therefore no, the member behavior cannot be extrapolated to 1.33W, the K_b value will remain the same

$(K := 1 + K_a \cdot K_b = 1.442)$ Adjustment Factor

$RF_{LT} := RF_L \cdot K = 1.142$ Adjusted Load Rating Factor for Legal Load Rating

RF_{LT} >= 1.0 therefore the Five Forks Bridge does not require restrictive posting.

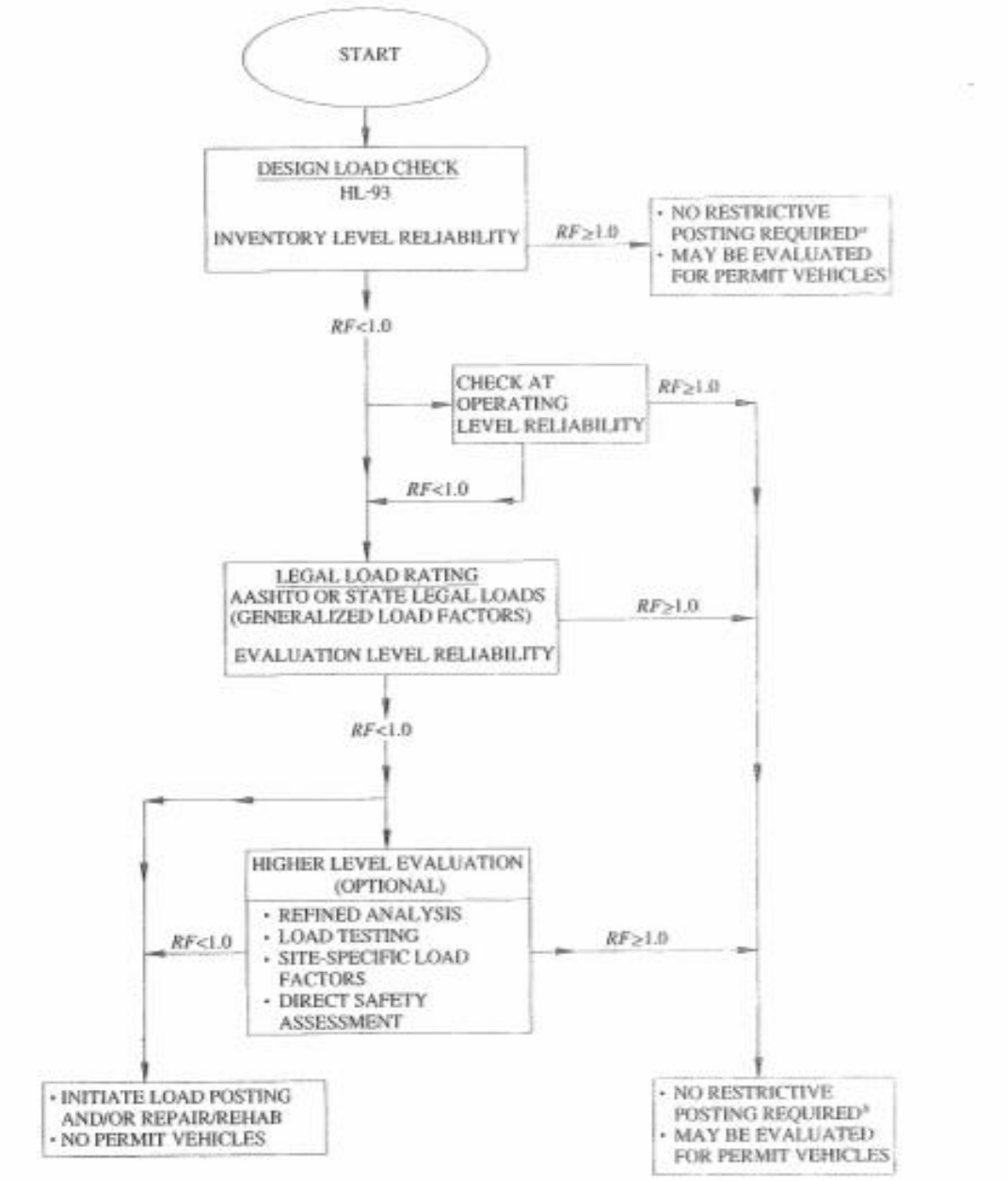

[a] For routinely permitted on highways of various states under grandfather exclusions to federal weight laws.

[b] For legal loads that comply with federal weight limits and Formula B.

Figure B 2: Load Rating Flow Chart from Appendix A6A of MBE

DISTRIBUTION FACTORS FOR MOMENT

Interior Beams

Equation for DFM the same for bridge types (i)* and (h) in Table 4.6.2.2.2b-1
*assuming girders in (i) connected enough to just prevent relative vertical deflection at interface

No skew and there are only 2 design lanes so the equations are applicable

$N_L := 2$ number of design lanes

$K_1 := 2.2$ preliminary value for channel

$\mu := .3$ poissons ratio

$y_b := 12.369in$

$y_t := 19in - y_b$

$$I_g := \frac{1}{12}\cdot 36.5in\cdot(5in)^3 + 36.5in\cdot 5in\cdot\left(y_t - 2.5in\right)^2 \ldots + 2\left[\frac{1}{36}\cdot .75in\cdot(2.5in)^3\right] + .5\cdot .75in\cdot 2.5in\cdot\left(y_t - 2.5in\cdot\frac{2}{3}\right)^2 \ldots + .5\cdot 2.5in.75in\cdot\left[y_t - \left(2.5in + 2.5in\cdot\frac{1}{3}\right)\right]^2 \ldots + 2\cdot\left[\frac{1}{12}\cdot 4.5in\cdot(14in)^3 + 4.5in\cdot 14in\cdot\left(y_b - 7in\right)^2\right] \ldots + 4\cdot\frac{1}{36}\cdot 1in\cdot(14in)^3 + \frac{1}{2}\cdot 1in\cdot 14in\cdot\left(y_b - 14in\cdot\frac{2}{3}\right)^2 = 9.588\times 10^3\cdot in^4$$

$$J := \frac{1}{3}\cdot\left[36.5in\cdot(5in)^3\cdot\left(1 - \frac{.63\cdot 5in}{36.5in}\right) + 2\cdot 14in\cdot(5.5in)^3\left(1 - \frac{.63\cdot 5.5in}{14in}\right)\right] = 2.558\times 10^3\cdot in^4$$

$$\sqrt{\frac{I_g}{J}} = 1.936$$

$b := 36.5in$ beam width

$d := 19in$ depth of beam

$$K_2 := \sqrt{(1+\mu)\cdot\frac{I_g}{J}} = 2.207$$

$L := 30ft$ span length

$(W := 33.583ft)$ edge to edge width of bridge

$\left(K_2 \cdot \left(\frac{W}{L}\right)\right) = 2.471$

K * (W/L) > K so use C = K

$(C := K_2 = 2.207)$

$\left(D := 11.5 - N_L + 1.4 N_L \cdot (1 - .2 \cdot C)^2 = 10.373\right)$ width of distribution per lane

$(S := 3.0417)$ girder spacing

$\left(DFM := \frac{S}{D} = 0.293\right)$ distribution factor for interior beam

Exterior Beams

Use Lever Rule:

Position truck wheel line of truck 2' from edge of barrier rail

$P_1 := 1kip$ at $x_1 := 18.375in + 24in = 42.375in$ from edge of bridge

$P_2 := 1kip$ at $x_2 := x_1 + 8ft = 124.375in$ from edge of bridge

$P_R := P_1 + P_2$ at $x_R := \frac{x_1 + x_2}{2} = 83.375in$ from edge of bridge

Force in girders will be assumed to occur at middle of girder

Force in the exterior girder (RE) at $x_3 := \frac{37.25in}{2} = 18.625in$

Force in first interior girder (RI) at $x_4 := 37.25in + \frac{36.5in}{2} = 55.5in$

Sum moments about first interior girder to determine ratio of truck load resisted by exterior girder

$P_R \cdot (x_4 - x_R) - R_E \cdot (x_4 - x_3)$ solve $\rightarrow$ $= \blacksquare \cdot 0$

The DFM for a girder can't be negative so the DFM for the exterior girder will be assumed to be equal to the DFM for the interior girder, 0.293.

Appendix D: Bridge Property Plots/Tables

Table D 1: DFM for Each Scenario and Run

	Scenario 1	Scenario 2	Scenario 3	Scenario 4	Scenario 5
Run 1	0.373	0.401	0.360	0.434	0.438
Run 2	0.366	0.365	0.383	0.462	0.433
Run 3	0.367	0.371	0.365	0.483	0.434
Run 4	0.352	0.391	0.376	N/A	
Run 5	0.351	0.380	0.318		
Run 6	0.350	0.378	0.394		
Run 7	0.371	0.409	0.297		
Run 8	0.374	0.416	0.290		
Run 9	0.363	0.418	0.340		

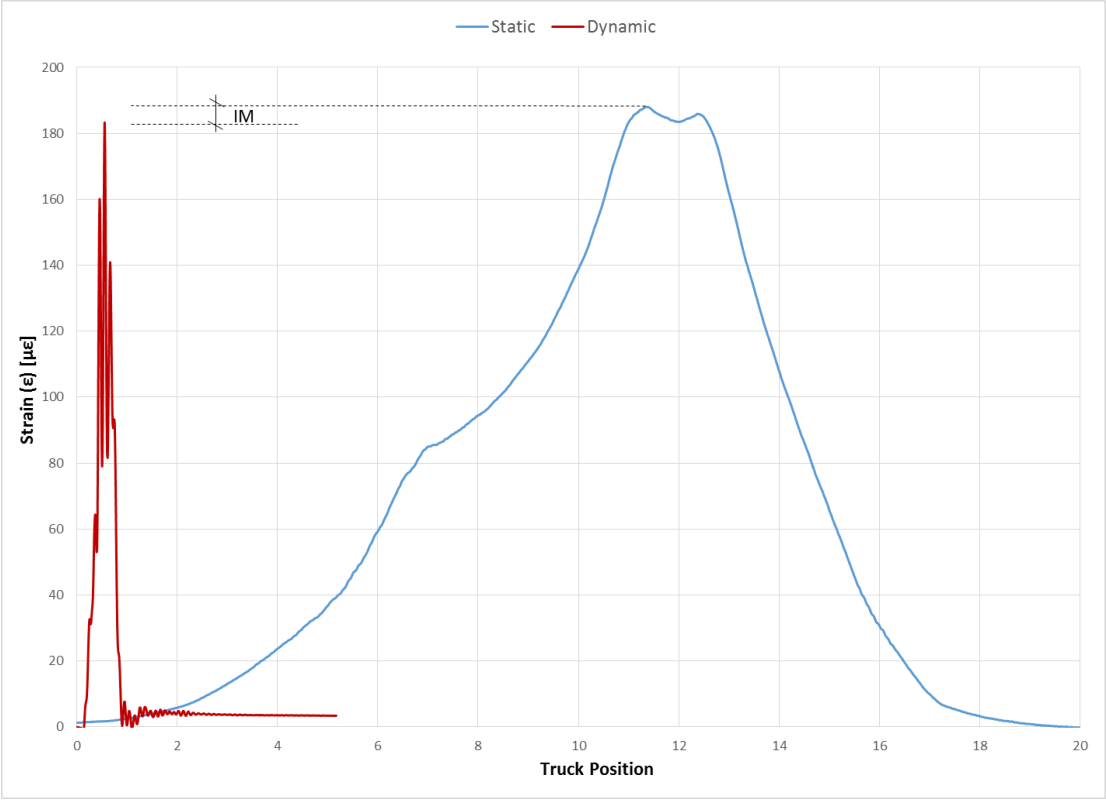

Figure D 1: IM for Girder 7

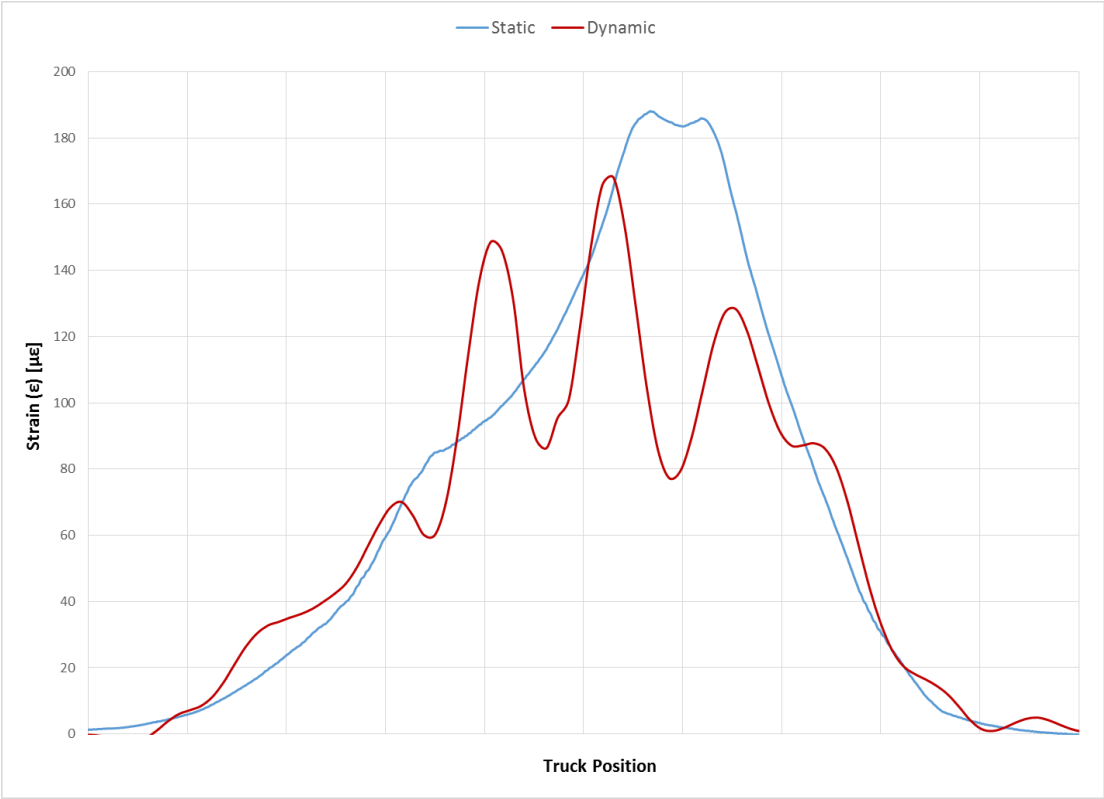

Figure D 2: Dynamic Strain Superimposed over Static Strain

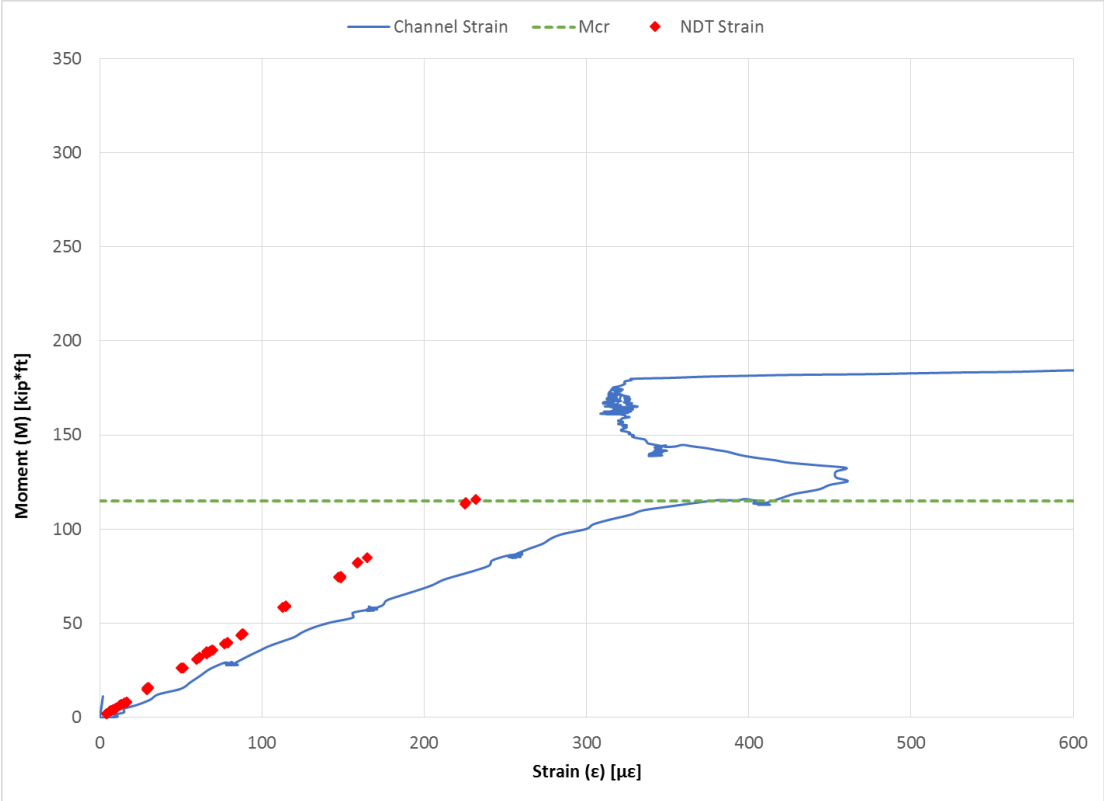

Figure D 3: Comparison of NDT and Channel Strain for Scenario Two

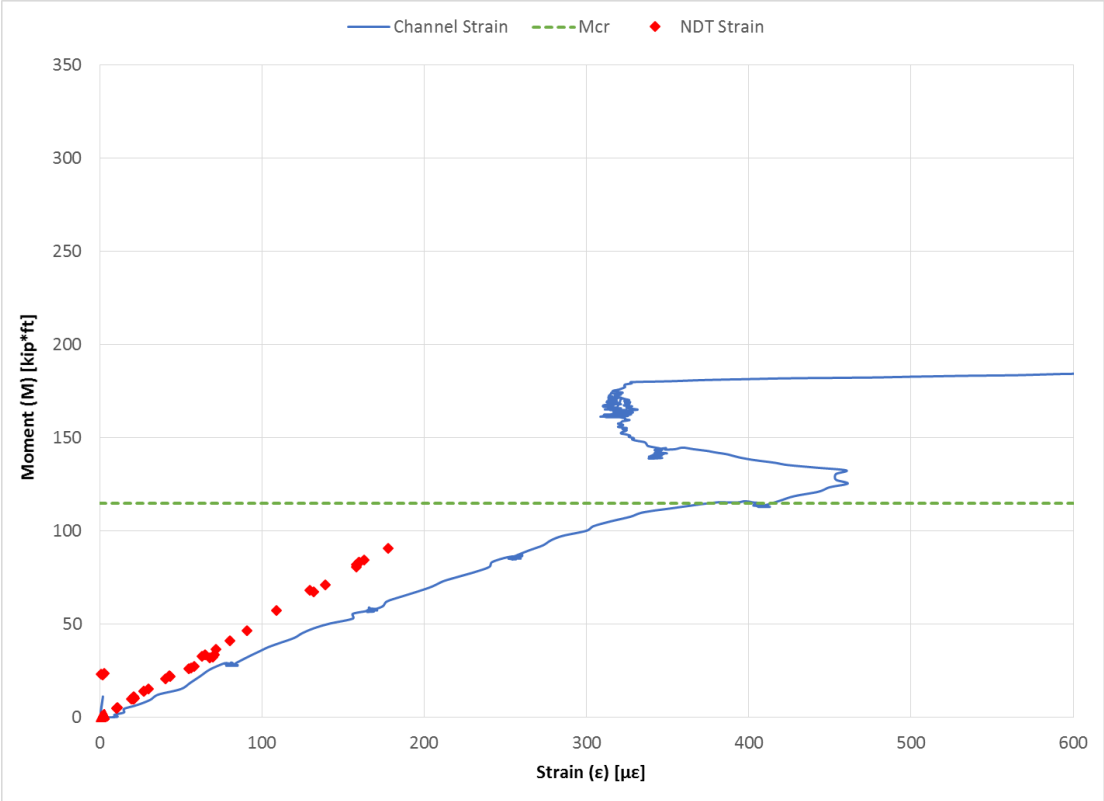

Figure D 4: Comparison of NDT and Channel Strain for Scenario Three